A THESIS SUBMITTED TO
THE GRADUATE SCHOOL OF NATURAL AND APPLIED SCIENCES
OF ÇANKIRI KARATEKİN UNIVERSITY

DEVELOPMENT AND COMPARISON OF THREE ALGORITHMS USED IN MPPT TECHNOLOGY TO EXTRACT MAXIMUM POWER FROM PHOTOVOLTAIC SYSTEM IN MATLAB/SIMULINK

IN PARTIAL FULFILLMENT OF THE REQUIREMENTS
FOR
THE DEGREE OF MASTER OF SCIENCE
IN
ELECTRICAL AND ELECTRONICS ENGINEERING

BY

ALAA SHAKIR MHMOOD AL-ARJEELI

ÇANKIRI

2022

DEVELOPMENT AND COMPARISON OF THREE ALGORITHMS USED IN MPPT TECHNOLOGY TO EXTRACT MAXIMUM POWER FROM PHOTOVOLTAIC SYSTEM IN MATLAB/SIMULINK

By Alaa Shakir Mhmood AL-ARJEELI

May 2022

We certify that we have read this thesis and that in our opinion it is fully adequate, in scope and in quality, as a thesis for the degree of Master of Science

Advisor : Asst. Prof. Dr. Mustafa TEKE
Co-Advisor : Asst. Prof. Dr. Mohannad Jabbar MNATI

Examining Committee Members:

Chairman : Assoc. Prof. Dr. Hayati MAMUR
Electrical and Electronics Engineering
Manisa Celal Bayar University

Member : Assoc. Prof. Dr. Fatih KORKMAZ
Electrical and Electronics Engineering
Çankırı Karatekin University

Member : Asst. Prof. Dr. Mustafa TEKE
Electrical and Electronics Engineering
Çankırı Karatekin University

Approved for the Graduate School of Natural and Applied Sciences

Prof. Dr. İbrahim ÇİFTÇİ
Director of Graduate School

I hereby declare that all information in this document has been obtained and presented in accordance with academic rules and ethical conduct. I also declare that, as required by these rules and conduct, I have fully cited and referenced all material and results that are not original to this work.

Alaa Shakir Mhmood AL-ARJEELI

ABSTRACT

DEVELOPMENT AND COMPARISON OF THREE ALGORITHMS USED IN MPPT TECHNOLOGY TO EXTRACT MAXIMUM POWER FROM PHOTOVOLTAIC SYSTEM IN MATLAB/SIMULINK

Alaa Shakir Mhmood AL-ARJEELI
Master of Science in Electrical and Electronics Engineering
Advisor: Asst. Prof. Dr. Mustafa TEKE
Co-Advisor: Asst. Prof. Dr. Mohannad Jabbar MNATI
May 2022

This thesis discusses the design and simulation of a photovoltaic system that use an MPPT charge controller to extract the maximum power from solar panels. Three different algorithms have been developed to be implemented in MPPT, namely, the Perturb and Observe (P&O) algorithm, the fuzzy logic controller (FLC) algorithm, and the particle swarming optimization (PSO) algorithm. The system was simulated using MATLAB/Simulink and simulation results have been compared to determine the best maximum power point tracking algorithm. The simulation results have shown the superiority of the developed (PSO) algorithm in increasing the system efficiency by extracting the maximum power from the solar panels and controlling the duty cycle of the converter to generate a constant voltage compared to the two algorithms (P&O, FLC). The (PSO) algorithm has achieved the highest efficiency under (STC) and changing conditions, so PSO is the best and most effective choice to increase the efficiency of the PV system.

2022, 129 pages

Keywords: Maximum power point tracking (MPPT), DC-DC boost converter, photovoltaic (PV) system, Perturb and Observe controller (P&O), fuzzy logic controller (FLC), Particle swarm optimization (PSO)

ÖZET

MATLAB/SİMULİNK'TE FOTOVOLTAİK SİSTEMDEN MAKSİMUM GÜÇ ELDE ETMEK İÇİN MPPT TEKNOLOJİSİNDE KULLANILAN ÜÇ ALGORİTMANIN GELİŞTİRİLMESİ VE KARŞILAŞTIRILMASI

Alaa Shakir Mhmood AL-ARJEELI
Elektrik ve Elektronik Mühendisliği, Yüksek Lisans
Tez Danışmanı: Dr. Öğr. Üyesi Mustafa TEKE
Eş Danışman: Dr. Öğr. Üyesi Mohannad Jabbar MNATI
Mayıs 2022

Bu tez, güneş panellerinden maksimum gücü çıkarmak için bir MPPT şarj kontrolörü kullanan bir fotovoltaik sistemin tasarımını ve simülasyonunu tartışmaktadır. MPPT'de uygulanmak üzere Perturb and Observe (P&O) algoritması, bulanık mantık denetleyicisi (FLC) algoritması ve parçacık swarming optimizasyonu (PSO) algoritması olmak üzere üç farklı algoritma geliştirilmiştir. Sistem MATLAB/Simulink kullanılarak simüle edilmiş ve en iyi maksimum güç noktası izleme algoritmasını belirlemek için simülasyon sonuçları karşılaştırılmıştır. Simülasyon sonuçları, geliştirilen (PSO) algoritmanın güneş panellerinden maksimum gücü çıkararak sistem verimliliğini artırmada ve dönüştürücünün görev döngüsünü kontrol ederek sabit bir voltaj üretmek için iki algoritmaya (P&O, FLC) göre üstünlüğünü göstermiştir. (PSO) algoritması, standart test koşulları ve değişken koşullarda en yüksek verimi elde etmiştir. Bu nedenle PSO, fotovoltaik sisteminin verimliliğini artırmak için en iyi ve en etkili seçimdir.

2022, 129 sayfa

Anahtar Kelimeler: Maksimum güç noktası takibi (MPPT), DC-DC boost converter, fotovoltaik (PV) sistem, Perturb and Observe denetleyicisi (P&O), bulanık mantık denetleyicisi (FLC), Parçacık sürüsü optimizasyonu (PSO)

PREFACE AND ACKNOWLEDGEMENTS

I would like to thank my thesis advisor, Asst. Prof. Dr. Mustafa TEKE and Asst. Prof. Dr. Mohannad Jabbar MNATI, for their patience, guidance, and understanding. After completing this work, first, I thank God a lot for helping me to accomplish it. Then there are many people whom I would like to thank and give them my respect and appreciation for standing with me, supporting me, and giving me valuable advice. A thousand thanks to those without whom I would not be. Whoever made my life full of love, I am very grateful to my mother and the mercy and forgiveness of my father in his grave, and my brothers for their prayers and continuous support. I would also like to express to those who have given me love, trust, and support, my dear wife, without whom I would not have been able to complete this work, and with the constant encouragement of my children, may God preserve them for me. Last but not least, I am very grateful to Çankırı Karatekin University and all its professors, and everyone who contributed to the completion of this valuable thesis. Thanks to all.

Alaa Shakir Mhmood AL-ARJEELI
Çankırı-2022

CONTENTS

LIST OF SYMBOLS

ΔD	The change in duty ratio
A	Ampere
$P_{I/P}$	The power extracted from the photovoltaic panel
P_{pv}	Theoretical photovoltaic power of the panel
R_L	The load resistance
W/m^2	Watt per square metre
η	Efficiency
Ω	Ohm

LIST OF ABBREVIATIONS

ANN	Artificial Neural Network
C	Capacitance
D	Duty Cycle
DC	Direct Current
E	Error
FLC	Fuzzy logic control
I	Current
IC	Incremental conductance
Impp	Current at Maximum Power Point
Iph	Photo Current
Irr	Irradiance
ISC	Short circuit current
L	Inductance
MPP	Maximum Power Point
MPPT	Maximum Power Point Tracking
P	Power
P&O	Perturb and observe
Pmax	Maximum power
P-n	p-n junction
PSO	Particle swarm optimization
PV	Photovoltaic
PWM	Pulse Width Modulation
R	Resistance
STC	Standard Test Condition
Tem	Temperature
V	Voltage
Vmpp	Voltage at Maximum Power Point
Voc	Open Circuit Voltage

LIST OF FIGURES

LIST OF TABLES

1. INTRODUCTION

The great development in industries and technology, the increasing demand for electric power, and the large population growth led to an increase in electricity consumption, forcing researchers to search for alternatives to traditional electric power generation methods from fossil fuels because of their high costs and shortages. For this reason, sustainable and renewable energy (Sasi 2017)was the best choice for several reasons such as its availability, accessibility, low cost, and noiselessness. All these factors and advantages and others made it the focus of researchers and scientists to develop it. And finding ways to extract it and maintain its stability with changing weather conditions. (Figure 1.1) represents the most important renewable energy sources.

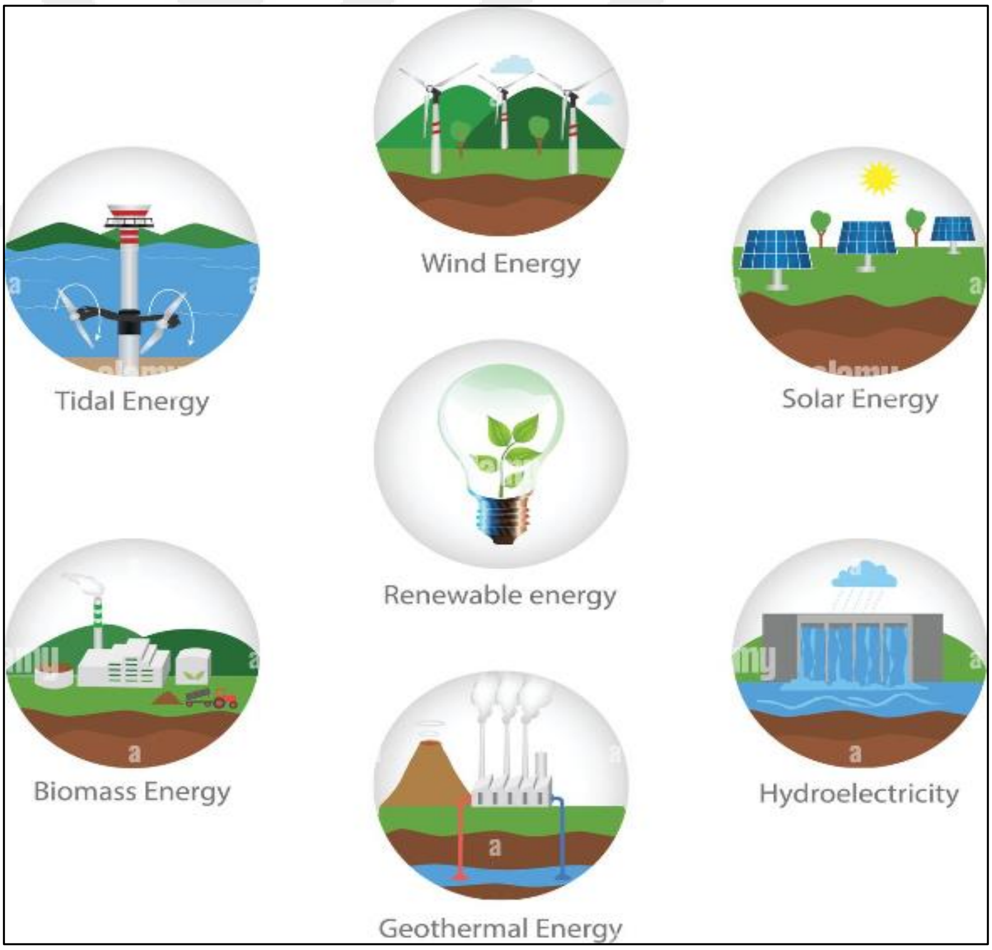

Figure 1.1 Renewable energy sources (Website 2009)

Renewable energy is also environmentally friendly and inexhaustible such as (Solar energy, Wind energy, Hydro energy, Tidal energy, geothermal energy, Biomass energy). Where solar energy is one of the most important and most widely used types of renewable energy today to generate electrical energy, solar energy is converted into electrical energy by shining sunlight on a photovoltaic cell (Sampaio and González 2017, Mnati *et al.* 2019) made of semiconductors, which in turn generate electrical energy whose value depends on two main factors, the intensity of solar radiation and temperature.

Electricity generated from solar energy is used in water pumps, homes, factories, street lighting, surveillance cameras, and homes in remote villages, water purification, sterilization plant, and agriculture. Solar energy is available to everyone and it is free. They are environmentally friendly, silent, and the solar cells are easy to install and maintain (Raof 2020). But there are problems with solar energy systems such as the high upfront costs of buying and installing panels, batteries, and chargers. The main problem that the solar energy system suffers from is its low efficiency and its great impact on the surrounding weather conditions.

Since photovoltaic (PV) systems responsible for generating electrical energy from converting solar energy (sunlight) into electricity suffer from the problem of the efficiency of the photovoltaic system is low and is affected by weather changes, the characteristics of the cell are not linear and depend on The intensity of solar irradiation and temperature, Where solar energy is directly converted into electricity by a solar photovoltaic (PV) module (Pathare *et al.* 2017).

Because of the low efficiency of solar panels, researchers have tended to find ways to increase the efficiency of photovoltaic systems by tracking the maximum power point (MPP) that the solar panels produce when exposed to radiation. These methods are called Maximum Power Point Tracking (MPPT) (Nadkarni *et al.* 2018, Talbi *et al.* 2021), a set of algorithms developed by researchers that are used to extract the best energy from solar panels, stabilize voltage and control the charging process of batteries (Mao *et al.* 2020). (Figure 1.2) shows the location of MPPT technology in the photovoltaic system.

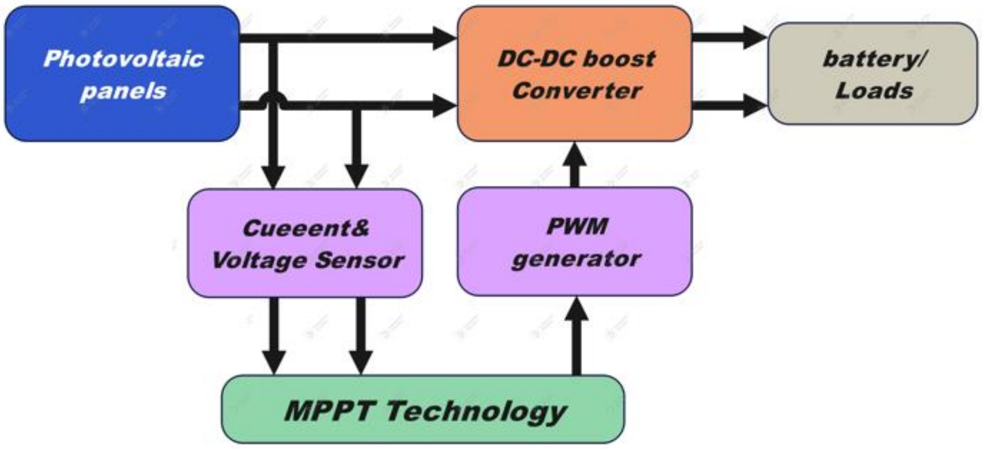

Figure 1.2 Shows the photovoltaic system with MPPT Technology (Mao *et al.* 2020)

To track the power output, many MPPT algorithms are applied in the literature, to get the point at which it can provide the maximum power (MPP), which is called the maximum power point. This point depends on the weather conditions and the load resistance, so it is not fixed. Therefore, we need to apply Maximum Power Point Tracking (MPPT), where researchers have worked on developing many MPPT methods, including traditional methods such as Perturb and Observe (P&O) (Abo-Sennah *et al.* 2021, Al-Majidi *et al.* 2018) and Incremental conductance (IC) (Ronilaya *et al.* 2018, Mohamed and Abd El Sattar 2019).

These algorithms are easy to implement and do not need to know the characteristics of the photovoltaic generator, so it works independently, and its efficiency is good under stable conditions but its problems appear when the weather conditions (solar radiation intensity and temperature) change as the algorithm starts to oscillate around the MPP point and cannot track the MPPT properly True and this reduces the efficiency of the entire system (Talbi *et al.* 2021).

The second type of algorithm is artificial intelligence algorithms such as the fuzzy logic control (FLC) algorithm, the artificial neural network (ANN) algorithm, etc... Where these algorithms are characterized by their high efficiency and high speed. Response, and accurately track the maximum power point under stable and changing weather conditions, but it is more complex compared to previous conventional methods (Abo-Sennah *et al.* 2021, Ali *et al.* 2021).

The third type of algorithms applied in MPPT technology is the optimization algorithm such as (Cuckoo search (CS), Ant colony optimization (ACO), Particle swarm optimization (PSO) algorithms) this type of modern algorithm is characterized by rapid convergence and high accuracy, especially under volatile weather conditions, which increase the efficiency of the photovoltaic system, (Zafar *et al.* 2020, Chao and Rizal 2021).

In this thesis, a photovoltaic system is built, which consists of three main parts, the solar panels and the MPPT type charge controller with a DC-DC boost converter. Where all parts were linked and simulated using the MATLAB/Simulink environment, and through the simulation results, three algorithms will be compared that will be used to track the maximum power point and find out the best performance by running each algorithm under stable and changing weather conditions (change in the intensity of solar radiation and change in temperature).

Where an algorithm was chosen as one of the three main techniques from which the algorithms are classified. The Perturbation and Observation (P&O) algorithm was chosen from the traditional method, the Fuzzy Logic Control (FLC) algorithm was chosen from the Artificial Intelligence method, and finally, the Particle Swarm Optimization (PSO) algorithm was chosen, which is one of the optimizations algorithms.

In the third section, the algorithms used in this thesis are presented that the MPPT technology is built based on these three algorithms and the electrical properties of the solar panel used (1Soltech 1STH-215-P) are also shown. From the solar panel datasheet, we can get a voltage of 29V, a current of 7.35A, and a power of 213.15W under standard test conditions (irr=1000W/m^2, tem=25^0C). Voltage, current, and power values vary with different weather conditions. Ambient (radiation intensity and temperature). Based on the values given in the datasheet of the solar panel used, the DC-DC boost converter has been designed using the equations mentioned in Section Three (3.4.1) which is designed to provide a voltage of (36-40) volts under standard and variable test conditions.

In the fourth section, the simulation of the PV system was carried out using MATLAB/Simulink and the design of MPPT technology based on three different algorithms in this thesis. Each algorithm was individually tested under standard test conditions (irr=1000W/m^2, tem=25^0C) and the measurements (current, voltage, power) that were extracted from the photovoltaic panels were recorded and then compared with the values given by the solar panel theoretically and the efficiency of the algorithm was calculated and also calculated DC-DC boost converter output values. And apply the same process to all algorithms and also note the curves of the characteristics of current, voltage, and power. Then repeat the same process, but when the test conditions change first, a change in the radiation intensity (600 1000 800 650 980 700) W/m^2 and the temperature is constant (25^0C), Secondly, the temperature changes (55°C, 45°C, 35°C, and 27°C) and the radiation intensity is constant (1000 W/m^2).

In the fifth section, the simulation results for the three algorithms were presented under standard and other variable test conditions. The efficiency of each algorithm was calculated based on the ability that was extracted from the solar panel, to compare between the three algorithms and determine which algorithm is better in raising the efficiency of the system and extracting the greatest power generated in the panel through MPP point tracking speed under various conditions. Then the results obtained, the efficiency of each algorithm, and the accuracy of controlling the duty cycle of the DC-DC boost converter to generate a voltage equal to or close to the voltage it was designed for (36-40 V) were discussed.

Finally, in the sixth section, the conclusion from this thesis was summarized, what are the most important results that we obtained, and future proposals for the development of work were given.

2. LITERATURE REVIEW

Great interest in sustainable energy, especially solar energy, because it is easy to obtain and is available free of charge, has made it the focus of attention of many researchers and scientists, but solar energy systems, in general, suffer from the problem of low efficiency due to being affected by changes in weather conditions significantly, which made their distinctive characteristics non-linear.

To address the problem of its low efficiency, researchers worked on finding ways to increase efficiency and reduce the impact of climate fluctuations on the photovoltaic system. One of the most important of these is the Maximum Power Point Tracking Technology (MPPT).

In 2021, Sarvi et al. presented that this technology improves efficiency and tracks Maximum Power Point (MPP) faster. This technique contains a large group of algorithms found and developed by researchers, which can be divided into (Sarvi and Azadian 2021):

1- Conventional methods:

- Perturb and observe(P&O).
- Incremental conductance(IC).
- Fractional open-circuit voltage(FOCV).
- Fractional short circuit current(FSCC).

2- Artificial intelligent techniques:

- Genetic algorithm(GA).
- Artificial Neural Network (ANN).
- Fuzzy Logic Controller (FLC).
- Differential evolution (DE).

3- Biologically inspired algorithms:

- Ant colony optimization algorithm (ACO).
- Cuckoo search (CS).
- Firefly algorithm (FA).
- Particle swarm optimization (PSO).

In this study, three algorithms will be applied, studied, and simulated in the Maximum Power Point Tracking Technology (MPPT) and compared between the simulation results of the three algorithms and knowing which algorithm is the best in tracking power and achieving higher efficiency through simulation results using MATLAB/Simulink. The algorithms that will be worked on are Perturb and observe (P&O) algorithm, fuzzy logic controller (FLC) algorithm, and particle swarm optimization (PSO) algorithm.

I will review a set of research papers submitted by researchers to apply and develop algorithms that work in the maximum power point tracking technology. And review their results.

Pathare *et al.* (2017) presented that the increasing demand for sustainable energy due to the depletion of non-renewable energy sources and the increase in its costs, and because sustainable energy is available, less expensive, free from pollution and noise, has made it the focus of the attention of major industrial companies in the production of photovoltaic cells, where solar energy is one of the most important sources of renewable energy because it is easily and abundantly available and its costs are low. But the main problem of solar energy is its instability and fluctuation with changing weather conditions (solar radiation intensity and temperature), so batteries are always connected between the PV panels and the load to compensate for the lack of energy during changing conditions as it is considered as a secondary source of energy. But these batteries can be easily damaged when the voltage produced by the cells rises, so the researchers resorted to finding a way to protect the batteries, as MPPT technology was reached, which has two main functions in the photovoltaic system. Whereas MPPT technology works mainly to track the maximum power point and extract maximum power from the photovoltaic cell, in addition to its other work, which is to protect the batteries from sudden voltage surges, the function of MPPT is also discussed in detail in the research paper (Pathare *et al.* 2017).

Alsumiri (2019). Presented that the grid-independent photovoltaic system includes solar panels, MPPT technology, DC-to-DC converter, and batteries. This system is used in locations far from the extensions of the electric grid and remote villages, where there must be space that allows access to sunlight easily and for the longest possible period at this time. The excess energy is stored in the batteries to be utilized when the solar radiation decreases or when it is dark. These systems' performance is related to the technology used in them to track the maximum power point to improve the harm of the system and increase its efficiency. This was explained in the research paper (Alsumiri 2019), where the MATLAB environment was used to implement the system with the use of the Incremental conductance (IC) algorithm. This method is more complex and costly compared to other methods. But it has a high-performance accuracy.

Nadkarni *et al.* (2018) presented that the role of MPPT technology is important in the photovoltaic system in tracking the maximum power point in stable conditions, but its role is more important when the weather conditions (solar radiation intensity and temperature) change, these two factors have a great influence on the efficiency of the solar system to control the energy production And efficiency in such conditions, the role of MPPT is highlighted by its control over the duty cycle of the DC-DC converter, MPPT technology consists of a large set of algorithms. The algorithm-based technology generates pulses to control the operation of the DC-DC converter and drive it to the required power output continuously despite changing conditions, and here the role of algorithms is highlighted by their speed in tracking the maximum power point. The researcher used in (Nadkarni *et al.* 2018), two types of algorithms, the traditional methods are the Perturb and Observe algorithm (P&O) and the Incremental conductance algorithm (IC) with DC-DC converter, and they were simulated using MATLAB / Simulink, where the simulation results showed that (P&O) is easy to implement but slow Respond as weather conditions change and continue to oscillate around the MPP causing power loss. As for the)IC) algorithm, the problem of oscillation around the power point has been addressed and has a faster response to track the energy point when conditions change, so it is considered better than the (P&O) algorithm.

Abdellatif *et al.* (2021) presented that to improve the efficiency of the photovoltaic system and increase the production capacity of the system that depends on the intensity of solar radiation and temperature, the researchers used traditional methods in MPPT technology, where they used two algorithms, the perturbation, and observation method (P&O) and the Incremental conductance method (IC), as well as the use of artificial intelligence techniques, such as the MPPT method based on the unit Fuzzy Logic Control (FLC). The three algorithms were simulated using MATLAB/Simulink and the results were compared to determine which methods are best to improve efficiency under changing climate conditions. Where the researcher mentioned that the simulation results showed that the MPPT technique based on the fuzzy logic algorithm is much better in terms of stability, high accuracy, and speed of MPP tracking than that based on the traditional MPPT methods (P&O and IC).

Mohamed and Abd El Sattar (2019) presented that the researcher proposed a technique for tracking the maximum power of photovoltaic panels based on the perturb and observe (P&O) algorithm, which is operated at high perturbation frequencies, which provides higher efficiency than the traditional (P&O) method of power tracking and better system performance under stable conditions.

Majaw *et al.* (2018) presented that MPPT technology plays an important role in the photovoltaic system by obtaining the maximum power point for the solar panel. In the research paper (Majaw *et al.* 2018), the simulation results of three methods of MPPT technique were studied and compared, which are the traditional method (P&O), the method of artificial intelligence fuzzy (FLC), and the method of particle swarm optimization (PSO). The role of MPPT appears greatly during the changing weather conditions (solar radiation intensity and temperature). The solar panels were connected with a buck converter and MPPT technology. The simulation results showed the superiority of the (PSO) algorithm in that it reaches the maximum power point in the shortest time and with the least oscillation around MPP point, and it has the advantage of fast convergence And high accuracy, where its efficiency was 99.3%, compared to the efficiency of the (FLC) algorithm, which was 99.04%, which came in second place, while the (P&O) algorithm achieved an efficiency of 97.03%.

Nasser *et al.* (2020) presented that the fuzzy logic control (FLC) algorithm was used for MPPT technology to increase the efficiency of the photovoltaic system and extract the maximum power produced in the cell under changing weather conditions. The technique was simulated along with the panels and DC-DC boost converter using MATLAB/Simulink environment. The simulation results proved that the fuzzy logic algorithm is characterized by a high response and less fluctuation around the MPP point compared to traditional methods. All this was clarified in the research (Nasser *et al.* 2020).

Kumar *et al.* (2017) presented that the presence of MPPT technology in the photovoltaic system is very necessary and indispensable if we want to increase the efficiency of the system and obtain the maximum energy from the solar system. This has been proven by researchers in (Kumar *et al.* 2017), where the photovoltaic system was simulated twice in the first case, the system was simulated only with a switch without using MPPT technology. In the second case, the photovoltaic system was simulated with the addition of an MPPT controller (P&O) and a DC-DC boost converter. In the first case, an output power of 95 watts was obtained under the influence of a radiation value of 85w/m2. When using MPPT technology, the value of the energy produced from the panels increased to 215 watts under the influence of the same value of the previous irradiation, so we can say that using MPPT technology based on the (P&O) algorithm increases the efficiency of the system by 120%.

Khodair *et al.* (2020) the researcher presents a comparative study between two traditional algorithms, the perturbation and observation (P&O) algorithm and the Incremental conductance (IC) algorithm, and It is compared with two algorithms whose variable step size has been modified (M-VSS-P&O and M-VSS-IC) that are implemented through the technique of MPPT control to control the duty cycle of a DC-DC boost converter. The simulation was carried out using MATLAB/Simulink with three different types of the solar panels (polycrystalline KC200GT, monocrystalline SQ85, and ST40 thin-film solar cells), the simulation of the photovoltaic system was carried out with the four algorithms under standard test conditions (STC) and tested under conditions in which the forms of solar radiation change. The simulation results obtained by the researchers showed the superiority of the modified traditional algorithms (M-VSS-P & O and M-VSS-INC) in terms of MPP tracking speed, efficiency, and performance compared to the traditional algorithms (P&O, IC).

Victor *et al.* (2019) presented that when designing the charge control unit, the electrical characteristics of the solar panels and the load circuit (battery) that will be fed by the control unit must be taken into account. Therefore, to charge the battery with high efficiency and with fewer energy losses, the type of charge controller must be chosen accurately. There are many charging control methods to know the characteristics of each type that were simulated using MATLAB/Simulink, where the simulation results showed, as discussed by the researcher in (Victor *et al.* 2019) that the traditional methods of charging, i.e. basic charge controllers, are undesirable because of their large loss of energy through the charging circuit itself. The most common charging methods in charging batteries in recent years are PWM and MPPT because of their low loss. We can use a PWM type controller when the battery voltage is similar to the voltage of photovoltaic panels, while at high voltage it is preferable to use the MPPT charge controller, which is more common nowadays because it Works well when weather conditions change (change of radiation intensity and temperature).

Majaw *et al.* (2018) presented that the researchers conducted a comparative study between the charge controllers used today and their importance in raising the efficiency of the photovoltaic system, increasing the energy produced and protecting the battery from damage. The most important charge controllers are Pulse Width Modulation (PWM) and Maximum Power Point Tracking (MPPT). It is necessary to have charge controllers in solar energy systems that contain batteries, as the chargers work to ensure that the batteries are recharged quickly and not completely discharged, which increases the battery life, as well as working to isolate the battery from the solar panels in times of darkness when there is no sunlight Where it does not allow the passage of reverse current. By comparing charge controllers, the researchers found the superiority of MPPT technology, as it increases the efficiency of the solar system by 30% compared to PWM technology.

Guran and Perișoară (2020) the researcher presented his research paper for the application of charge controllers for the photovoltaic cell in smart solar-powered cars, where the solar cell was installed on the vehicle and the charge controller and batteries were linked with a DC to DC converter and a digital screen to display the results. A comparison was made between the charge controllers (PWM, MPPT) in terms of increasing the efficiency of the system, providing protection for the batteries, tracking the power cut, and isolating the batteries from the panels when there is no solar light, as well as isolating the batteries from the load when the car stops. Through the results reached by the researcher, it was found that MPPT technology is superior to PWM technology.

Sepulveda *et al.* (2019) the researcher presented a practical comparison of charge controllers (PWM, MPPT), as these devices are an important part of the photovoltaic system, and through charge controllers, the efficiency of the entire system can be increased. The researchers conducted a practical experiment to charge batteries using solar panels, charge controllers (PWM and MPPT), and a DC-DC converter and found that the efficiency of MPPT technology is better in terms of response speed, waste reduction, and battery charging speed, but its problem lies in its high costs compared to PWM technology, which is suitable For those who want a simple and low-cost charging controller.

Acharya and Aithal (2020) presented that Solar energy is one of the most important types of renewable energy used, which has become the focus of researchers and manufacturers to address its problems, which are severely affected by weather conditions. Therefore, charge controllers are a major and important part of the photovoltaic system that controls the flow of current and voltage from the solar panels to the batteries and the load. In (Acharya and Aithal 2020) a detailed study of the most important types of charge controllers (MPPT, PWM) and what are the advantages and disadvantages of each type and the differences between them in terms of battery charging speed, system efficiency, and cost.

Pilakkat *et al.* (2020) presented that the photovoltaic properties of solar panels and several MPPT algorithms are discussed in this paper. The MPPT response time for the solar radiation step was calculated using some comparisons. Compared with traditional algorithms and artificial intelligence algorithms, the performance of biologically inspired algorithms under the Partial Shaded Conditions (PSC). Finally, the particle swarm optimization (PSO) algorithm and the Firefly algorithm (FA) appear to be more accurate, fast, and stable than traditional MPPT methods.

Ali *et al.* (2020) the researchers presented a general review on an important part of the photovoltaic system, which always suffers from the problem of low efficiency and its non-linear characteristics because it is affected by weather conditions. Therefore, MPPT maximum power point tracking technology is considered the best option to address the problems of the photovoltaic system, raise its efficiency and extract MPP from it. Therefore, the researchers presented in this paper a general review of the most important MPPT methods, identifying the advantages and disadvantages of each type, and finding the best to apply it under standard and changing conditions.

Bollipo *et al.* (2020) presented that 23 research papers on MPPT methods used to raise the efficiency of the photovoltaic system and increase the production capacity during stable conditions and partial shade (PSC) conditions are reviewed, where the algorithm is divided into three main groups which are traditional methods, artificial intelligence and optimization. Where the algorithm is chosen according to the working conditions. In stable conditions, it is preferable to use traditional methods for their simplicity and low costs. In PSC conditions, it is preferable to use artificial intelligence algorithms or optimization algorithms.

Ali *et al.* (2020) presents a comparison between the Incremental conductance (IC) algorithm and the fuzzy logic control (FLC) algorithm that works through MPPT technology in a photovoltaic system that suffers from low efficiency and is affected by weather conditions. The system was simulated with a DC-DC boost converter, and the simulation results showed the superiority of (FLC) algorithm over (IC) algorithm. (FLC) is characterized by rapid response and low oscillation, which increases the efficiency of the system, especially in changing weather conditions.

Mohamed *et al.* (2020) presented that presents the Maximum Power Point Tracking MPPT technology based on the Modified perturbation and observation (MP&O) algorithm to be used in solar energy systems to extract the most energy from it under different weather conditions. The photovoltaic system was simulated using MATLAB/Simulink environment with a detailed circuit diagram of the MP&O-based charge controller, and the simulation results were compared with the results of conventional algorithms (P&0, IC). Where the results showed the superiority of the traditional modified MP&O algorithm under different weather conditions quickly and the proposed method provides high performance and increases the efficiency of the system from 94% to 98%.

Salem *et al.* (2021) presented that the photovoltaic cell suffers from the disadvantages of low energy conversion efficiency and high initial cost, so MPPT methods are used to extract the maximum power point MPP. In the paper (Elbarbary and Alranini 2021), the researcher presented a simulation of two traditional algorithms (P&0, IC) to compare them under constant weather conditions in radiation intensity and temperature with a DC-DC boost converter. The simulation results showed that the P&O algorithm has a better response speed than the IC algorithm under standard test conditions (temperature = 25°C, radiation intensity = 1000 W/m^2).

Kareem (2019) Presented that MATLAB/Simulink was used to model a self-contained photovoltaic system. Incremental conductance (IC) technology was used to track the maximum power point. The simulation results show that the MPPT method based on the IC algorithm is characterized by high speed and accuracy response under rapidly changing radiation and temperature conditions, but the algorithm is more complex than other traditional methods, which is what the researcher mentioned in (Kareem 2019).

Pathy *et al.* (2019) presented that The researchers discussed in (Pathy *et al.* 2019) the problem of the photovoltaic cell being exposed to partial shading or changing the intensity of solar radiation or temperature, and its great impact on the work of the photovoltaic system, which results in multiple peaks in the system output, making the process of tracking the maximum power point fail in traditional methods such as (voltage Open circuit (FOCV), perturbation and observation (P&O) and the Incremental conductance (IC) algorithm ...etc.). Therefore, the researchers in this paper propose a set of optimization algorithms (PSO, DE, ABC, ACO, BFOA) where these algorithms are qualified to work under changing conditions or partial shade, it is characterized by a fast response, accuracy, and high efficiency.

Sutikno *et al.* (2021) presented that to harvest the maximum energy coming out of the photovoltaic panels, a high-voltage DC-DC converter is used with MPPT technology based on the fuzzy logic control (FLC) algorithm to improve the system performance and raise its efficiency under changing weather conditions. The photovoltaic system was simulated using MATLAB/Simulink with the use of various Membership Functions (triangle, trapezoid, Gaussian, and GBell) available in the membership function editor to compare them and choose the optimal function to work in such conditions. The simulation results show that the GBell function can track MPP with high accuracy, can optimally transfer power, and has stable performance under various conditions. This is explained in detail in the research paper (Sutikno *et al.* 2021).

Jeannot *et al.* (2020) The researchers proposed a solution to maintain the maximum power point under changing atmospheric conditions (change in solar radiation intensity and temperature change) through a simulation using MATLAB environment for a photovoltaic system consisting of solar panels, DC-DC boost converter, and MPPT based on Fuzzy logic control algorithm. The simulation results showed fuzzification and defuzzification of the input and output variables of the converter. The high efficiency of the proposed algorithm in power point tracking under changing conditions.

Nour (2019) The researcher used an artificial neural network to replace the traditional methods such as (P&O, IC) in tracking the maximum power point of the PV system and addressing the problems encountered by the traditional methods, while the ANN technology can provide a better response when well trained. The MPPT based on the

ANN algorithm in the literature has used solar radiation and temperature as its inputs. In this research, the researcher suggested new inputs to improve the performance of the ANN algorithm, and he also suggested a second improvement using the Genetic Algorithm (GA) to design the ANN algorithm by adjusting the number of neurons in each layer, the type of learning algorithm, and the activation function, and after simulating the system using MATLAB/Simulink, the results appeared The modified and improved ANN algorithm has better performance, reliability, and responsiveness than traditional methods and increases the efficiency of the solar system.

Villegas *et al.* (2021) presented that Because of its cleanliness and low noise, the demand for solar energy has increased, especially in recent years, due to the ease of obtaining it, and it is an energy that does not run out and is available on most days of the year, but its problem lies in its lack of efficiency. Is the most important obstacle, and has become the concern of most researchers to find ways to increase the efficiency of the photovoltaic system. The MPPT method allows us to extract the maximum amount of energy from the solar panels. This technique has a set of algorithms. The research (Villegas *et al.* 2021) dealt with the method of Artificial Neural Network (ANN), where the speed and accuracy of MPP tracking depend on the nature of the algorithm used in the hidden layer and the quality of its training. The researcher stated that the application of ANN-based MPPT technology provides average efficiency of up to 98% under uniform conditions, high convergence velocity, and lower fluctuations around the MPP.

Kota and Bhukya (2019) the researchers proposed a new MPPT technique scheme based on the ANN algorithm for MPP point tracking under partial shading (PSC) conditions and compared the results of the proposed algorithm (ANN) with the optimization algorithm (PSO) and (ABC) algorithm. From the results obtained by the researcher, it was found that the proposed ANN algorithm excels, as it is faster, more accurate, and less expensive compared to (PSO, ABC) algorithms whose costs are considered high.

Jyothy and Sindhu (2018) presented that MPPT technology is implemented based on the Artificial Neural Network (ANN) algorithm to track the maximum power point and extract the maximum power from the photovoltaic panels under variable irradiation conditions and temperature by simulating them in MATLAB/Simulink and comparing the results of the ANN algorithm with traditional charge control methods. Such as (P&O, IC, FOCV) simulation results showed that MPPT technology based on ANN algorithm provides better performance through tracking speed, fewer oscillations around the MPP, and lower settling time requirements.

Putri *et al.* (2019) the researchers presented a research paper on improving the efficiency of the electrical system under partial shading conditions that the solar panels are exposed to using MPPT technology based on the PSO particle swarm optimization algorithm. The photovoltaic system was simulated using MATLAB/Simulink to compare two solar cell designs, one using MPPT technology based on PSO, and the second without using MPPT technology. According to the simulation results, the researcher showed that using the PSO algorithm improves the performance of the system and increases its system efficiency under the conditions of PSC.

Ritu *et al.* (2020) presented that MPPT technology based on the PSO particle swarming optimization algorithm was used to control the duty cycle of the DC-DC boost converter to extract the maximum power from the photovoltaic panels under partial shading (PSC) conditions. Conventional methods can fail under PSC conditions because multiple peaks appear in the system characteristic curve. The system was simulated using a MATLAB/Simulink environment, and the researcher showed that by using PSO under appropriate PSC conditions, it has a high convergence rate and low oscillation when MPP is reached.

Irwanto *et al.* (2020) presented that photovoltaic panels are greatly affected by the change of solar radiation and temperature, which leads to its production of unstable energy, so it cannot be supplied directly to the batteries or the load. For this reason, the researcher suggests in (Irwanto *et al.* 2020) the use of a DC-DC boost converter based on the PID controller unit to control the work cycle. A boost converter is used to charge a 12-volt battery. The results of the simulation of the boost transformer showed that the transformer works to regulate the current and voltage flowing to charge the battery, in addition to protecting the battery from damage and prolonging its life.

Palanisamy *et al.* (2019) the researchers studied five algorithms most commonly applied in MPPT technology in photovoltaic systems, namely Perturb and Observe (P&O), Incremental Conductance (INC), Fractional Open Circuit Voltage (FOCV), Ripple Correlation Control (RCC) and Extremum Seeking Control (ESC). The system was simulated with three types of DC-DC converter (Boost, Buck, and Buck-Boost), the simulation results showed that the (IC) algorithm and (ESC) algorithm are the best MPP point tracking among the MPPT controllers, and the DC-DC buck-boost converter is the best among the three converters.

3. MATERIALS AND METHODS

3.1 PV Conversion Chain

In general, the photovoltaic system consists of four main parts (solar panel, MPPT charge controller, DC-DC converter, Batteries or loads). Figure 3.1 shows the photovoltaic conversion process chain, Where the maximum power point (MPP) is obtained by controlling the duty cycle of a DC-DC converter using maximum power point tracking (MPPT) techniques, Which works to improve and raise the efficiency of the system and transfer the maximum energy from the photovoltaic cell to the load (Akiza *et al.* 2021). MPPT technology is based on many traditional algorithms, optimization algorithms, and artificial intelligence, and the algorithm is selected according to weather conditions and speed required to track the point of maximum power and efficiency (Rougab *et al.* 2021).

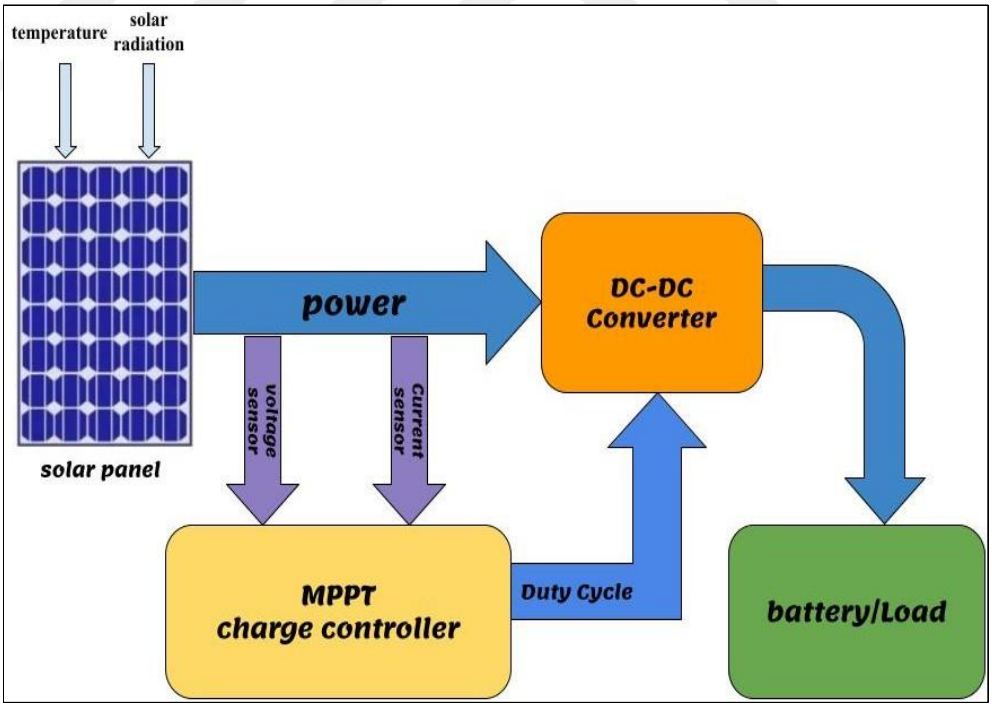

Figure 3.1 The basic photovoltaic conversion chain

The photovoltaic panel that we will study in this paper is 1Soltech 1STH-215-P (Nkambule *et al.* 2019). Where Table 3.1 shows the electric characteristics of the panel under the standard test conditions (STC), as it is the two most important factors affecting the work of the photovoltaic system are solar irradiation and temperature, whose values are in the standard test conditions, irradiation (irr = 1000 W/m^2) and temperature (tem= 25^{O}C) (Kabalci and Boyar 2020, Remoaldo and Jesus 2021). Where one cell connected in parallel and one in series will be used in this study as a model used in the simulation.

Table 3.1 Trina Solar 1Soltech 1STH-215-P Photovoltaic modules datasheet

Module Parameters	
Maximum Power (W)	213.15
Open Circuit Voltage (Voc)	36.3
The voltage at maximum power point (Vmpp)	29
Temperature coefficient of Voc(%/deg.C)	-0.36099
Cells per module (Ncell)	60
Short-circuit current Isc (A)	7.84
Current at maximum power point (Imp)	7.35
Temperature coefficient of Isc (%/deg.C)	0.102
Light-generated current IL(A)	7.8649
Diode Saturation Current Io (A)	2.9259e-10
Diode ideality factor	0.98117
Shunt resistance Rsh (ohms)	313.3991
Series resistance Rs (ohms)	0.39383

3.1.1 Photovoltaic system

Mathematical model and equivalent circuit for a PV cell: A photovoltaic module converts sunlight into electricity. To put it another way, when a PV module is exposed to solar radiation, it creates a direct current without causing any noise or pollution. Solar modules feature photovoltaic cells connected in series and/or parallel. These cells are essentially semiconductor diodes with a photosensitive p-n junction (Kamran *et al.* 2020, Senthilkumar *et al.* 2022). PV modules can be linked in series and/or parallel to create PV arrays.

Single-diode and two-diode models are two types of equivalent circuits often used to simulate a PV cell. Single diode, double diode, vulture, and other models are available.

There are a lot of equivalent circuits being created. In comparison to the single-diode equivalent circuit, the two-diode equivalent circuit has a more complicated structure and exhibits more nonlinear features. As a result, units with two diodes are rarely used. Because it produces realistic results, the single-cell circuit model is the most popular. The single-diode equivalent circuit model was chosen in this investigation (Mars *et al.* 2017, Eltamaly and Abdelaziz 2020).

The PV cell output voltage-current (V-I) characteristic is quite similar to the diode characteristic in the absence of sunshine. The electron mobility generated by photons falling on the panel creates an electric current when there is sunlight. This current completes the circuit through the external load when the PV panel is short-circuited. In the equivalent circuit model, when the circuit is open, it completes through the p-n combination diode (Raof 2020, Mars *et al.* 2017).

The photovoltaic cell is represented in the equivalent circuit shown in Figure 3.2 where the incident light flux is represented by the current source, the cell is polarized by the diode connected in parallel with the source, Parallel resistance for leakage current, while the connected resistance in series represents the losses due to the loss of the metal network, communications and bus current assembly. This circuit is a model of the photocell for easy mathematical representation (Syafaruddin *et al.* 2018).

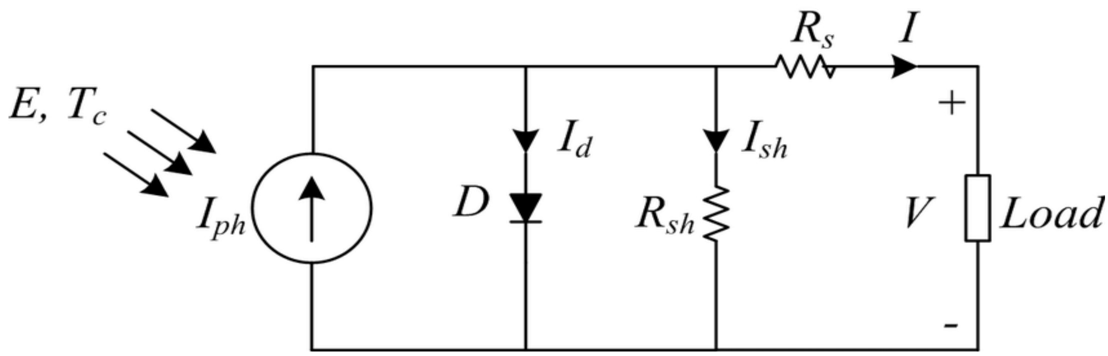

Figure 3.2 Equivalent circuit of a photovoltaic cell (Syafaruddin *et al.* 2018)

Furthermore, the mathematical expression is derived from the aforementioned circle. The single-diode equivalent circuit model was used to do the MPPT analysis of the solar panel system in this study. The equations that define the PV module model are as follows (Syafaruddin *et al.* 2018, Mars *et al.* 2017) Equation 3.1:

$$I = I_{ph} * N_p - I_d - I_{sh} \tag{3.1}$$

Where I_{ph} represents a photocurrent, I_d represents a diode current, and I_{sh} represents a shunt current. The module photo-current was rated as follows Equation 3.2:

$$I_{ph} = G_k\left[I_{sc} + K_I\left(T - T_{ref}\right)\right] \tag{3.2}$$

The equation for the shunt current is as follows Equation 3.3:

$$I_{sh} = \frac{V_{pv} + I_{pv} * R_s}{R_{sh}} \tag{3.3}$$

The equation for calculating the dark current I_d is as follows Equation 3.4:

$$I_d = I_s\left[\exp\left(q\ \frac{V_{pv} + R_s * I_{pv}}{N_s * V_t}\right) - 1\right] \tag{3.4}$$

The following equation describes how the reserved saturation current varies with temperature Equation 3.5:

$$I_s = I_{rs}\left(\frac{T}{T_{ref}}\right)^3 * e^{\left[\frac{qEg}{nk}\left(\frac{1}{T} - \frac{1}{T_{ref}}\right)\right]} \tag{3.5}$$

Finally, the total current can be calculated using the following formula Equation 3.6:

$$I = N_p * I_{ph} - N_p * I_s \left[exp\left(\frac{q*V_{pv}+R_s*I_{pv}}{N_s*V_t}\right) - 1\right] - N_p \frac{V_{pv}+I_{pv}*R_s}{R_{sh}} \quad (3.6)$$

The equivalent shunt resistance of a perfect PV cell is extremely high, whereas the analogous series resistance is extremely low (Simplification R_{sh} >>>R_s).

When the values of the resistors

R_s=0 R_{sh}=∞

The previous equation will become as follows Equation 3.7:

$$I = N_p * I_{ph} - N_p * I_s \left[exp\left(\frac{A*V_{pv}}{N_s*\text{n}}\right) - 1\right] \quad (3.7)$$

<u>Nomenclature</u>

V: PV cell output voltage [V].

I: PV cell output current [A].

N_s: The number of modules that are connected in a series.

N_p: The number of modules that are connected in parallel.

I_{ph}: Current generated by light in a PV cell [A].

I_s: Saturation current in PV cells [A].

R_s: The series resistance of a PV cell [Ω].

A: Ideality factor.

T: Cell temperature [Kelvin].

q: The electron charge constant (1.602x10-19 C)

T_{ref}: Reference temperature [Kelvin].

I_{sc}: PV cell short-circuits current at 25°c and 1000[w/m2].

R_{sh}: Shunt resistance of a PV cell [Ω].

Eg: The band gap for silicon [eV]

From the above last equation, we can notice that the output current of the photovoltaic cell mainly depends on the photovoltaic cell current produced by the beam falling on it, which depends on the solar irradiation and the junction temperature of the unit cells (Nasser *et al.* 2020). Thus, we can consider that the power of the photovoltaic cell depends on the radiation intensity and temperature, for this reason, the output characteristics of the photovoltaic system are always non-linear (Nasser *et al.* 2020, Syafaruddin *et al.* 2018).

PV panel manufacturers develop module values based on testing conducted at 25 degrees Celsius and a 1000 W/m2 irradiation intensity. These are referred to as standard testing conditions. Maximum power (Pmax), open-circuit voltage (Voc), short-circuit current (Isc), current at the maximum power point (Impp), and voltage at the maximum power point (Vmpp) can all be acquired from a PV panel under these conditions.

Curves of characteristics for PV systems: To obtain the highest efficiency of the photovoltaic cell, it is necessary to study and know its properties, which mainly depend on the intensity of solar radiation and temperature. Therefore the voltage-current (V-I) and power-voltage (P-V) characteristics must be specified to express changes under standard conditions at a temperature of 25^0C and radiation values of 1000 W/m^2.

All photovoltaic cell manufacturers adopt standard conditions when manufacturing them for the intensity of solar irradiation and temperature (tem= 25^0C and irr=1000 W/m^2) because it is difficult to predict the changing weather conditions and study their properties (Al-Majidi *et al.* 2018), so there is a technology that controls the work of the photovoltaic cell in such conditions. This technique is called Maximum Power Point Tracking (MPPT) (Zhang *et al.* 2021), which will be studied in detail in the next paragraph. This technology helps in obtaining the maximum power point (MPP) in the output regardless of changing weather conditions. This study will work on the photovoltaic cell type 1Soltech 1STH-215-P whose data sheet was mentioned in the previous paragraph (3.1). The characteristics of this cell will be determined under standard test conditions (STC) and variable conditions.

The characteristic curve inspection of the photovoltaic panel is based on standard test conditions (STC): Using the equivalent circuit model of a photovoltaic cell whose type and mathematical equations were mentioned earlier, and whose electrical specifications are given in Table 3.1, we can plot the characteristic curves of current-voltage (I-V) and power-voltage (P-V) according to standard test conditions (STC) using radiation intensity and temperature constant (tem = 25°C and irr = 1000 W/m^2) as shown in Figure 3.3, where a characteristic curve will be adopted to illustrate the most important points and then the curve is plotted using Matlab/Simulink for the same cell type previously selected to plot the electrical specifications (Syafaruddin *et al.* 2018).

One point at the top of the PV curve is called the maximum power point (MPP), which shows that the photovoltaic panel operates at maximum efficiency and produces the highest output power (P_{mpp}). This power is the product of the maximum current (I_{mpp}) and the maximum voltage (V_{mpp}) of the cell (Kumar *et al.* 2017).

But there is a problem that solar energy systems suffer from, the lack of stability of this point in light of changing environmental conditions Figure 3.3.

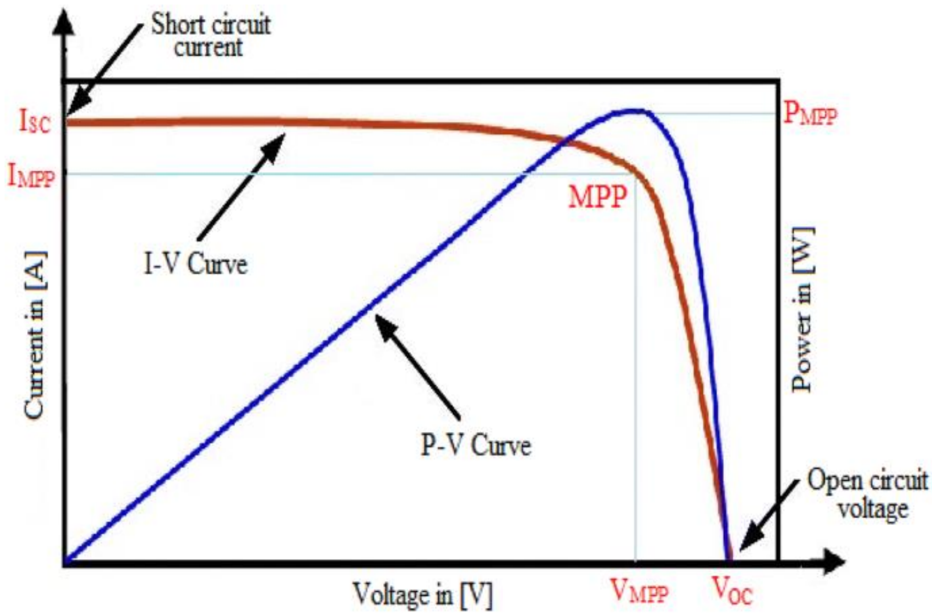

Figure 3.3 Diagram showing the characteristics of the PV module under (STC) (Mohamed and Abd El Sattar 2019)

Figure 3.4 shows the results of characteristic curves when simulating a photovoltaic panel representing the current-voltage (I-V) and power-voltage (P-V) curves using a 1Soltech 1STH-215-P solar cell that has been selected to work on in this thesis and which consists of one panel connected in series and one Connected in parallel, we can see that the simulation results are similar to the results of the electrical cells in the datasheet.

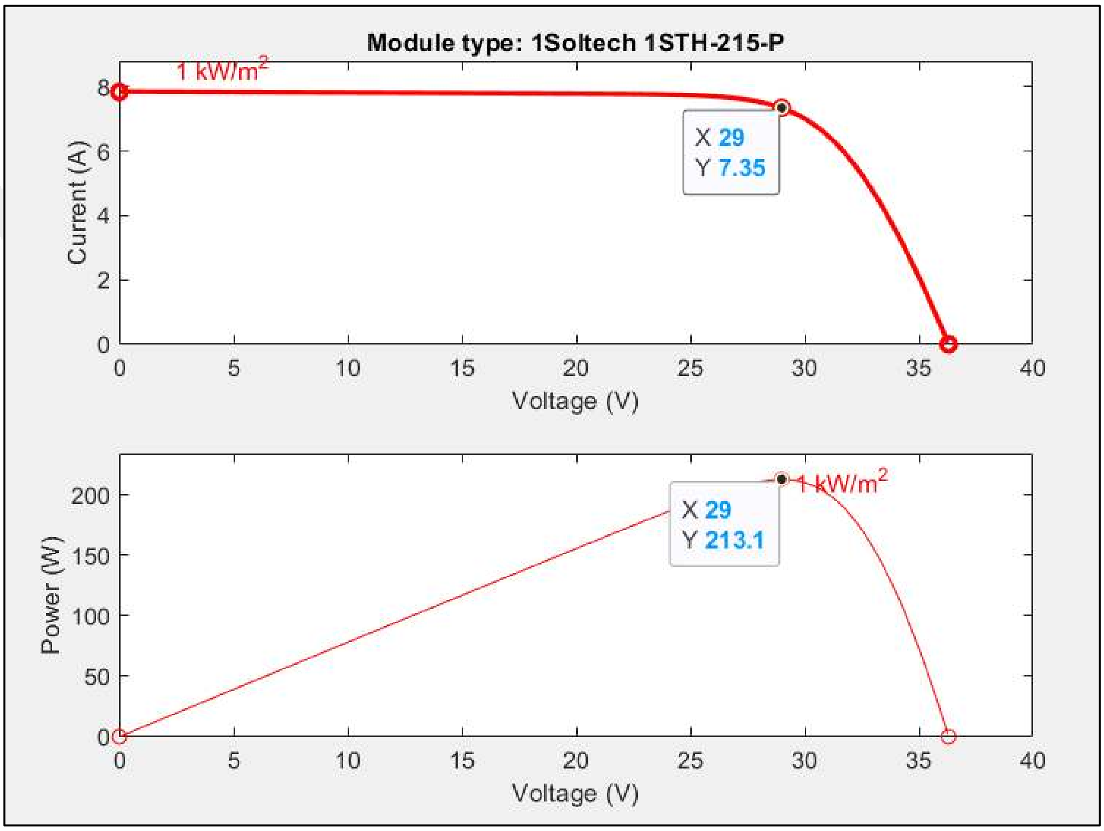

Figure 3.4 Under STC conditions, a PV module's I–V and P–V characteristics

Study of the characteristic curve of the photovoltaic panel when the temperature is constant and the intensity of solar radiation is variable: To obtain the highest efficiency of the photovoltaic system, the working stability of the system must be maintained at the maximum power point (MPP), but there is a problem that this point is not constant because the system performance is strongly affected by both irradiation intensity and temperature (Al-Ghezi *et al.* 2022). It can be seen how the MPP is affected by plotting the I-V and P-V characteristics curves of the photovoltaic cell when the temperature is constant(25°C) and radiation intensity is different (1000 W/m^2, 800 W/m^2, 600 W/m^2, 400 W/m^2) (Converter 2017), as shown in Figure 3.5 .

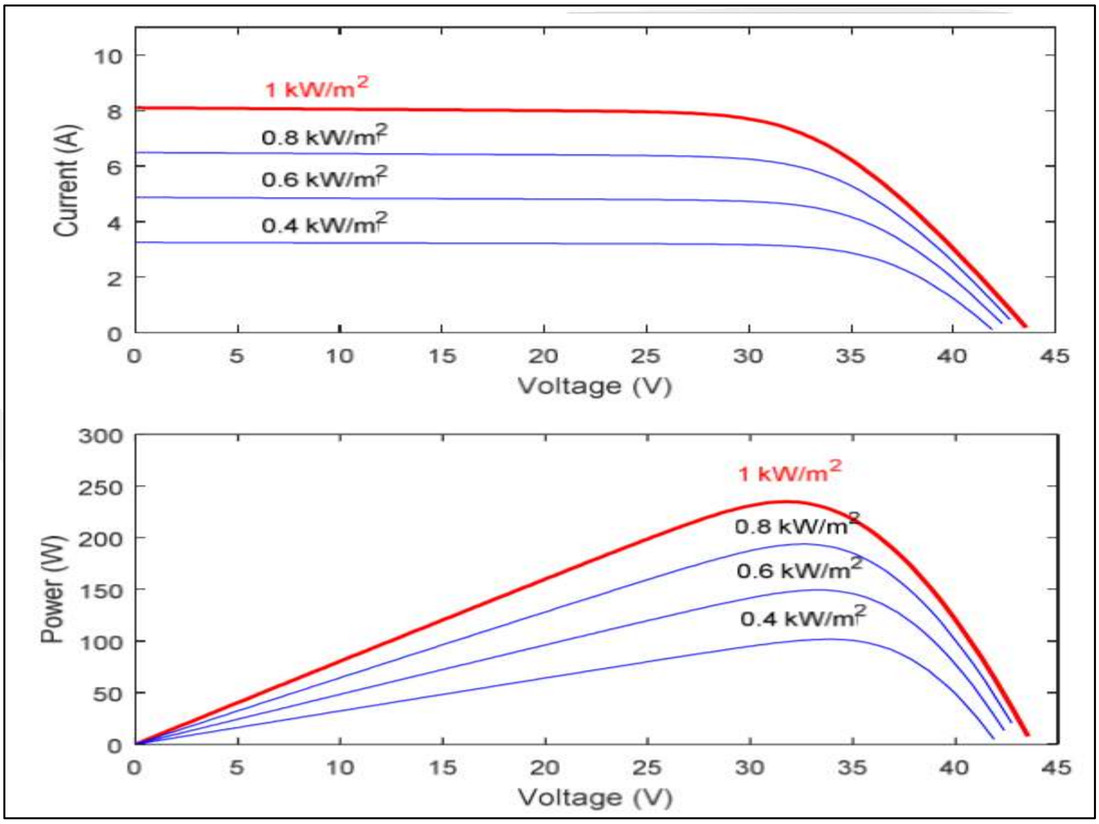

Figure 3.5 Characteristics curves (I-V & P-V) of PV panel under constant temperature and different irradiation

It can be seen from the results that the characteristics of the photovoltaic panel are not linear. The MPP varies according to the intensity of solar irradiation. The maximum energy point can be obtained when the irradiation intensity is the highest value (1000 W/m^2) and the energy point begins to decrease with the decrease in the intensity of irradiation (Rougab *et al.* 2021). The output current of the photovoltaic unit is greatly affected when the intensity of solar irradiation changes, it increases with the increase of irradiation, while the voltage remains almost constant (very little change).

Study of the characteristic curve of the photovoltaic panel when the temperature is variable and the intensity of solar irradiation is constant: In the previous paragraph (D) the effect of changing the irradiation intensity on the characteristics of the photovoltaic cell (I-V & P-V) was studied Figure 3.6.

In this paragraph, the radiation intensity will be constant (1000 W/m^2) and we change the temperature in values (55°C, 45°C, 35°C, 25°C) and study their effect on the characteristics of the photovoltaic panels as shown in Figure 3.6 (Chaibi *et al.* 2019, Al-Ghezi *et al.* 2022).

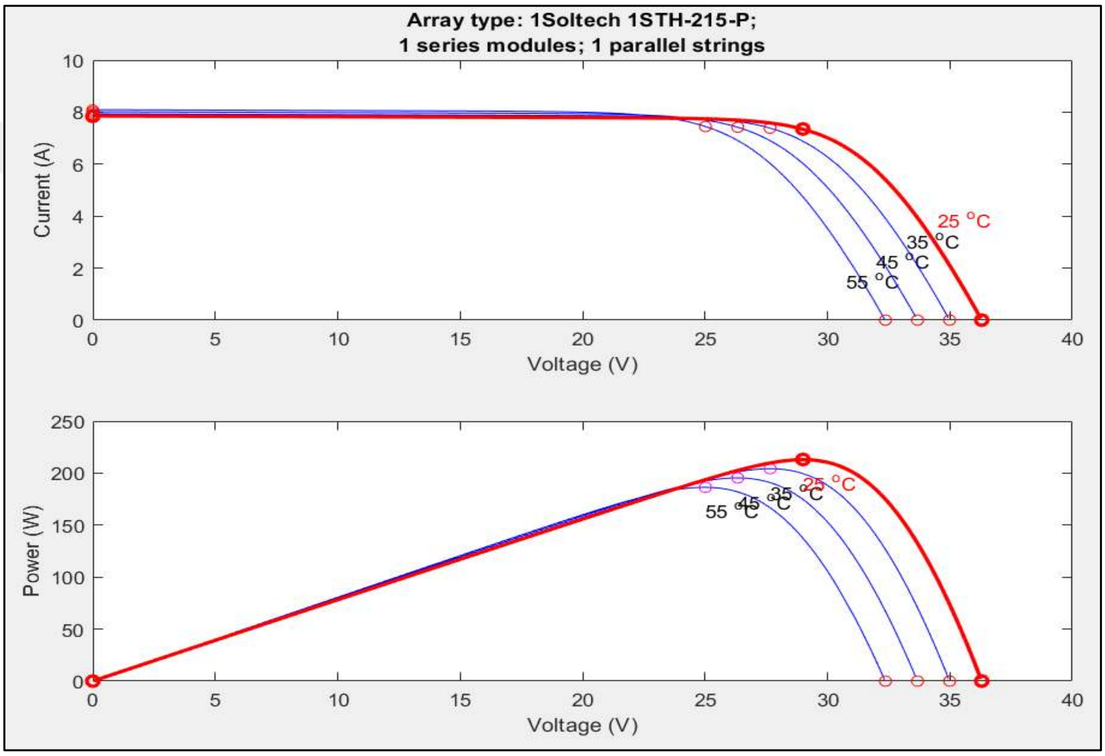

Figure 3.6 Characteristics curves (I-V & P-V) of the photovoltaic panel under variable temperature and constant irradiation

It can be seen from the results that the characteristics of the PV panel are not linear. As the MPP varies according to the temperature change, the maximum power point can be obtained when the temperature is the lowest and the energy point starts decreasing as the temperature increases. The output voltage of the PV module is greatly affected when the temperature changes, and increases with its decrease, while the current remains almost constant (very little change) (Al-Ghezi *et al.* 2022).

3.2 Solar Charge Controller

As we mentioned earlier, the maximum power point given by the solar panels is not fixed and is affected by changes in weather conditions such as radiation intensity and temperature, and the voltage and current leaving the cell are also not constant.

For this reason, it was necessary to find a technology that regulates the work of the photovoltaic cell and controls its output when the weather conditions are different. Therefore, a system was designed to track the maximum power point, regulate voltage and current, and perform impedance matching between the photovoltaic source and the load (Salman *et al.* 2018).

Therefore, this technology is considered a major part of the PV system, as its presence increases the efficiency of the system by 30% to 35% (Panchal *et al.* 2019, Ahmed and Salam 2017). It enables the system to work close to MPP and with maximum efficiency.

This technology is generally called a solar charge controller. The charge controller plays a vital role in ensuring that the battery is not overcharged or undercharged, that is, it ensures that the battery is charged efficiently.

Where they control how much energy is transferred from the solar panels to the battery bank. Overcharging is prevented via charge controllers, which reduces the danger of battery damage. When the batteries are fully charged, the charge controller should turn off the photovoltaic modules. The charge controller also avoids overvoltage, which can harm the battery's performance and shorten its life significantly. There are two types of charge controllers (Panchal *et al.* 2019, Victor *et al.* 2019).

3.2.1 PWM (pulse width modulation) charge controllers

The Pulse Width Modulation (PWM) charge controller is one of the most effective technologies for charging a constant voltage battery by adjusting the duty cycle of the switches (MOSFET) (Sepulveda *et al.* 2019).

In a PWM charge controller, the current flowing from the photovoltaic panel increases or decreases according to the battery's need for recharging. When the battery voltage reaches the desired level, the PWM algorithm slowly reduces the flow of charging current from the plates to avoid overheating of the battery and the release of gases (Yilmaz *et al.* 2022, Majaw *et al.* 2018).

PWM charging technology has many advantages such as maintaining the battery life for a long time, reducing the excessive temperature in the battery, and the stress on the battery is less.

PWM controller technology is not a DC-DC converter. The PWM controller is a switch that is connected to the photovoltaic panels on one side and the battery on the other. When the switch is closed, the board and the battery will be connected. The voltage will begin to flow from the plates to the battery, where the voltage will increase slowly as the battery state of charge increases. When the battery voltage reaches full, the PWM controller will start reducing the flow until the board is disconnected and reconnected to prevent overcharging (that's why it's called a PWM charge controller) (Majaw *et al.* 2018).

There are disadvantages in this type of charge controller, as it converts voltage from the solar cell to the battery as much as the battery needs over a long period, and the voltage of the battery’s need is lost, and this causes a decrease in the efficiency of the entire system, and it also takes a long time to charge the battery (Yilmaz *et al.* 2022, Majaw *et al.* 2018).

3.2.2 Maximum power point tracking (MPPT) charge controller

Since the output characteristics of the PV system are not linear and vary with different weather conditions (solar radiation intensity and temperature), to obtain the maximum MPP power point, it must be tracked and made constant under different conditions to increase the efficiency of the system. This is the reason behind the design of a charge-control technology called Maximum Power Point Tracking (MPPT) (Acharya and Aithal 2020).

One of the most advanced technologies is (MPPT) solar charge controller. This technology is more advanced and more expensive. It has many advantages over acharge controller (PWM). The application of MPPT technology increases the efficiency of the photovoltaic system by 20% to 40% under Standard Test Conditions (STC) and low temperatures (Szczepaniak *et al.* 2022).

The MPPT generates DC-DC converter control pulses to control its duty cycle. The higher voltage of the solar panels reduces the battery charging voltage or raises the lower voltage. It will control the input voltage to get the most power from the PV panels and then convert that power to meet the variable voltage needs of the battery as well as the load (Sepulveda *et al.* 2019).

MPPT charge controllers are several algorithms working in tandem with a DC-DC converter that can convert high voltage power to low voltage power (Majaw *et al.* 2018). Keeping the amount of power constant, therefore, if the output voltage is less than the input voltage, the output current will be higher than the input current to compensate for the difference, so that the power produced P = VI remains constant in all cases. Under specific conditions, MPPT charge controllers are applied to obtain the maximum power produced from the PV module so that the voltage in the PV module is capable of producing the maximum power called the "maximum PowerPoint". The maximum power point is affected by solar radiation and temperature. Therefore, Maximum Power Point Tracking (MPPT) technology is used to improve the efficiency of photovoltaic panels (Guran and Perișoară 2020).

The advantage of this technology (MPPT) is that it uses all the voltage produced by the photovoltaic cell as it takes the required voltage to charge the battery and converts the excess voltage into the current to increase the speed of the battery charging time. Therefore, this method is considered more efficient than PWM technology (Sepulveda *et al.* 2019, Majaw *et al.* 2018). Figure 3.7 shows the I-V characteristics of MPPT, while Figure 3.8 shows the difference between the two technologies (PWM) and (MPPT) in terms of production capacity and working area under the curve.

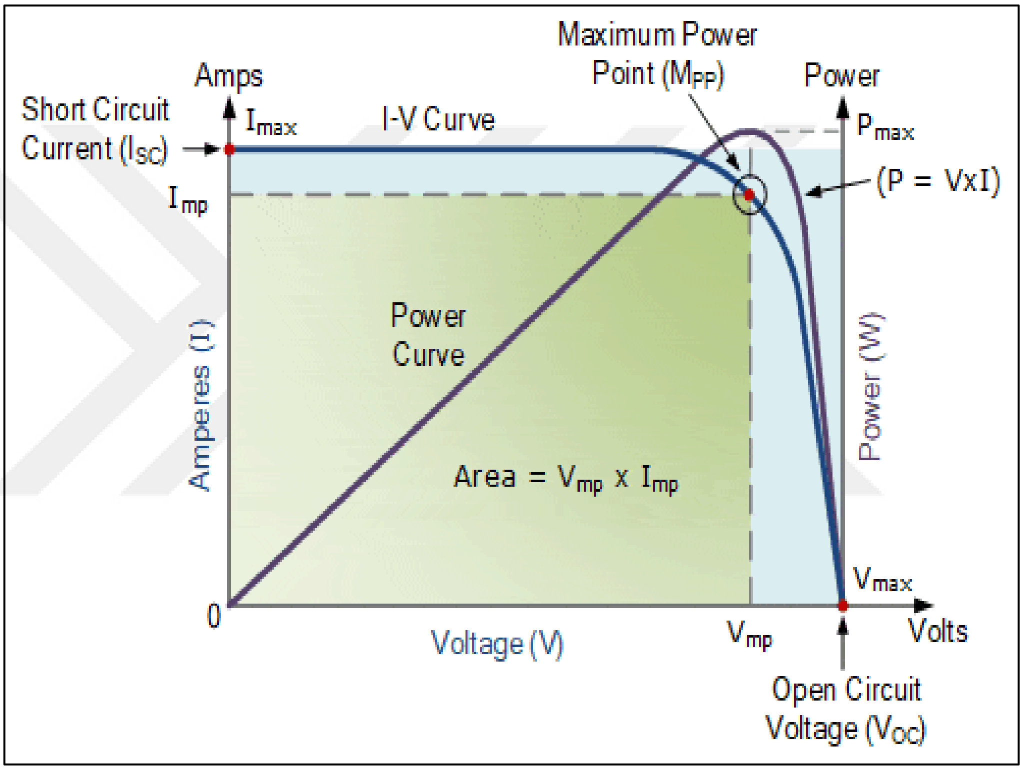

Figure 3.7 The I-V characteristics of MPPT (Anowar and Roy 2019)

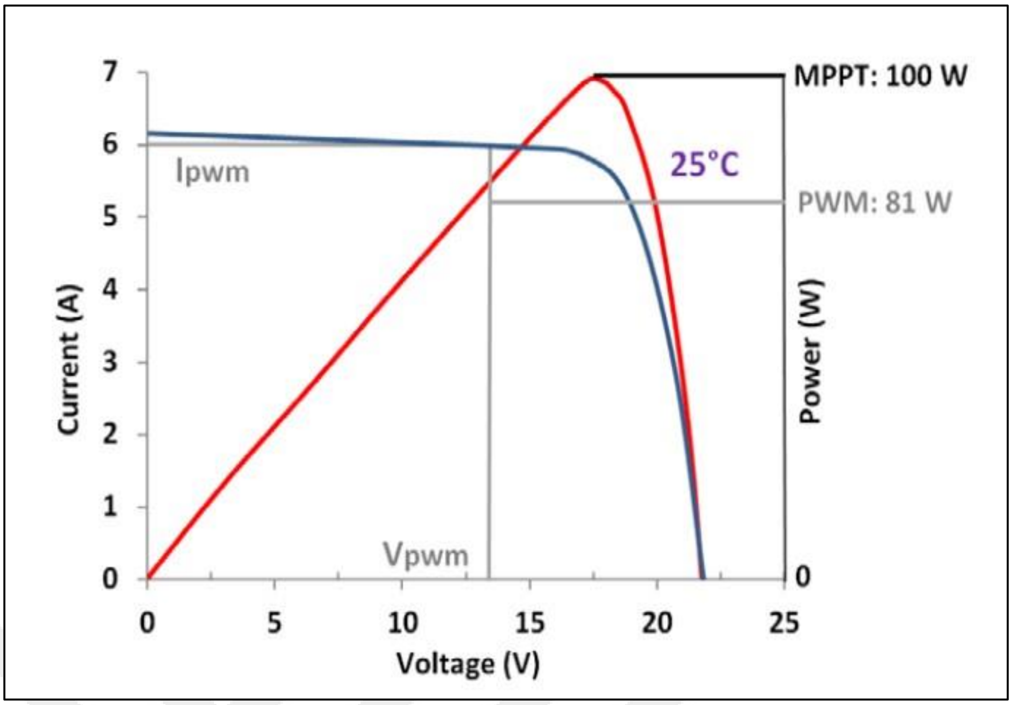

Figure 3.8 PV and I-V characteristics of MPPT& PWM (Majaw *et al.* 2018)

3.3 Maximum Power Point Tracking Algorithms

The use of MPPT technology based on several algorithms is necessary for PV applications because the maximum power point (MPP) of solar panels is not constant and is greatly affected by the change of radiation intensity and temperature applied to the solar cell, so the use of MPPT in PV systems is an indispensable part for tracking and Extracting the greatest energy from solar panels and regulating its flow to batteries (Farooqui *et al.* 2022).

Over the past years, researchers have developed, discovered, and published several MPPT methods for finding the maximum power point (MPP). The techniques used differ in many points such as the required current and voltage sensors, their effectiveness, their efficiency, the complexity of their form, their cost, the speed of convergence, the correct tracking when the irradiation intensity is variable, and/or the change in temperature, the devices needed for their installation and implementation, among others. A full review of a large number of different MPPT algorithms can be found in (Pilakkat *et al.* 2020, Ali *et al.* 2020, Mnati *et al.* 2019).

The maximum power point MPP and input and output values of solar panels can be monitored using MPPT technology and properly designed modeling calculations. The efficiency of solar energy tracking systems is directly related to the capabilities of the algorithm used. Thanks to these algorithms, the output of the system is ensured despite sudden changes in temperature and radiation (Farooqui *et al.* 2022, Bollipo *et al.* 2021). Several methods of theMPPT technique have been used in the literature. Figure 3.9 (Bollipo *et al.* 2020) lists the most popular algorithm strategies. It is classified into three main groups (traditional algorithms, artificial intelligence algorithms, and optimization algorithms) (Bollipo *et al.* 2021).

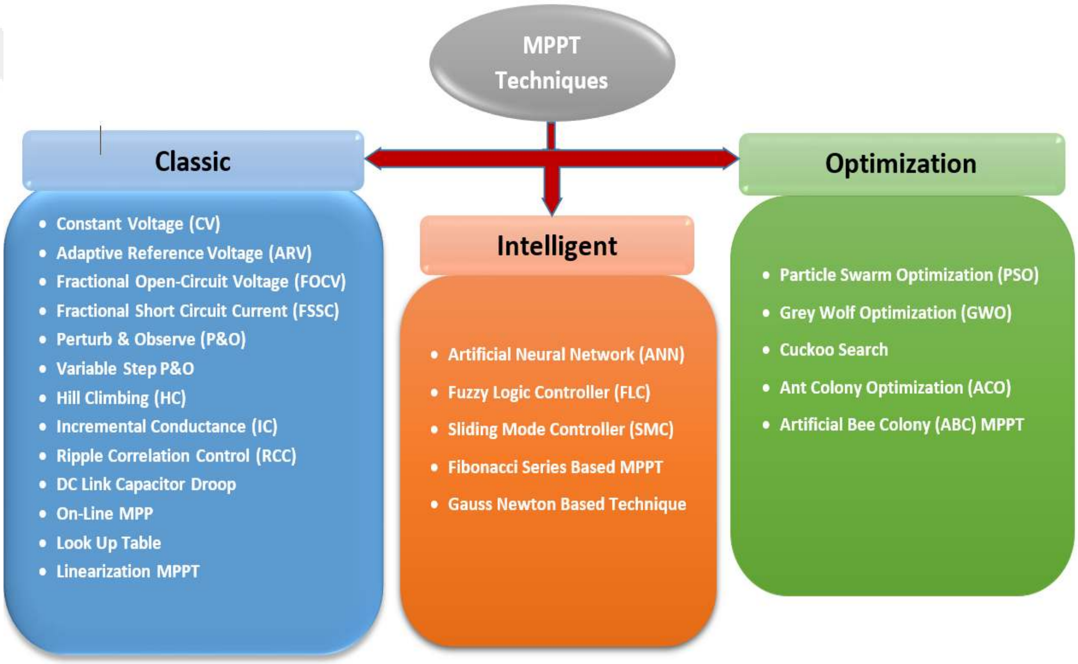

Figure 3.9 Classification of MPPT techniques

MPPT technology is connected with the photovoltaic panels through current and voltage sensors coming out of the panels. The algorithm based on the signal of the sensors generates control pulses to control the duty cycle of the DC-DC converter to supply constant power to the batteries or loads despite the change of weather conditions. Some of the most popular MPPT algorithms will be discussed in the next section (Abdellatif *et al.* 2021, Bollipo *et al.* 2021).

3.3.1 Perturb and observe (P&O)

The P&O algorithm is one of the most popular and widely used MPPT techniques due to its simplicity, ease of use, low costs, and simple results, especially under stable conditions (Ali *et al.* 2020, Mohamed Abdelwahab *et al.* 2020).

P&O operates by increasing the perturbation of the panel operating voltage regularly, allowing the power output to be recorded and compared during regular perturbation cycles. If the power difference is positive, more disturbance is added to the operating voltage in the same direction, and the output power is measured again. The perturbation process continues until the energy difference becomes negative. As a result, the disturbance direction of the operating voltage must be reversed (Junichi *et al.* 2003). The P&O method operates by increasing the voltage, which causes the power output to rise when the operating point is placed to the left of the MPP, as shown in Figure 3.10. When the operating point is to the right of the MPP, the P&O will reduce the voltage, increase the power output, and operate in the opposite direction (Kamran *et al.* 2020).

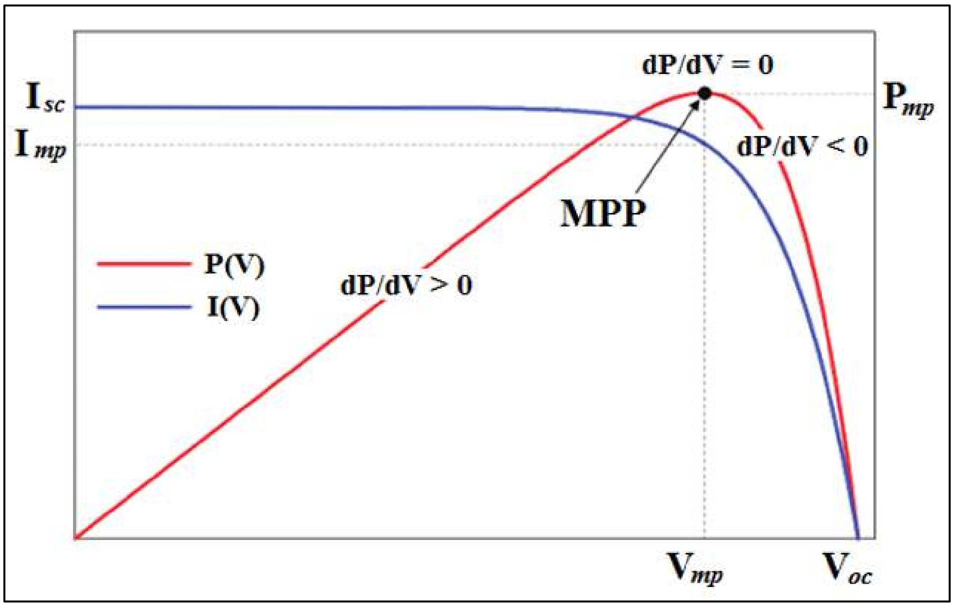

Figure 3.10 The Perturb and observe method's P-V curve (Mnati *et al.* 2019)

When the perturbation causes the power to increase by $\frac{dP}{dV} > 0$, it indicates that the operating point has been shifted towards MPP. Therefore the next perturbation must be kept in the same direction to bring the actuation point as close to MPP until MPP is reached. On the other hand, if the perturbation causes the energy to drop to $\frac{dP}{dV} < 0$, that is, the operating point has shifted away from the MPP, then the perturbation steps must be reversed in the opposite direction to correct this. The photovoltaic panel voltage is regulated by the P&O algorithm to obtain the corresponding voltage (VMPP) of the MPP. The MPP is monitored and updated periodically to ensure that the power slope equation $\frac{dP}{dV} = 0$ is met (Bollipo *et al.* 2021). The equations below show the mathematical relationships of a technique for the P&O algorithm (Elbarbary and Alranini 2021, Bollipo *et al.* 2020) Equation 3.8, Equation 3.9 and Equation 3.10.

- ❖ $\frac{dP}{dV} = 0$ at the MPP (3.8)

- ❖ $\frac{dP}{dV} > 0$ *at the* left side of MPP (3.9)

- ❖ $\frac{dP}{dV} < 0$ at the left side of MPP (3.10)

For measuring the plate operating voltage V and current I, the P&O algorithm uses only two sensors (Bollipo *et al.* 2020). Figure 3.11 shows a flowchart that explains the details of the P&O algorithm. As we can see, lowering the operating voltage reduces output power; therefore, the next essential action must be positive, i.e., raising the voltage.

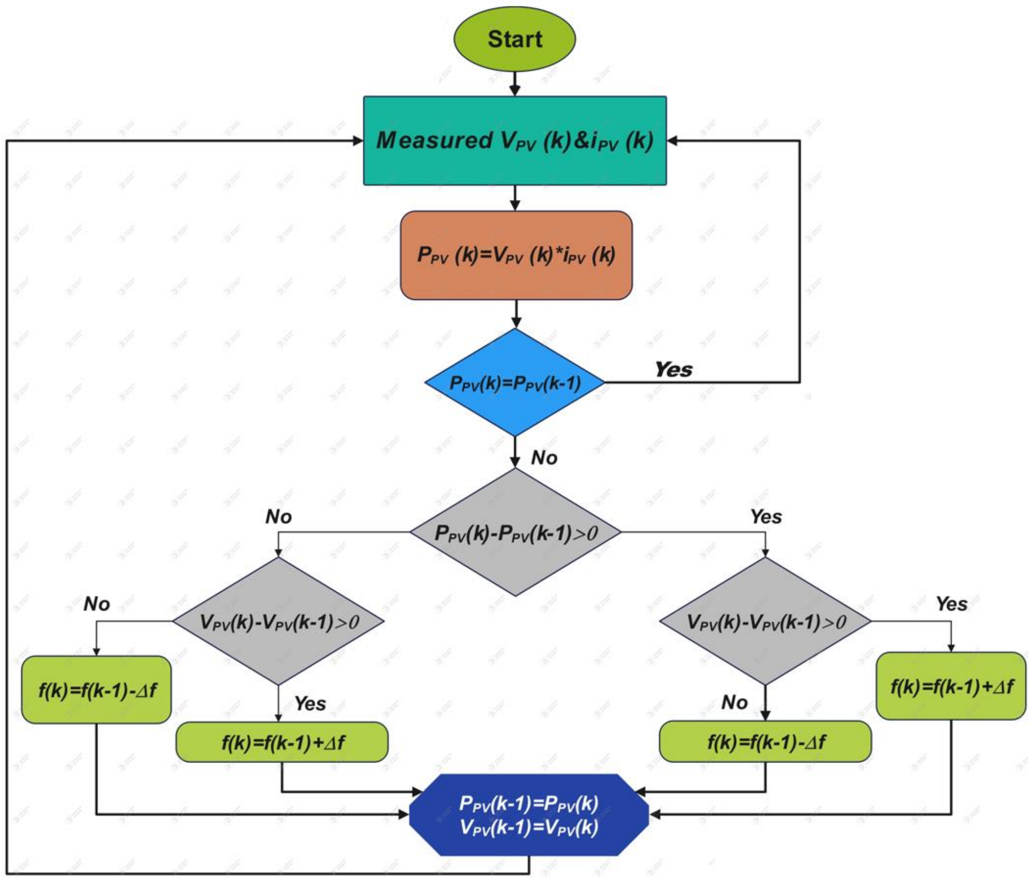

Figure 3.11 P&O algorithm flowchart

There are certain flaws in the P&O algorithm, such as slow response to rapid changes in weather conditions and searching in the wrong side of the maximum energy point during sudden shifts in conditions. The system is not fixed here when it reaches its maximum power point because it is always doing P&O. The system may constantly oscillate near the maximum power point, resulting in some energy loss in the system and a decrease in the efficiency of the PV system (Pilakkat *et al.* 2020).

3.3.2 Incremental conductance (IC)

The Incremental conductance (IC) algorithm is designed to address the shortcomings of the P&O algorithm while dealing with rapidly changing weather conditions (Necaibia *et al.* 2017, Dhaouadi *et al.* 2019).

The conductance $\frac{I}{V}$ and the incremental conductance $\frac{dI}{dV}$ are selected using voltage and current measurements so that the operating voltage can be increased or decreased depending on whether the operating point is to the left or right of the MPP. The IC algorithm's working principle is based on the fact that the photovoltaic power curve slope is negative to the right of MPP, zero at MPP, and positive to the left of MPP (Necaibia *et al.* 2017, Mohamed *et al.* 2020), as shown in Figure 3.12 and as proven by the mathematical equation below (Dhaouadi *et al.* 2019) Equation 3.11, Equation 3.12 and Equation 3.13.

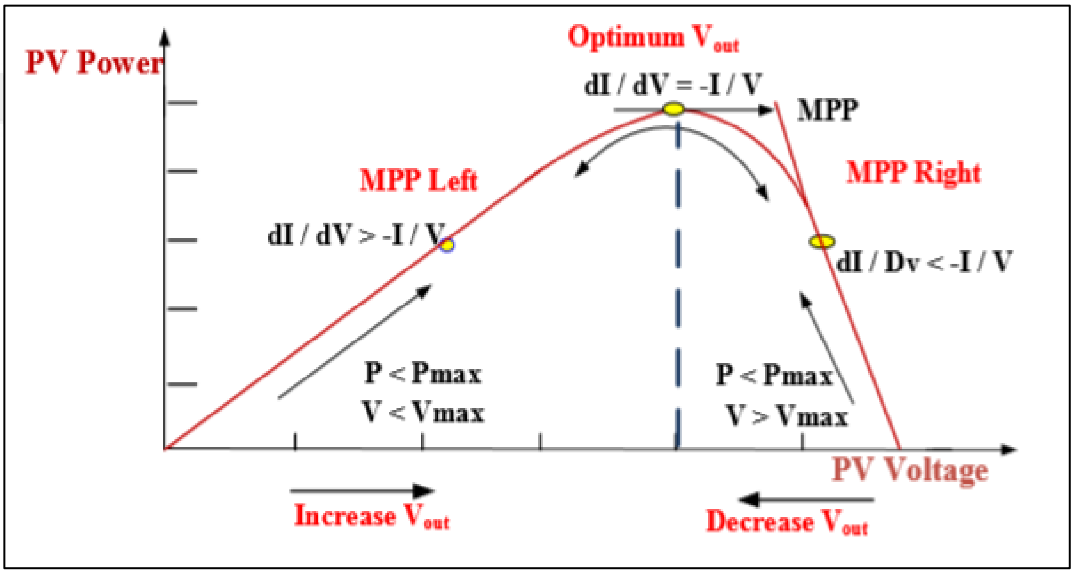

Figure 3.12 Incremental conductance algorithm P-V curve (Mohamed Abdelwahab *et al.* 2020)

$$\frac{dI}{dV} > -\frac{I}{V} \quad \text{left of MPP} \tag{3.11}$$

$$\frac{dI}{dV} = -\frac{I}{V} \quad \text{at MPP} \tag{3.12}$$

$$\frac{dI}{dV} < -\frac{I}{V} \quad \text{right of MPP} \tag{3.13}$$

Data sufficient to locate the MPP is provided by the incremental conductance (IC) technique. Making special measurements and comparisons of $\frac{dI}{dV}$ and $\frac{I}{V}$ make this possible. The MPP setpoint reference voltage at which the PV system must operate is V_{MPP} (Mohamed *et al.* 2020). Figure 3.13 the flow chart below illustrates the detailed working concept of (IC) algorithm (Kareem 2019).

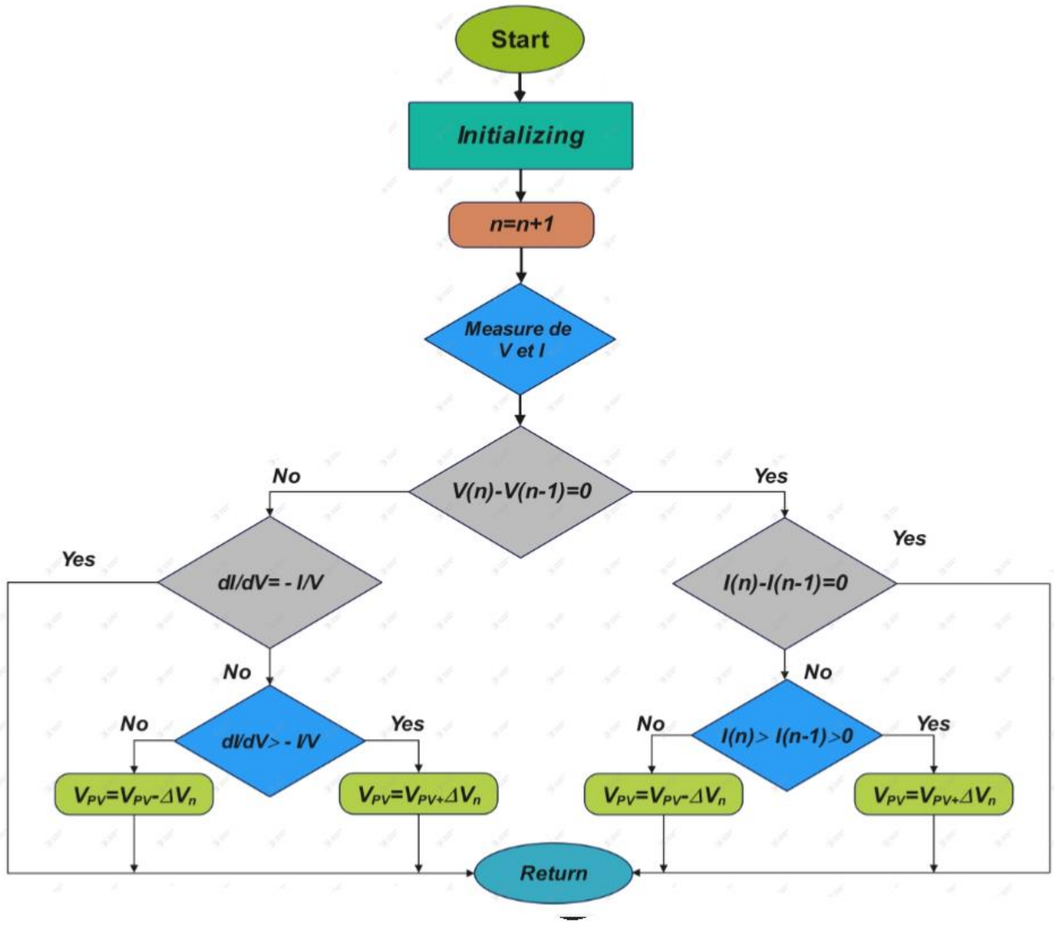

Figure 3.13 Incremental Conductance Algorithm Flow Chart.

According to the flow diagram of the IC algorithm shown in Figure 3.13, an evaluation test is carried out on one side after measuring voltage and current if the test difference on the side between voltage and current is respectively zero, and the contrast voltage is zero on the other side, a condition will be obtained Equilibrium $\frac{dI}{dV} + \frac{I}{V} = 0$ at MPP. If this condition is met, no changes will occur in the operation of the IC algorithm. If the equilibrium condition is not satisfied, the (IC) algorithm increases or decreases the voltage according to the amount of difference in current or the condition $\frac{dI}{dV} + \frac{I}{V}$ more or less at zero respectively (Necaibia *et al.* 2017, Kareem 2019).

In general, the IC algorithm is one of the most widely used MPPT techniques (Dhaouadi *et al.* 2019). However, until the MPP is achieved, the slope of the photovoltaic curve affects the duty cycle of the converter with fixed or variable step sizes in the (IC) algorithm. The time required to trace the MPP is reduced when the step size is larger, yet oscillation around the MPP is still present (Owusu-Nyarko *et al.* 2021). On the other hand, a small step size reduces the oscillation around MPP under extreme weather conditions more effectively, but it also slows down the tracking speed (Ali *et al.* 2020).

The disadvantages of this algorithm (IC) are mainly three. First, it can easily deviate from the MPP path if atmospheric conditions such as the intensity of solar radiation and temperature changes (Siddique *et al.* 2020, Azad *et al.* 2020) change. The second drawback that the two algorithms (IC and P&O) suffer from is the oscillations in voltage and current around the stationary state MPP point but in the (IC) algorithm this problem is addressed but at the expense of The MPP tracking speed is lower (Azad *et al.* 2020). The third problem is the complexity of the devices used in their application (Mnati *et al.* 2019).

3.3.3 Fuzzy logic control (FLC)

The PV panel parameters vary depending on the ambient conditions. To address these changing environmental circumstances, variable step sizes are employed to manage the increase in the duty ratio of the power converter (Bollipo *et al.* 2021, Bollipo *et al.* 2020) which is controlled by MPPT technology algorithms.

Application of MPPT technology based on fuzzy logic control (FLC) algorithm in solar systems with non-linear characteristics. As the FLC algorithm does not need to use complex mathematical models or system parameters. Therefore, FLC-based MPP point tracking and charge control technologies have become one of the most popular MPPT technologies due to this feature. Fuzzification, inference system and defuzzification are the primary components of Fuzzy Logic Controller (FLC) for MPPT Technologies (Alshareef 2021, Abdellatif *et al.* 2021). Figure 3.14 shows the most important parts of the fuzzy logic control (FLC) algorithm (Baramadeh *et al.* 2021).

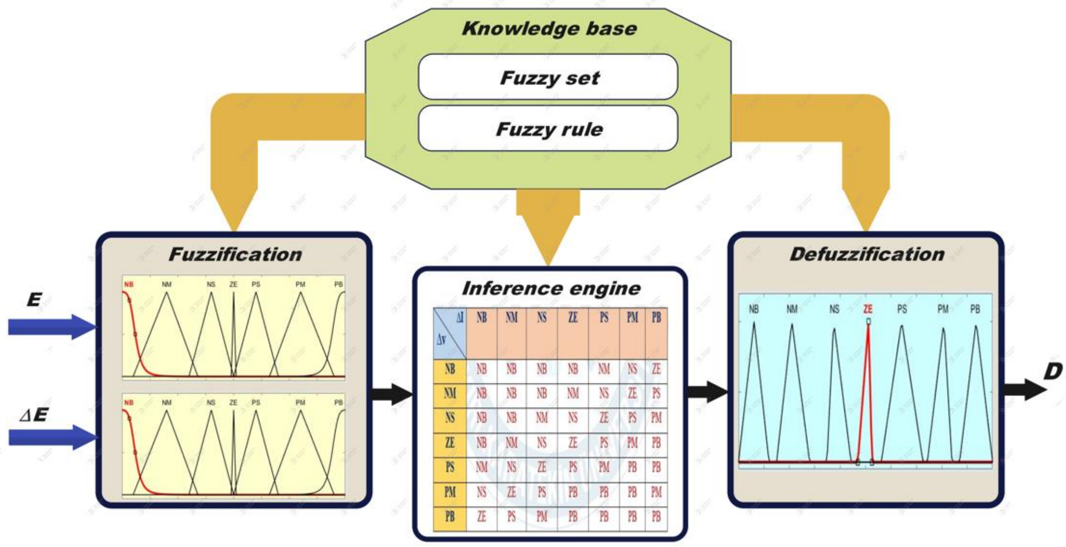

Figure 3.14 Illustrates the structure of an FLC.

The system's specified input and output variables have a direct impact on the performance of MPPT algorithms. Because of the soft calculation features of fuzzy logic, fuzzy logic systems achieve their maximum power point faster during load or under fluctuating atmospheric circumstances. After reaching the maximum power, Fuzzy Logic based on MPPT systems continues to operate without oscillation or at a low level. This system responds more quickly to changing environmental conditions (Aly and Rezk 2021), which allows it to quickly reach its maximum power point. As a result, the efficiency of the system that works with the FLC algorithm is superior to other traditional systems. MPPT technology based on the fuzzy logic control algorithm has several advantages over traditional P&O and IC algorithms (Abdellatif *et al.* 2021).

One of the types of artificial intelligence techniques and the most used in recent years is the fuzzy logic algorithm. Fuzzy logic is based on the idea that human decision-making is not just a matter of "ones and zeros" or "yes-no". IF-THEN rules (Junichi *et* *al.* 2003), or ambiguous control rules. The fundamental constituents of fuzzy logic are fuzzy sets. Fuzzy sets are represented by membership functions. This strategy employs fuzzy numbers as membership functions (Abdellatif *et al.* 2021, Ali *et al.* 2021). Figure 3.15 shows a comparison of Boolean logic and fuzzy logic.

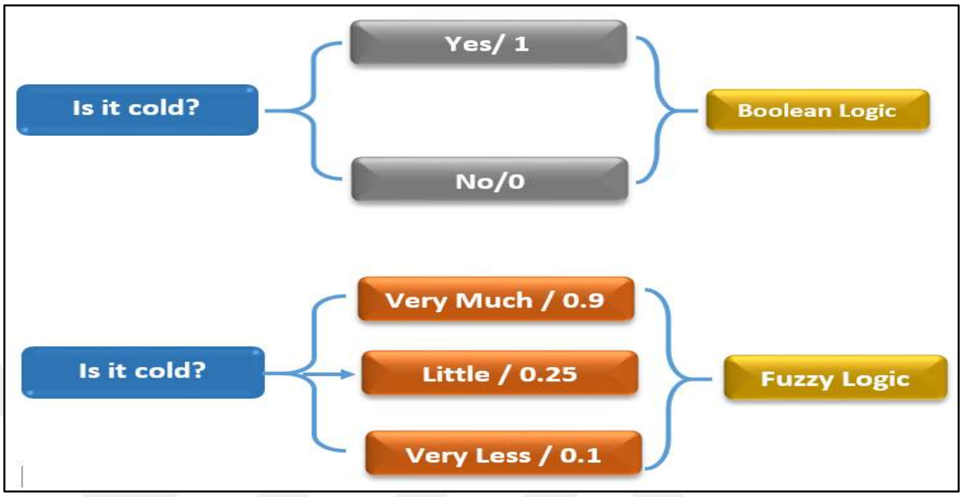

Figure 3.15 Illustrates the differences between Boolean and fuzzy logic.

Membership functions are used to represent a fuzzy set. Membership functions should be defined as continuous functions since the object's space frequently contains real values (Junichi *et al.* 2003). Figure 3.16 depicts the most commonly used membership functions.

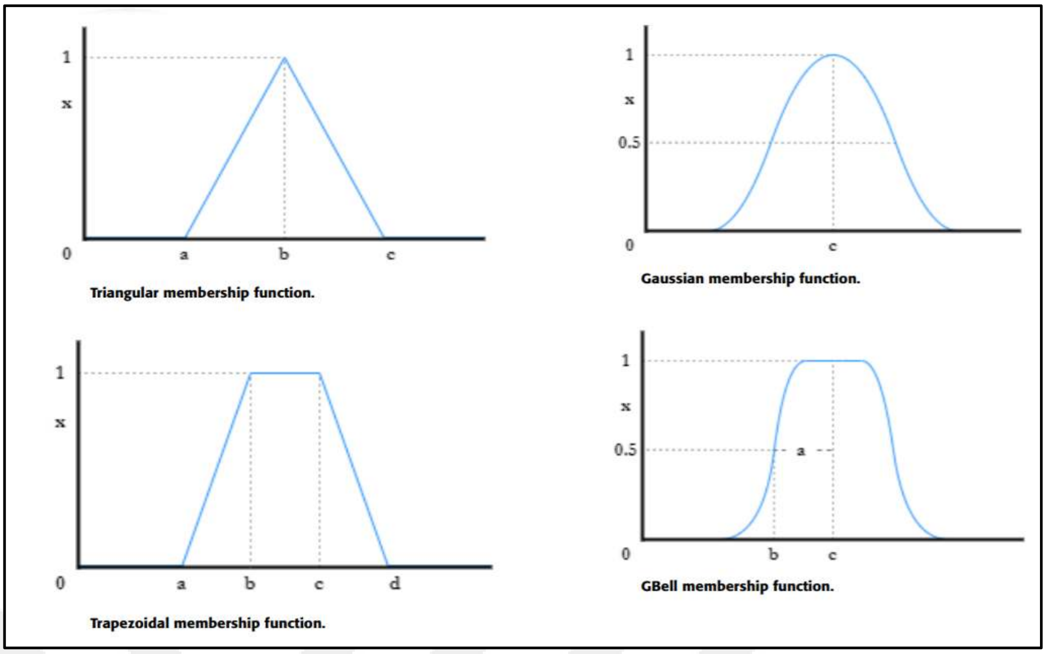

Figure 3.16 Different types of Fuzzy Membership Functions (Sutikno *et al.* 2021).

The appropriate membership functions are selected according to the designer's skills. The following describes the mathematical equations for each membership function (Sutikno *et al.* 2021, Junichi *et al.* 2003).

The triangular curve is the meeting of two straight lines at an angle, and it is defined by three coefficients (a, b, c). The x-coordinates of the three angles of the trigonometric membership function are given by the parameter (a, b, c) with a < b < c (Sutikno *et al.* 2021, Junichi *et al.* 2003) Equation 3.14.

$$\text{triangle}(x; a, b, c) = \begin{cases} 0 \quad for \;\; x \leq a \\ \frac{x-a}{b-a} \quad for \; a \leq x \leq b \\ \frac{c-x}{c-b} \quad for \; b \leq x \leq c \\ 0 \quad for \; x \geq c \end{cases} \tag{3.14}$$

The shape of a Trapezoidal curve resembles that of a Triangular curve, however, it has a membership value of 1 at multiple locations. The Trapezoidal membership function differs from the Triangular in that it has a flat top and is hence not fuzzy. The four parameters that make up the trapezoidal membership function are: (a,b,c,d) *(Sutikno et al.* 2021,Junichi *et al.* 2003) Equation 3.15.

$$\text{trapezoid}(x; a, b, c, d) = \begin{cases} 0 \quad for\ x \le a \\ \frac{x-a}{b-a} \ \ for\ a \le x \le b \\ 1\ for\ b \le x \le c \\ \frac{d-x}{d-c} \ \ for\ c \le x \le d \\ 0 \ \ for\ x \ge d \end{cases} \tag{3.15}$$

The Gaussian membership function has a smooth peak, unlike the Triangular membership function, which has a sharp peak (Sutikno *et al.* 2021, Junichi *et al.* 2003) Equation 3.16.

$$gauss(x; \sigma, c) = e^{\frac{-(x-c)^2}{2\sigma^2}} \tag{3.16}$$

In probability theory, the GBell membership function is a generalized Cauchy distribution (Sutikno *et al.* 2021, Junichi *et al.* 2003) Equation 3.17.

$$bell(x; a, b, c) = \frac{1}{1+\left|\frac{x-c}{a}\right|^{2m}} \tag{3.17}$$

To assign a grade to each linguistic phrase, membership functions such as those shown in Figure 3.16 are used. The number of membership functions utilized varies depending on the controller's precision, although it is normally between 5 and 7 (Salleh *et al.* 2017, Ali *et al.* 2021). NB (Negative Big), NM (Negative Medium), NS (Negative Small), ZE (Zero), PS (Positive Small), PM (Positive Medium), and PB (Positive Big) are the seven fuzzy levels in Figure 3.17. The values a, b, and c are based on the numerical variable's range of values. For improved accuracy, the membership functions are sometimes chosen less symmetrically or even optimized for the application (Asif *et al.* 2020).

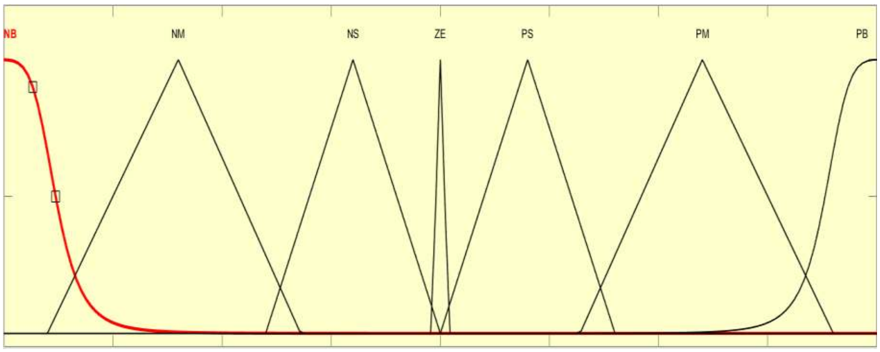

Figure 3.17 Fuzzy Membership Function.

Fuzzification: is possible to pass from real to fuzzy variables using fuzzification. The power (P = V×I) of a PV generator may be estimated by continually measuring the voltage (V) and current (I). At a sampling instant k, the control is defined by satisfying two requirements relating to two input variables of the proposed controller, namely error E (which represents the slope of the P-I characteristic) and change of this error (CE) (Baramadeh *et al.* 2021). The following is how the variables E and CE are expressed (Asif *et al.* 2020) Equation 3.18 and Equation 3.19:

$$E(k) = \frac{P(k)-P(k-1)}{I(k)-I(k-1)} \tag{3.18}$$

$$CE(k) = E(k) - E(k-1) \tag{3.19}$$

The PV generator's power and current, respectively, are $P(k)$ and $I(k)$. As a result, the input $E(k)$ indicates whether the operating point at time k is on the left or right of the MPP on the P-I characteristic, whereas the input $CE(k)$ indicates the point's displacement direction. As the suggested controller's output, the change in duty ratio (ΔD) of the DC-DC converter is used (Kabalci and Boyar 2020, Baramadeh *et al.* 2021).

Fuzzy Rule base and inference engine: In the fuzzy logic controller, the inference phase is one of the most important operations. People's ability to infer and make decisions is the driving force of this section. The fuzzy rule base and fuzzy implication sub-blocks make up the bulk of the inference engine. The inputs are now fuzzified and given to the inference engine, which applies the rule base. Four different inference strategies are commonly employed during the extraction procedure (Abdellatif *et al.* 2021). Max-Dot, Min-Max, Tsukamoto, and Takagi- Sugeno are some of the inference techniques that are used. In this study, the Mamdani method is used, which is similar to the max-min method. The rule base is used to generate several If-Then rule(Junichi *et al.* 2003, Boutabba *et al.* 2018). Inputs and outputs are addressed on the If and then sides of the rule, respectively. You have the option of choosing between and/or connections.

The number of rules is proportional to the number of input membership functions that are employed. Each input contains seven membership functions in this study, resulting in 49 rules as indicated in Table 3.2.

Table 3.2 Fuzzy logic rules.

ΔI / Δv	NB	NM	NS	ZE	PS	PM	PB
NB	NB	NB	NB	NB	NM	NS	ZE
NM	NB	NB	NB	NM	NS	ZE	PS
NS	NB	NB	NM	NS	ZE	PS	PM
ZE	NB	NM	NS	ZE	PS	PM	PB
PS	NM	NS	ZE	PS	PM	PB	PB
PM	NS	ZE	PS	PB	PB	PB	PM
PB	ZE	PS	PM	PB	PB	PB	PB

Defuzzification: the inference methods, it was discovered, give a function for the resulting membership variable, which acts as fuzzy information. Given that the DC-DC converter requires a precise control signal D at its entry, it is required to consider transforming this fuzzy data into deterministic data, known as defuzzification. Defuzzification is generally accomplished using two algorithms: the Center of Area (COA) and the Max Criterion Method (MCM). The identification of the final combined fuzzy set's center of gravity (COA) is the most commonly utilized defuzzification approach (Boutabba *et al.* 2018, Baramadeh *et al.* 2021).

Using the maximum aggregation approach, the final combined fuzzy set is defined as the union of all rule output fuzzy sets. The center of gravity (ΔD) is computed point-wise for a sampled-data representation by (Baramadeh *et al.* 2021) Equation 3.20:

$$\Delta D = \frac{\sum_{j=1}^{n} \mu(\Delta D j).\Delta D j}{\sum_{j=1}^{n} \mu(\Delta D j)} \tag{3.20}$$

After defuzzifying by Equation (3.20) and measured by $S_{\Delta D}$ gain, the output of the ambiguous controller, change of work ratio$\Delta D(k)$, is converted to actual duty ratio $D(k)$ by (Kabalci and Boyar 2020, alshareef 2021) Equation 3.21:

$$D(k) = D(k-1) + S_{\Delta D}.\Delta D(k) \tag{3.21}$$

The fuzzy logic control (FLC) output, the duty ratio, is used to control the MOSFET switches on the DC-DC converters using the PWM generated by the FLC to control it and control a coin based on the output parameters of the photocell (Baramadeh *et al.* 2021).

Software for Matlab's fuzzy logic toolbox: The Matlab fuzzy logic toolbox allows users to create and edit fuzzy inference systems. These systems also make use of graphical tools as well as command-line functionalities. Users of the Simulink software can use a block diagram to create and simulate their fuzzy systems. To develop, update and display fuzzy inference systems, the graphical tools are used Fuzzy Logic Designer the fis file is imported and the created system is monitored. Membership Function Editor, Rules Editor, Rules Viewer, and Surface Viewer are described in detail in Figure 3.18 (Naderpour *et al.* 2017, Mala *et al.* 2019).

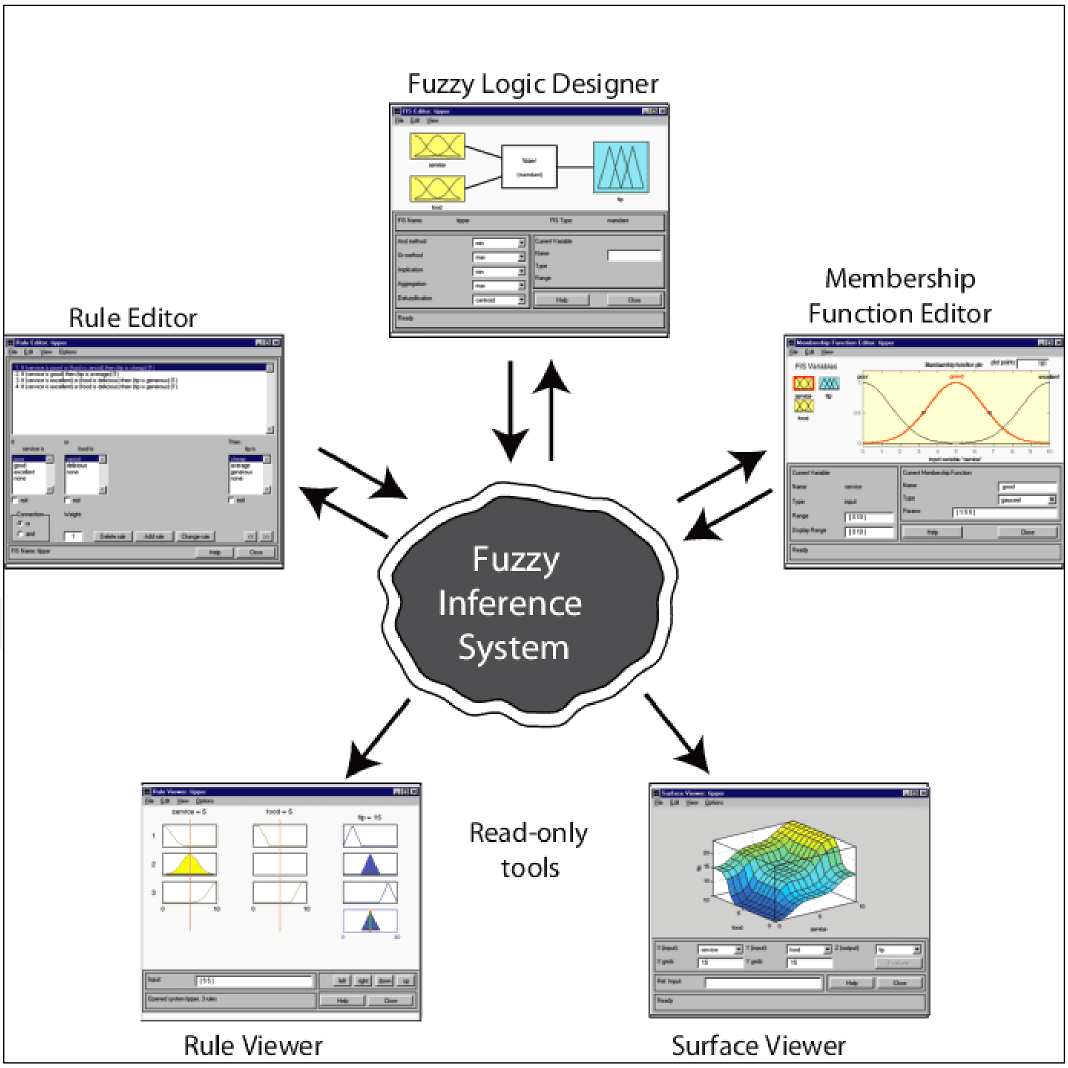

Figure 3.18 Fuzzy Logic Toolbox (Mala *et al.* 2019).

The editor for the membership function: Users can edit membership functions in the membership function editor. Here you can set the input and output numbers. Membership function simulation model in Figure 3.19 (The mathworks inc 2019).

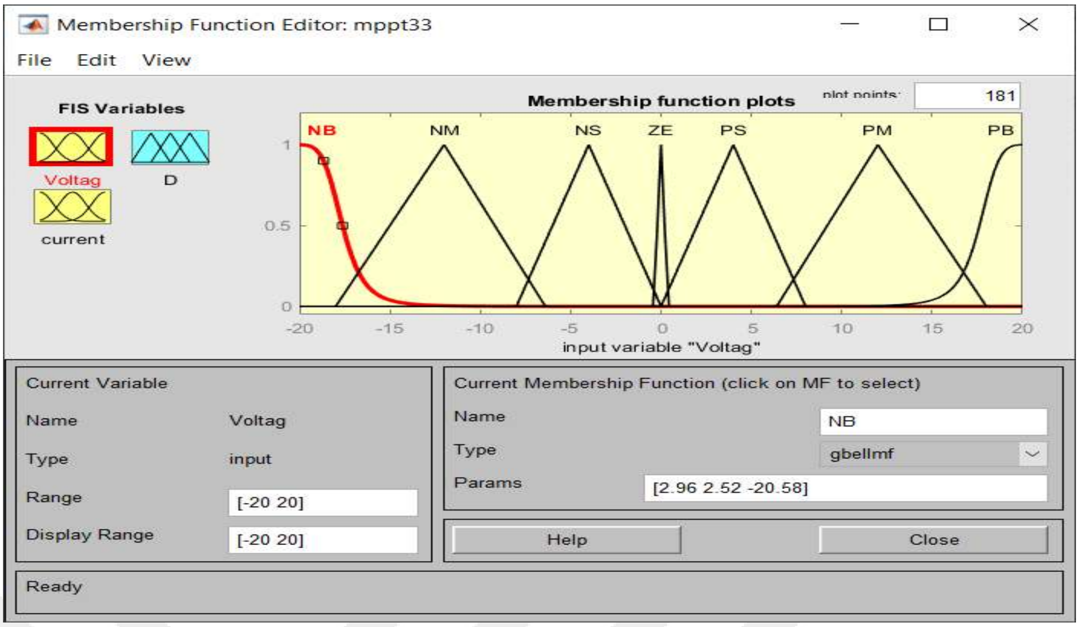

Figure 3.19 Editor's interface for membership functions.

The rule editor in the fuzzy logic controller: The rules between the input and output values are designed by the designers in this window shown in Figure 3.20. The convergence we achieve at the output improves as the number of rules used increases. The order in which the rules will be created is determined (Junichi *et al.* 2003).

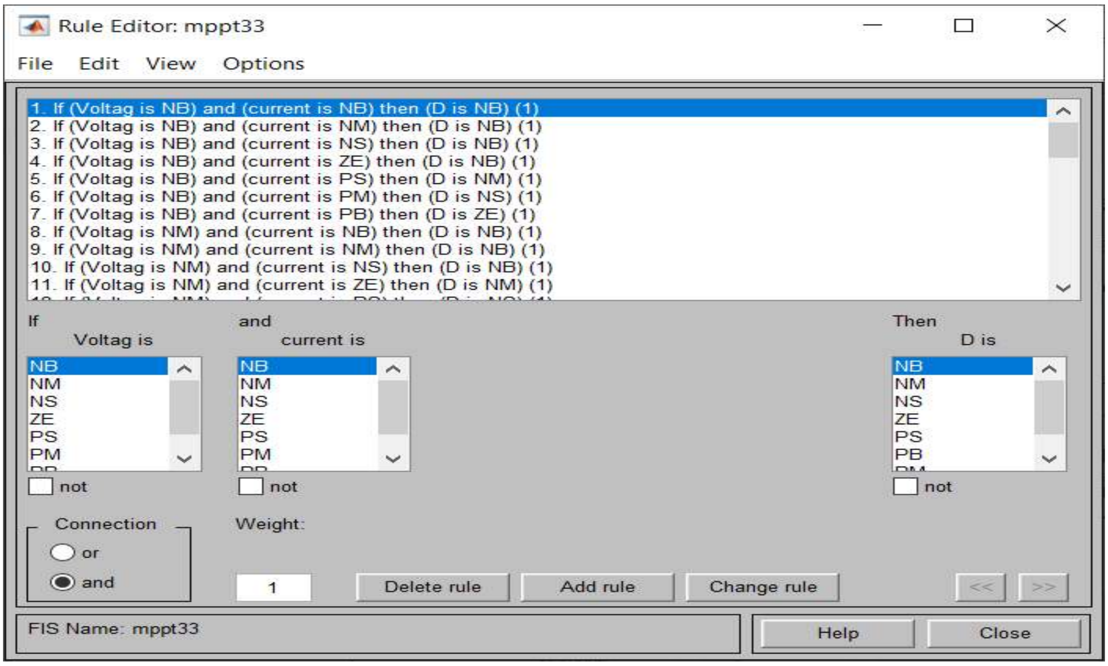

Figure 3.20 Rules Editor Interface.

The rule viewer in the fuzzy logic controller: The rule viewer displays the relationship between the fuzzy inference's inputs and outputs as shown in Figure 3.21. Columns and rows, as well as variables, are used to represent rules. Users can shift the red line and change the value of the input variables by clicking on the rule. It's also possible to look at how the output variable changes at the same time (Junichi *et al.* 2003).

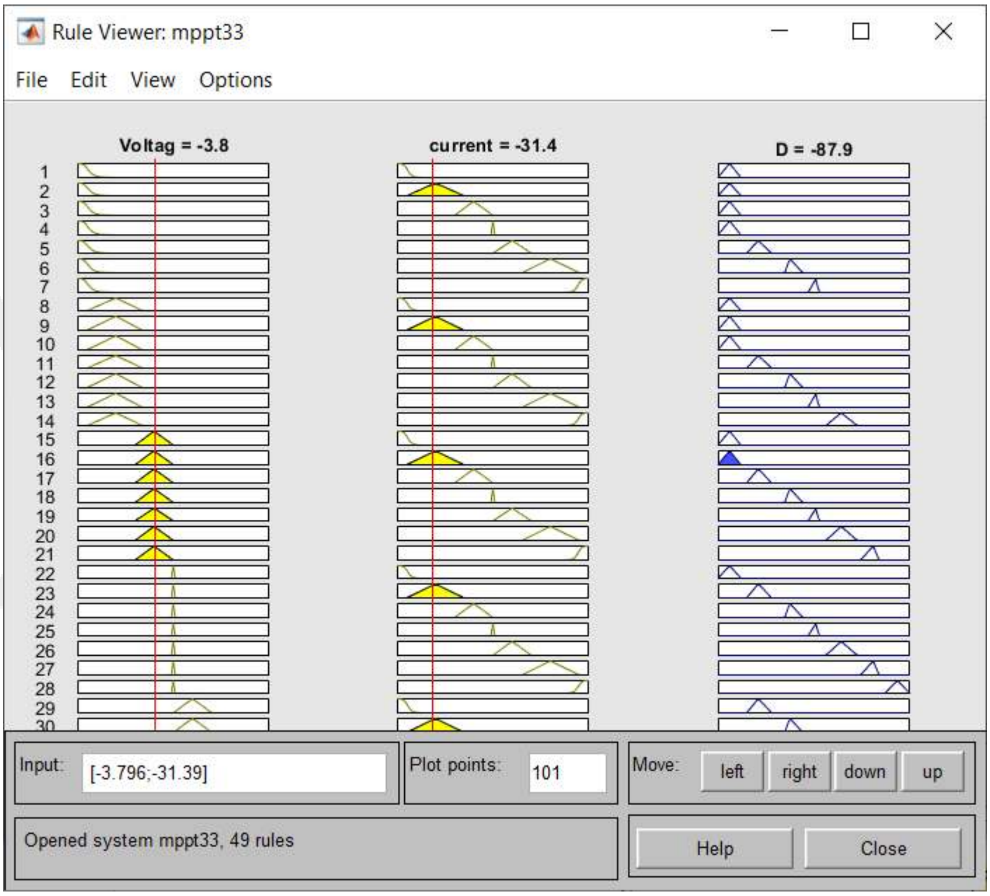

Figure 3.21 Rules Viewer Interface.

Surface view of fuzzy: A three-dimensional display is available, with the ability to explore the x, y, and z directions as needed and Figure 3.22 illustrates this.

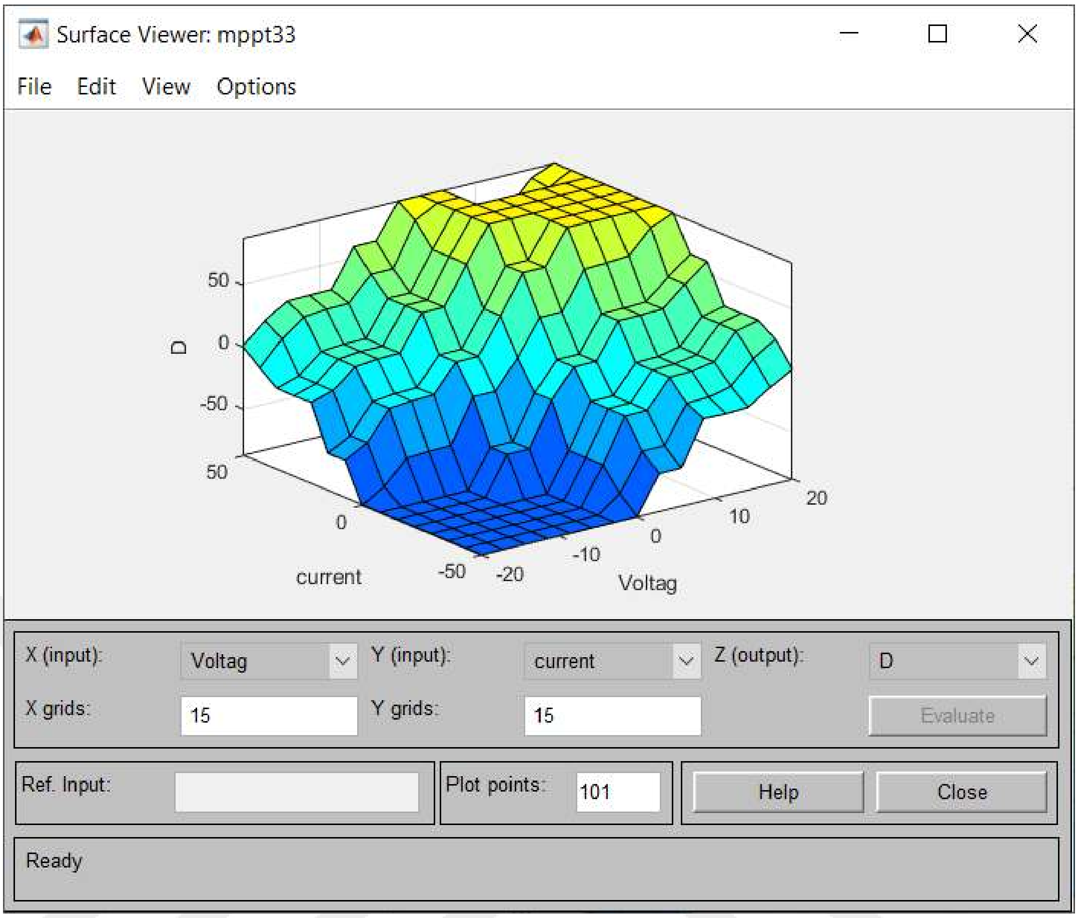

Figure 3.22 Fuzzy input versus output functions from the surface.

3.3.4 Artificial neural network (ANN)

In addition to the fuzzy logic control (FLC) algorithm, a new algorithm appeared next to it called the neural network algorithm (Kota and Bhukya 2019), which is more suitable in microcontroller applications, as it is another method of MPPT algorithms. The basic architecture of this algorithm is generally made of three main layers which are the input layers (Eltamaly and Abdelaziz 2020), the hidden layer, and the output layer which are the most common layers in neural networks, as shown in Figure 3.23 (Jyothy and Sindhu 2018).

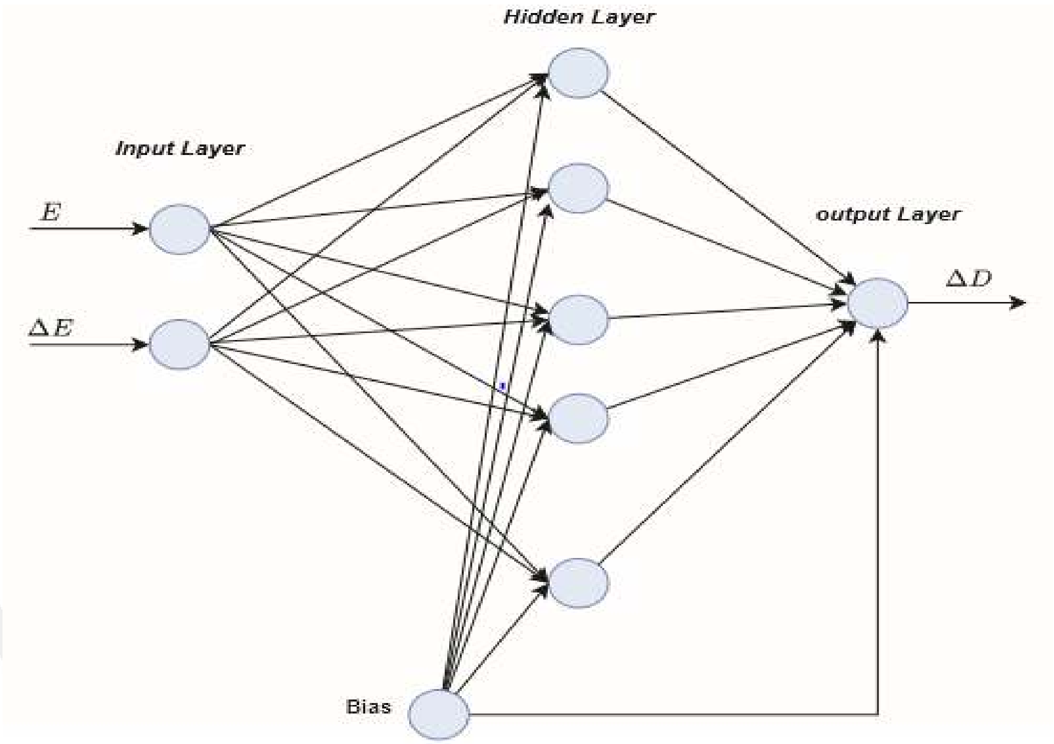

Figure 3.23 The MPPT ANN architecture (Ali *et al.* 2021).

The nodes used in each layer will be different depending on the design of the user. The input variables can be the parameters of the PV system such as the open-circuit voltage (VOC) and the short circuit current (I_{SC}), or it can represent the data of the atmosphere surrounding the photovoltaic system such as the intensity of solar radiation and temperature, or any variables related to the solar panels. The output is often one or more reference signals, such as a duty cycle signal, which are used to drive the transducer to run at or near the MPP (Jyothy and Sindhu 2018, Kota and Bhukya 2019).

The functions that the hidden layer uses are very important as the performance of the neural network depends mainly on it and how well the neural network is trained. The weights of all links between nodes are estimated. In Figure 3.23, wij represents the weight between the nodes i and j. During the training process of the neural network, the weights are modified. About the patterns between the input and output of the neural network, data is collected over a long period, to implement the training process, allowing to track the maximum power point (MPP) reliably (Farooqui *et al.* 2022, Jyothy and Sindhu 2018).

The approach of the ANN for the MPPT training process is depicted in a flowchart, as illustrated in Figure 3.24 (Nour 2019).

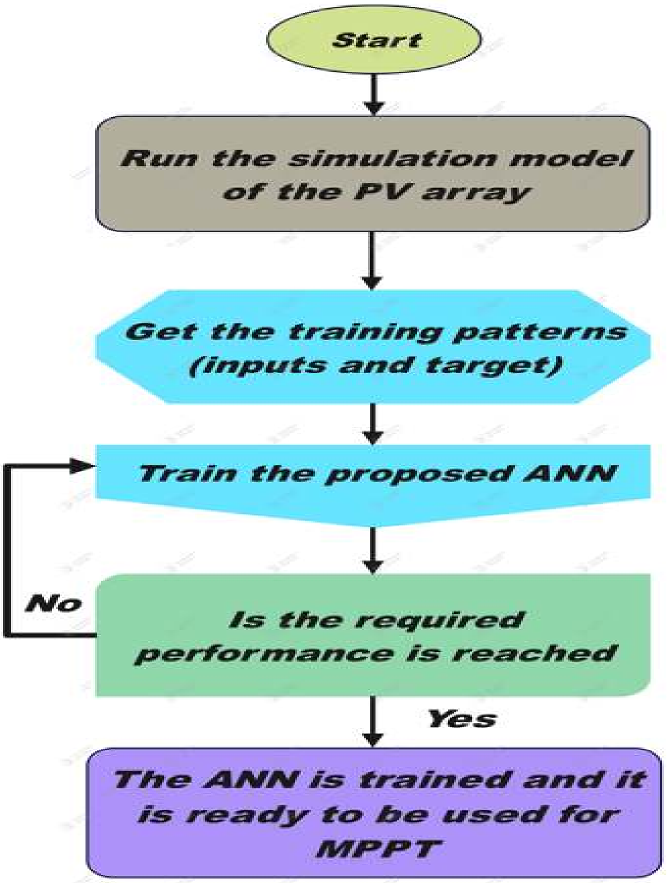

Figure 3.24 A flowchart depicting the ANN's training procedure for MPPT.

The primary drawback of the neural network-based MPPT technique is that the data required for the training process must be obtained separately for each PV array and site since the features of the PV array differ based on the model and the weather conditions vary depending on the geographical location. The neural network features change over time, so you need to train regularly (Farooqui *et al.* 2022, Villegas-Mier *et al.* 2021).

3.3.5 Particle swarm optimization (PSO)

PSO is a type of optimization algorithm based on the principle of social behavior of flocks of birds or fish. The PSO algorithm is designed based on the social behavior of the organism as an individual and as a herd (swarm). Academic and industry researchers widely use this population-based optimization (PSO) method due to its simple algorithm structures and fast convergence rates that are regulated by only a few parameters (Putri *et al.* 2019, Ritu *et al.* 2020). The PSO optimization algorithm uses the following equations (Hu *et al.* 2019, Putri *et al.* 2019) Equation 3.22:

$$v_i^{k+1} = wv_i^k + c_1.r_1 * \left(pbest - S_i^k\right) + c_2.r_2 * \left(gbest - S_i^k\right) \tag{3.22}$$

Equation 3.23 is used to update the inertia weight value for each iteration.

$$W = W_H - \left(\frac{W_H - W_L}{K_H}\right).K \tag{3.23}$$

As for the frequency of the particle's position, it is updated through Equation 3.24.

$$S_i^{k+1} = S_i^k + v_i^{k+1} \tag{3.24}$$

Where: v_i^{k+1} is the particle velocity at iteration k, w is the inertia weight factor, c1 and c_2 are acceleration constants, r_1 and r_2 are random numbers, and S_i^k is the particle position in the search space at iteration k, $pbest$ is called local best and $gbest$ is called global best (Putri *et al.* 2019).

For the MPPT tracking technology designed based on the PSO algorithm, the particle positions are chosen as duty cycle (D) that will be fed to the DC-DC boost converter, and the particle moving speed is set as the duty cycle variable, while the objective value or function of the fitness assessment function is chosen as the maximum power generated in the photovoltaic system. Figure 3.25 shows the flowchart of the PSO algorithm design technique (Putri *et al.* 2019, Ritu *et al.* 2020).

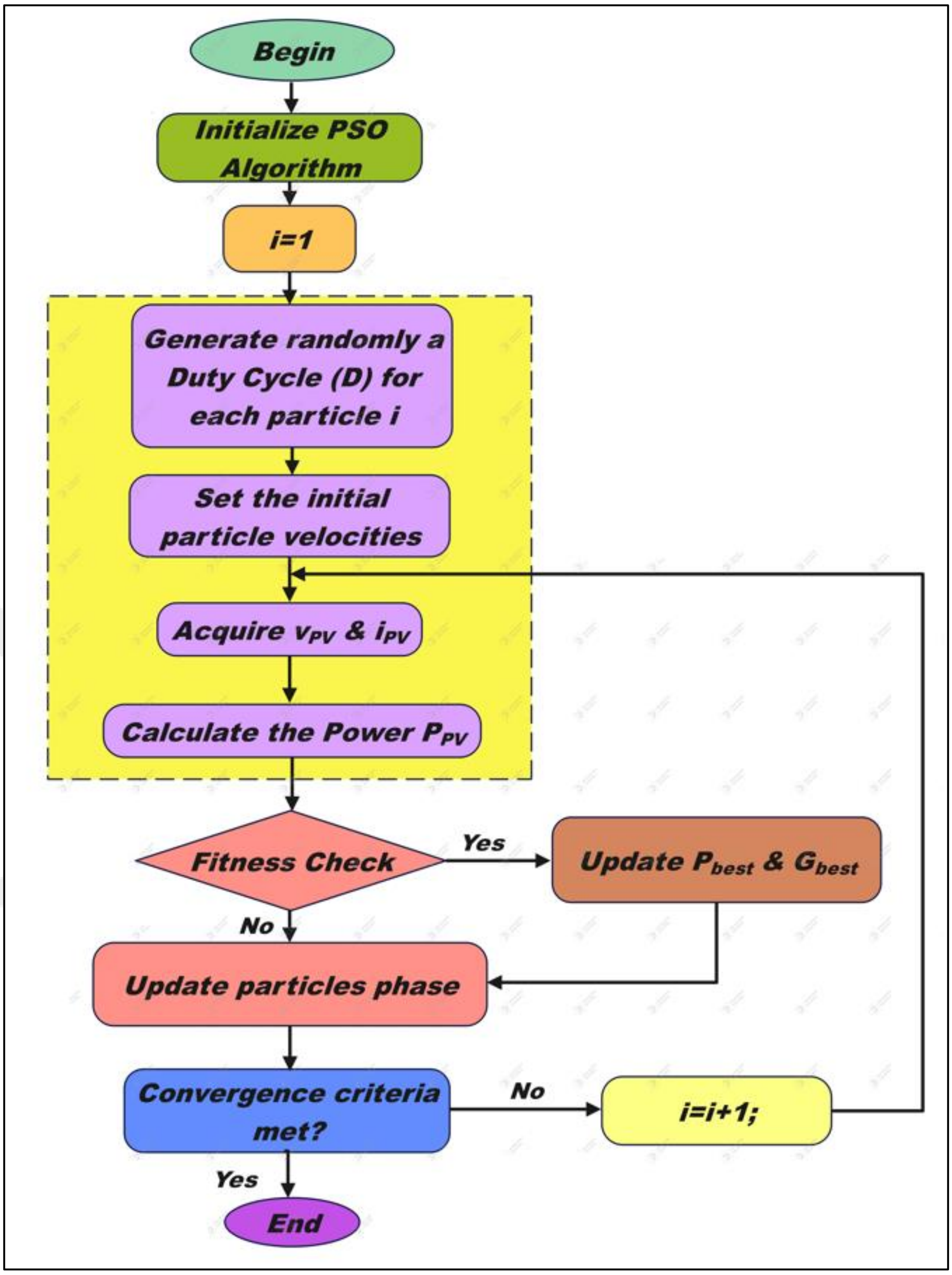

Figure 3.25 Flowchart of the PSO algorithm.

3.4 DC-DC Converters

Because they are greatly affected by weather conditions, solar energy systems are not ideal for generating constant power. Therefore, it is very difficult to transfer the maximum power generated by the photovoltaic panels directly to the loads continuously even if the maximum power point (MPP) is obtained from them. Since the PV system is affected by the intensity of solar radiation and temperature, some adjustments must be made to the load curve according to weather changes (Irwanto *et al.* 2020, Palanisamy *et al.* 2019). All this can be achieved by placing a smart electronic system between the solar panels and the load and Figure 3.26 shows the location of the converter (Shadlu 2018, Prabhu and Babu 2021). This system contains MPPT technology to control the duty cycle of the converter.

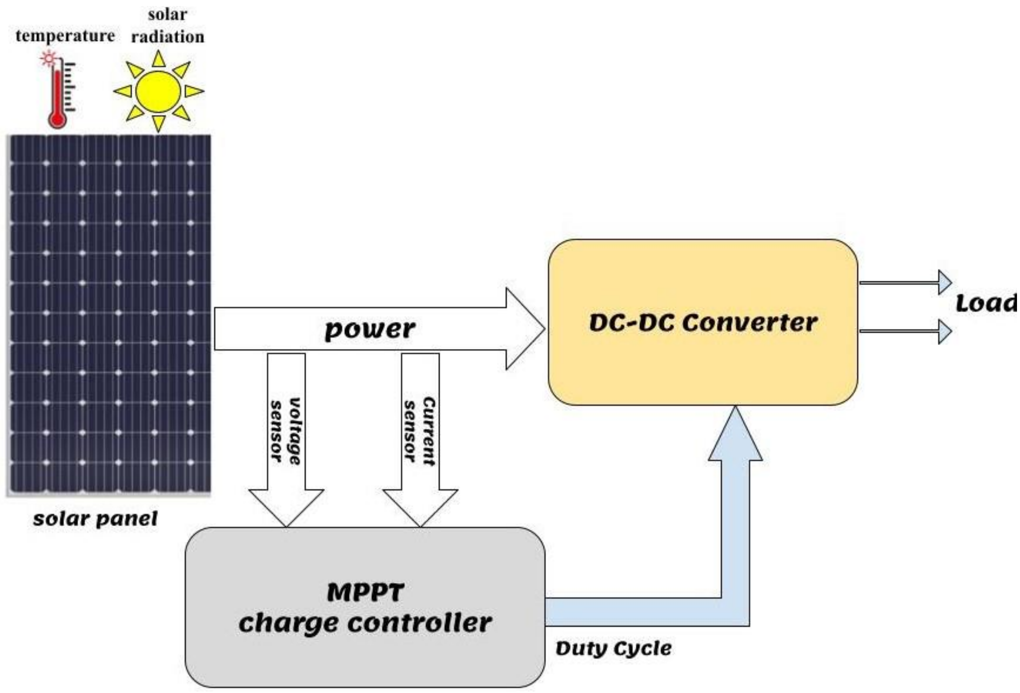

Figure 3.26 DC-DC converter for MPP operation.

To apply the Maximum Power Point Tracking (MPPT) technology in photovoltaic systems, one of the main and important parts of it is the DC-DC converter. It is an indispensable part, without which, MPPT tracking technology is not designed. It has wide applications in solar systems (Raof 2020, Irwanto *et al.* 2020).

In the previous paragraphs, the Maximum Power Point Tracking (MPPT) technique was introduced, and the most important algorithms applied in this technique were identified. In this section, we will address the DC-DC converter, which consists of three main types.

Three types of topologies are most common in DC-DC converters: buck-boost, Buck, and boost (Palanisamy *et al.* 2019). Buck transformers provide an output voltage that is less than the input voltage obtained from solar panels, while boost transformers produce an output voltage that is higher than the input voltage, and buck-boost systems can produce a voltage higher or less than the input voltage to them as needed (Prabhu and Babu, 2021, Shadlu 2018).

All types of converters contain a switch (MOSFET) that is controlled by the control pulses generated by the MPPT technology through the algorithms used in this technique, in this study we will use one type which is a boost converter (Irwanto *et al.* 2020, Hashim *et al.* 2018)

3.4.1 The DC-DC boost converter

To increase the power conversion of solar panels, a DC-DC Boost converter is usually preferred. It is commonly utilized in MPPT applications to reduce shadowing issues, and it has reached maximum power point. To adjust the duty cycle and switching frequency, the converter is placed between the photovoltaic panels and the loads. Where it works to increase the voltage entering it and coming from the solar panels and controlling it steadily with the change of surrounding conditions (Irwanto *et al.* 2020, Hashim *et al.* 2018). Figure 3.27 shows a boost converter circuit.

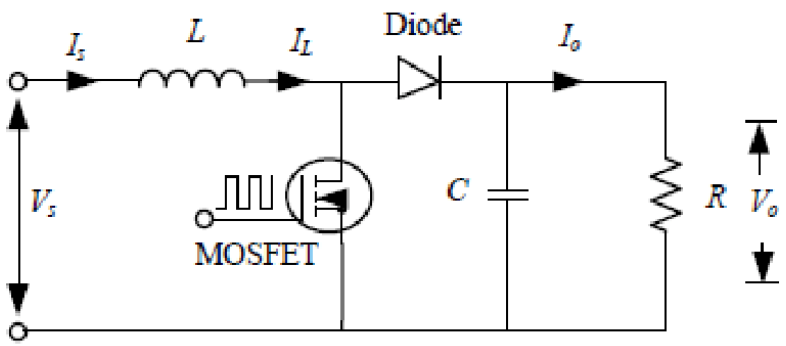

Figure 3.27 DC-DC boost converter (Irwanto et al., 2020).

When the MOSFET (electronic transistor) is on i.e. when its switch is off, it will allow current to flow through the coil connected in series with the solar panels where the coil stores energy when current passes through it. Then after changing the duty cycle, the MOSFET is extinguished, the switch opens and it becomes an open circuit through it so that the path turns towards the diode and then the load as the charging current in the coil begins to flow from the coil to the diode D and then to the capacitance C and the load resistance. The coil discharges its stored energy and the voltage polarity on the coil is the same as the voltage source polarity and the same polarity is transferred to the load via diode D (Palanisamy *et al.* 2019). Thus, the output voltage of the DC-DC converter connected to the loads is increased (Arunkumari and Indragandhi 2017, Junichi *et al.* 2003).

According to the researchers, a DC-DC conversion based on the Boost converter may address Buck flaws, overcome parasitic effects, and eliminate ripples at output voltage and current waveforms. However, using the Boost adapter in staging applications has a problem with the mean time between failures (MTBF), which restricts the adapter's reliability (Ba *et al.* 2018, Irwanto *et al.* 2020).

The following is the boost converter's design (Hashim *et al.* 2018) Equation 3.25 and Equation 3.26:

$$V_s \times t_{on} - (V_o - V_s) \times t_{off} = 0 \tag{3.25}$$

$$V_s \times D \times T = (V_o - V_s).(1 - D).T \tag{3.26}$$

Assuming that $P_{in} = P_{out}$ is an ideal converter with equal input and output power Equation 3.27, Equation 3.28, Equation 3.29, Equation 3.30, Equation 3.31, Equation 3.32 and Equation 3.33.

$$V_s.I_s = V_o.I_o \tag{3.27}$$

$$\frac{V_o}{V_S} = \frac{I_S}{I_o} = \frac{1}{(1-D)} \tag{3.28}$$

$$V_s = V_o.(1-D) \tag{3.29}$$

$$I_s = \frac{I_o}{(1-D)} \tag{3.30}$$

$$R_s = \frac{V_S}{I_S} = \frac{V_o.(1-D)}{\frac{I_o}{(1-D)}} = \frac{V_o}{I_o}\,(1-D)^2 \tag{3.31}$$

$$R_L = \frac{V_o}{I_o} \tag{3.32}$$

$$R_s = R_L(1-D)^2 \tag{3.33}$$

Photovoltaic maximum load is defined as Equation 3.34, Equation 3.35 and Equation 3.36:

$$R_{MPP} = \frac{V_{MPP}}{I_{MPP}} \tag{3.34}$$

$$D = \frac{t_{on}}{T} \tag{3.35}$$

$$T = \frac{1}{f_s} \tag{3.36}$$

D: The duty cycle

V_o: The output voltage.

V_s: The input voltage.

I_s: The input current.

I_o: The output current.

R_s: The input resistance

R_L: The load resistance.

T: The switching period.

R_{MPP}: The maximum load resistance.

f_s: The switching frequency.

t_{on}: The switching on time

Maximum Power Point Tracking (MPPT) technology is used to adjust the input impedance rating of the DC-DC converter so that it becomes equal to or very close to the maximum power point impedance $R_s = R_{MPP}$. But this process is not done if the value of R_{MPP} is not within the level of permissible values of R_s, that is, the method fails to reach the MPP if the value of $R_L < R_{MPP}$. But the method can be successful when $R_L \geq R_{MPP}$. The value of inductance L is calculated by using Equation (3.37) so that the inductance current I_L is allowed to continue flowing and never reaches the value of zero (Ayop and Tan 2018).

$$L = \frac{V_s . D}{\Delta i_L . f_s} \tag{3.37}$$

V_s: Input voltage

Δi_L: ripple current of the inductor

We can also calculate the output capacitance from Equation (3.38) (Soriano *et al.* 2017):

$$C_o \geq \frac{I_o . D}{f_s . \Delta V_o} \tag{3.38}$$

C_o: The output capacitance

ΔV_o: The output voltage ripple.

3.5 Design of MPPT Based on Several Algorithms Using MATLAB / Simulink

3.5.1 Solar energy system

In this study, we try to extract the best energy generated from the photovoltaic cell by simulating the Maximum Power Point Tracking (MPPT) system using different algorithms and comparing the simulation results to determine the best algorithm to increase the production capacity and raise the efficiency of the photovoltaic system.

A photovoltaic system is simulated using MATLAB/Simulink to produce electrical energy through solar light falling on solar panels and take advantage of sunlight and convert it into electricity for homes in villages and remote countryside where the national electricity grid is not available and also used in water pumps for farmers, water wells, water purification systems, and street lighting Because of the high costs of electricity generated from fossil fuels, scientists are forced to find alternative ways to produce energy, and the most important of these methods is solar energy because it is sustainable, clean and environmentally friendly energy.

In the sections below, three algorithms will be simulated to apply in MPPT technology to track MPP points and increase system efficiency. The solar panel input values will be checked under standard test conditions and variable conditions (radiation intensity and temperature) to see how they affect the photovoltaic system's output. Figure 3.28 shows the most important parts of a solar energy system.

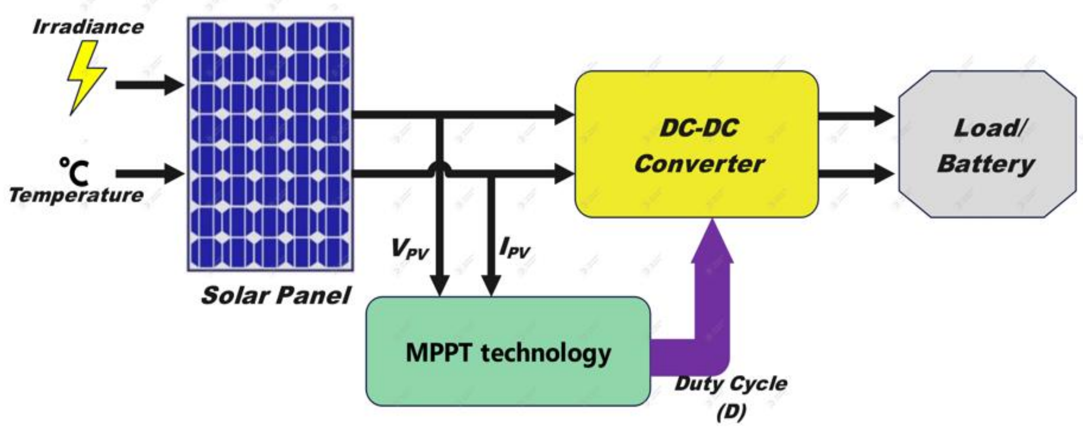

Figure 3.28 A solar photovoltaic system with MPPT

3.5.2 Solar panel

The PV module considered in the simulation is Suntech 1Soltech 1STH-215-P where the datasheet of the PV panel used is shown in Table 3.3 (Ronilaya *et al.* 2018). The photovoltaic system consists of one series panel and one parallel panel.

Table 3.3 Trina Solar 1Soltech 1STH-215-P Photovoltaic modules datasheet

Module Parameters	
Maximum Power (W)	213.15
Open Circuit Voltage (Voc)	36.3
The voltage at maximum power point (Vmpp)	29
Temperature coefficient of Voc(%/deg.C)	-0.36099
Cells per module (Ncell)	60
Short-circuit current Isc (A)	7.84
Current at maximum power point (Imp)	7.35
Temperature coefficient of Isc (%/deg.C)	0.102
Light-generated current IL(A)	7.8649
Diode Saturation Current Io (A)	2.9259e-10
Diode ideality factor	0.98117
Shunt resistance Rsh (ohms)	313.3991
Series resistance Rs (ohms)	0.39383

Figure 3.29 shows the characteristic curve of the photovoltaic system (I-V and P-V) when the temperature is constant at 25°C and the radiation intensity varies. Within five different values of radiation (1000 W/m^2, 800 W/m^2, 600 W/m^2, 400 W/m^2 and 200 W/m^2).

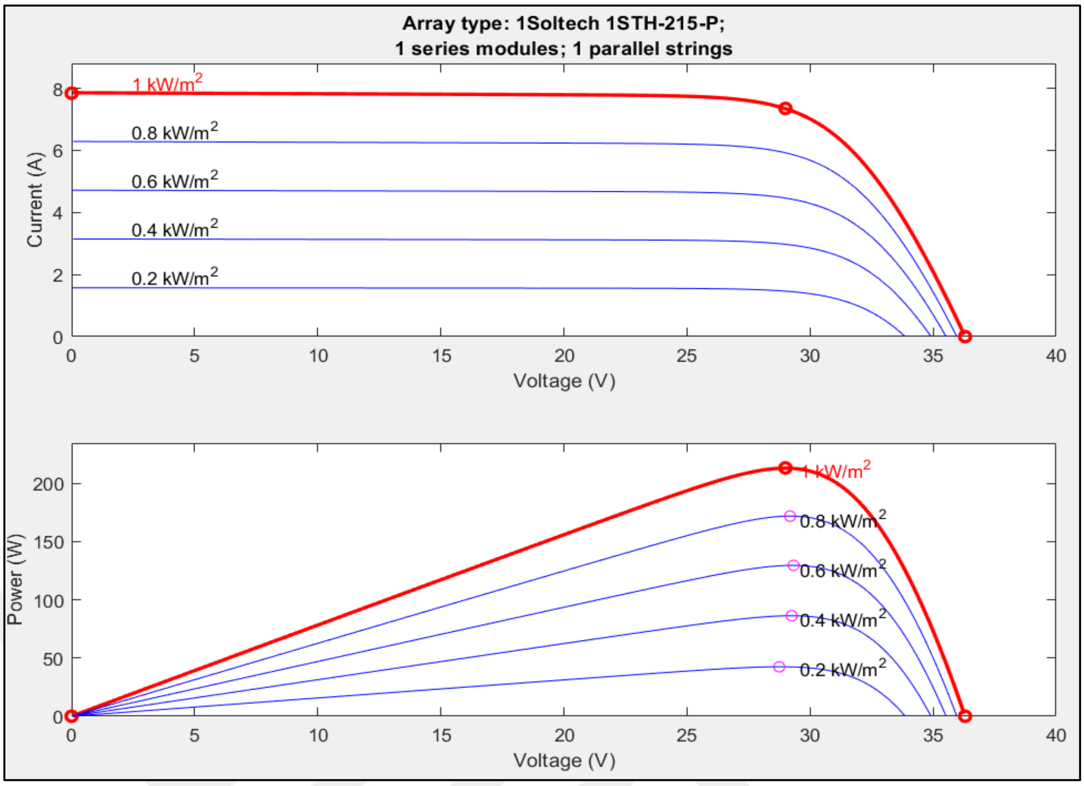

Figure 3.29 Characteristics curves PV panel under constant temperature and variable irradiation.

Figure 3.30 shows the characteristics (PV and I-V) of the photovoltaic panel when the radiation intensity is constant (1000 W/m^2) and at different temperatures. Within five different temperature values (55 °C, 45 °C, 35 °C, 25 °C, 15 °C).

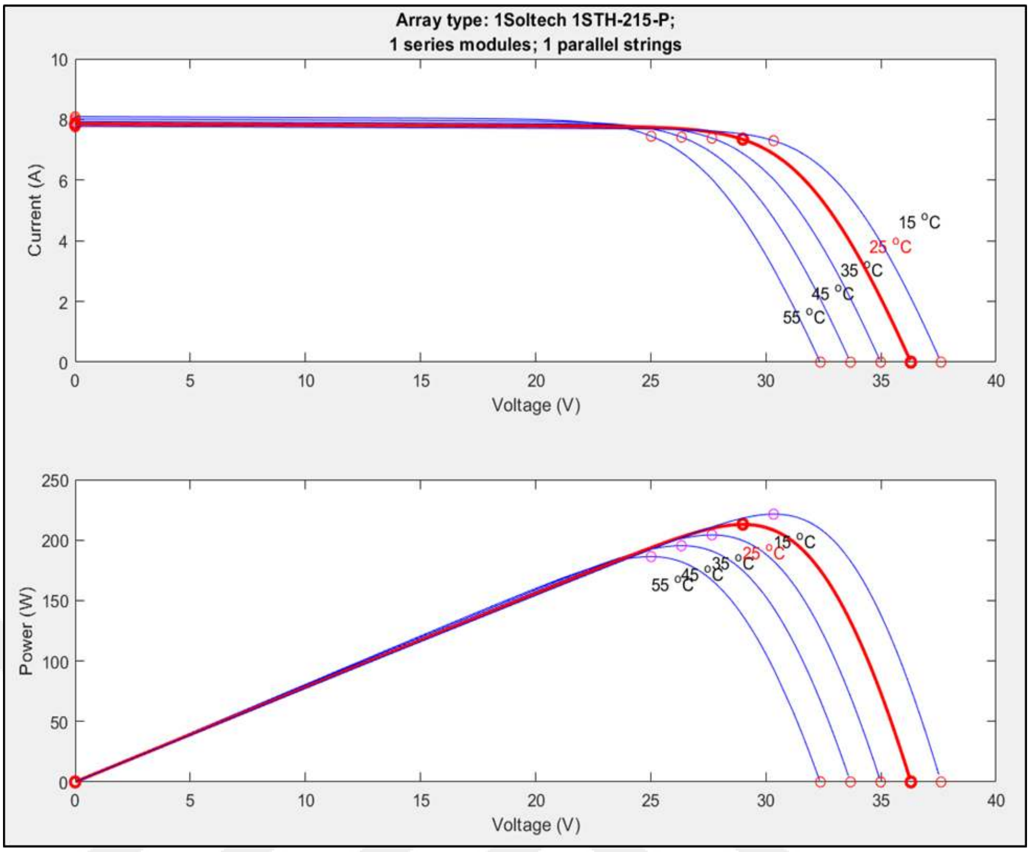

Figure 3.30 Characteristics curves PV panel under constant irradiation and different temperature.

3.5.3 DC-DC converter

In this thesis, a DC-DC boost converter will be designed using the mathematical equations mentioned in paragraph (2.4.1) and simulated using MATLAB/Simulink based on the results of current and voltage values produced by the solar panel, which produces a voltage of 29V and a current of 7.35 A, while the boost converter produces an output voltage of (36-40) V based on the design.

Where a DC-DC boost converter is located between the solar panels and the batteries or the load, it regulates the power flowing from the panels to the batteries, and the duty cycle of the converter is controlled through MPPT technology. Figure 3.31 shows the electronic elements used in the design of the DC-DC boost converter and the method of connecting components to the solar panel.

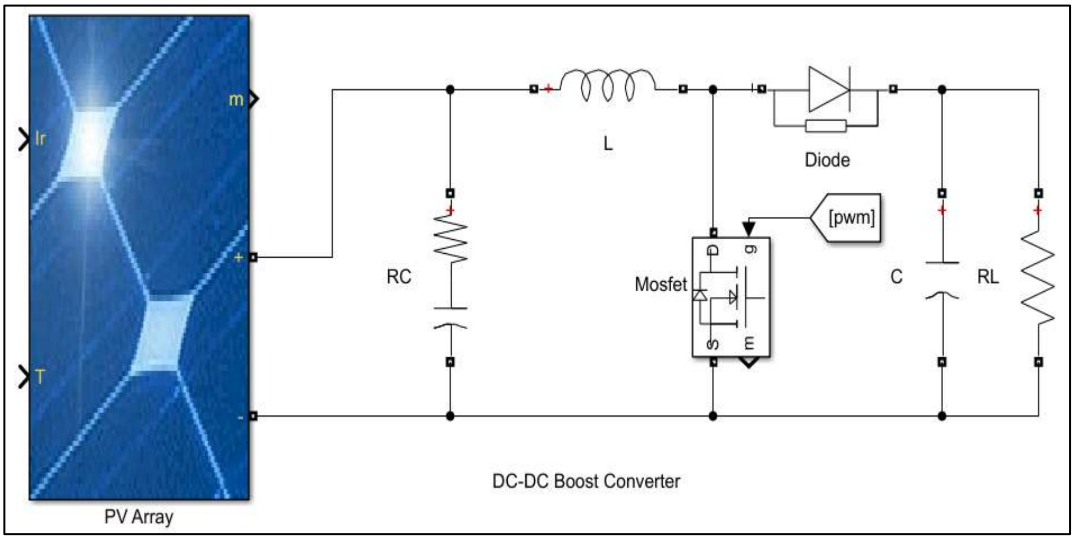

Figure 3.31 Mathematical model of DC-DC Boost converter circuit with solar panel.

The values and details of the items used in the DC-DC boost converter circuit simulation are shown. Capacitor and resistance in series, inductance, MOSFET, diode, capacitor, and RL load respectively are shown in Figure 3.32, Figure 3.33, Figure 3.34, Figure 3.35, Figure 3.36, and Figure 3.37.

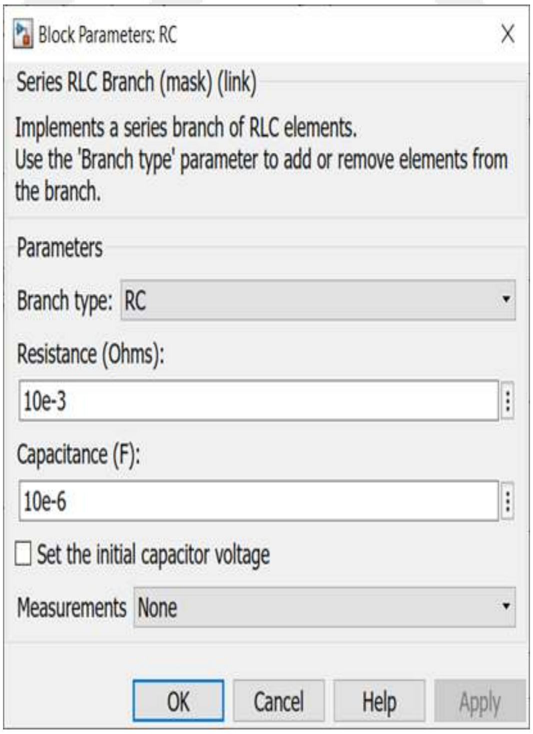

Figure 3.32 Value of Capacitor and resistance in series

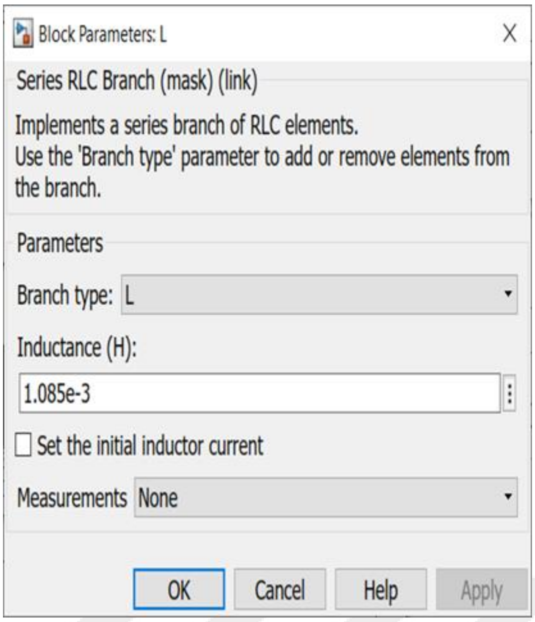

Figure 3.33 Value of inductance

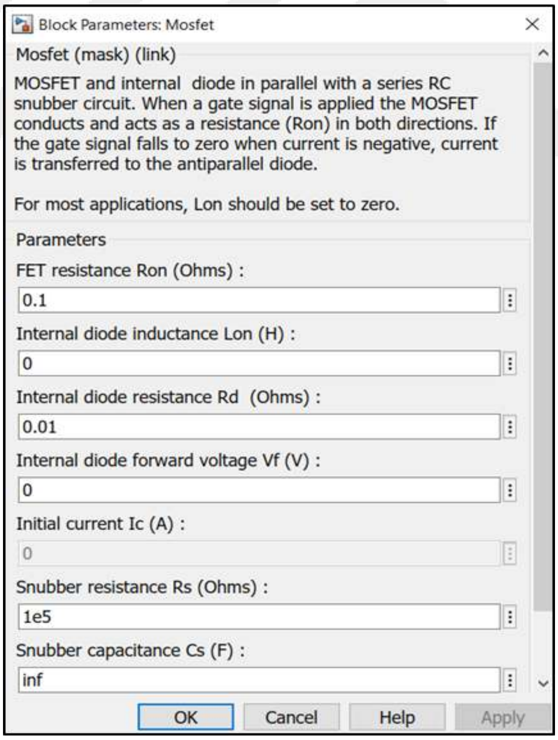

Figure 3.34 A window of the MOSFET

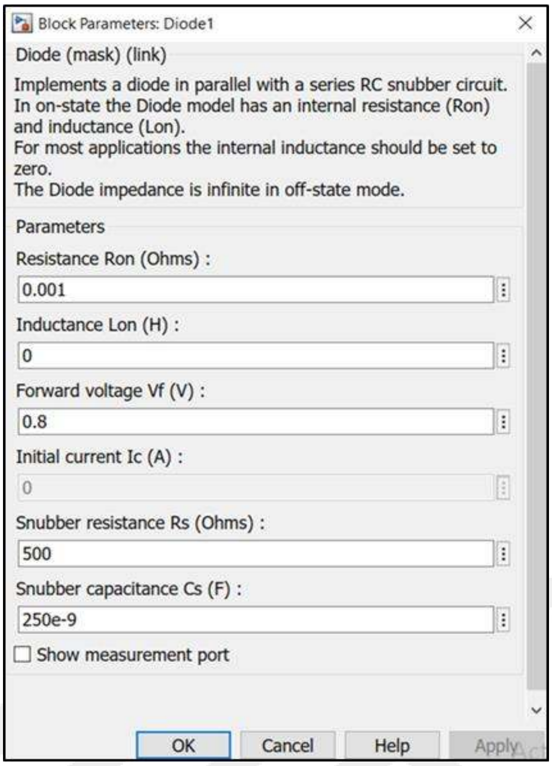

Figure 3.35 A window of the diode

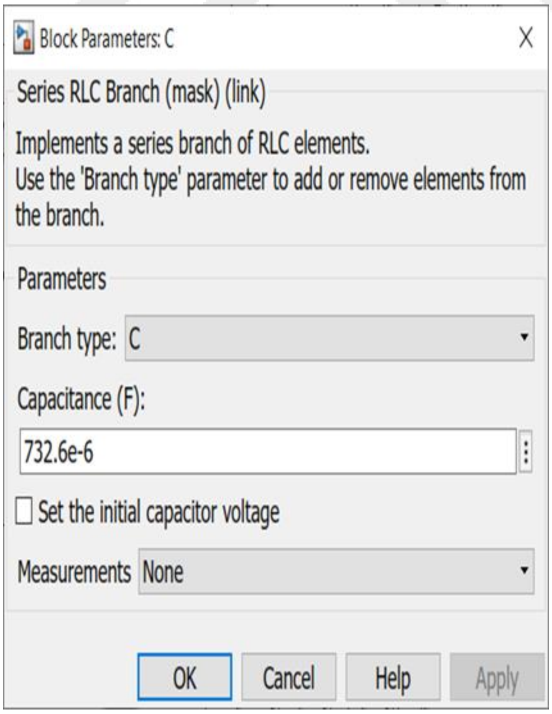

Figure 3.36 Value of the capacitor

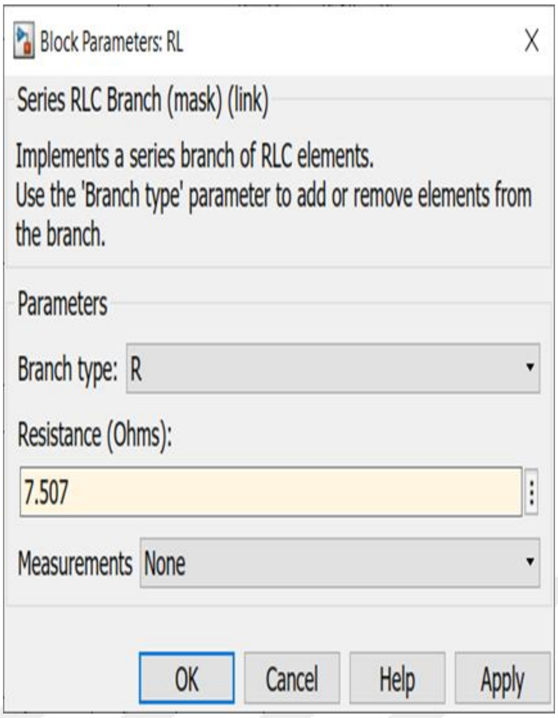

Figure 3.37 Value of the load resistan

3.5.4 Maximum power point tracking MPPT technology

In this thesis, MPPT technology will be built on the basis of three algorithms and simulation using MATLAB/Simulink, and compare the simulation results in terms of tracking accuracy, the efficiency of each algorithm, and the amount of effort it extracts from solar panels. The algorithms used are:

1. Perturb and Observe(P&O)
2. Fuzzy Logic controller (FLC)
3. Particle Swarm Optimization (PSO)

Each algorithm was tested under two test cases:

1- Under standard test conditions (STC) when the temperature (25°C) and radiation intensity (1000W/m^2).
2- Tested under changing weather conditions

- ❖ Change in the intensity of the solar radiation.
- ❖ Temperature change.

Photovoltaic system simulation with MPPT technology based on P&O algorithm:Figure 3:38 shows a simulation of a photovoltaic system with MPPT technology based on the Perturb & Observe (P&O) algorithm using MATLAB/Simulink. Where the P&O algorithm tracks the MPP that extracts the maximum power from the solar panels by controlling the duty cycle of the DC-DC boost converter connected to the solar panel, which contains two inputs, one for the intensity of solar radiation and the other for the temperature Figure 3.38.

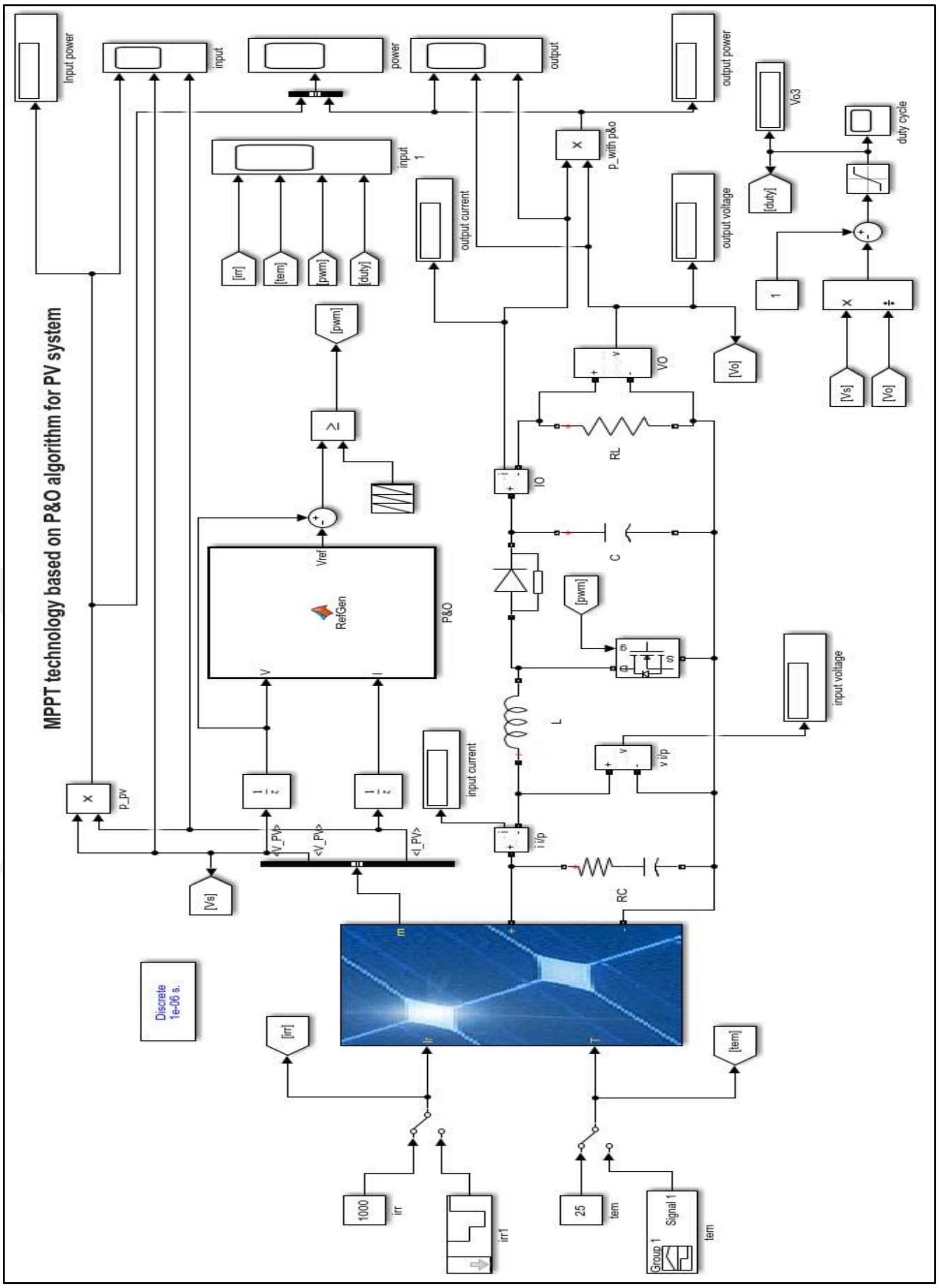

Figure 3.38 MPPT technology based on P&O algorithm with a DC-DC boost converter.

Table 3.4 shows simulation results using the resulting MATLAB/Simulink values (current, voltage, and power) obtained from solar panels as well as DC-DC boost converter output after applying the Perturb and Observe (P&O) algorithm when tested under volatile weather conditions (radiation different and constant temperature).

Table 3.4 P&O algorithm simulation results when the irradiation intensity is variable.

Irradiation at 25^{O} C	$P_{I/P}$ (W)	$V_{I/P}$ (V)	$I_{I/P}$ (A)	$P_{O/P}$ (W)	$V_{O/P}$ (V)	$I_{O/P}$ (A)	MPPT Technology Efficiency %
1000 W/m^2	206	26.89	6.934	196	36.49	5.37	95.14
800 W/m^2	171.3	29.49	6.331	146.8	31.59	4.648	85.69
600 W/m^2	129.5	29.26	4.547	125.6	29.21	4.298	96.98
400 W/m^2	68.44	21.97	3.115	65.93	21.17	3.115	96.33
200 W/m^2	17.9	11.44	1.565	16.65	10.64	1.565	93.01

Table 3.5 shows simulation results using the resulting MATLAB/Simulink values (current, voltage, and power) obtained from solar panels as well as DC-DC boost converter output after applying the Perturb and Observe (P&O) algorithm when tested under volatile weather conditions (The intensity of solar radiation is constant and the temperature is variable).

Table 3.5 P&O algorithm simulation results when the temperature is different.

Temperature at 1000 W/m^2	$P_{I/P}$ (W)	$V_{I/P}$ (V)	$I_{I/P}$ (A)	$P_{O/P}$ (W)	$V_{O/P}$ (V)	$I_{O/P}$ (A)	MPPT Technology Efficiency %
15° C	212.8	28.01	8.582	194.5	36.35	5.349	91.40
25° C	206	26.89	6.934	196	36.49	5.37	95.14
35° C	202.4	28.51	7.157	190.5	35.98	5.294	94.12
45° C	195	26.07	7.99	181.8	35.15	5.172	93.23
55° C	178.1	22.63	8.086	174.8	34.47	5.071	98.14

Solar system test with MPPT based on P&O algorithm in two test cases:

1. Testing the P&O algorithm under standard test conditions (STC):

In this case, the photovoltaic system based on the (P&O) algorithm was tested under standard test conditions (irr = 1000W/m^2, tem = 25°C) and plotted the input and output signals (voltage, current, power) Using MATLAB / Simulink Figure 3.39, Figure 3.40 and Figure 3.41.

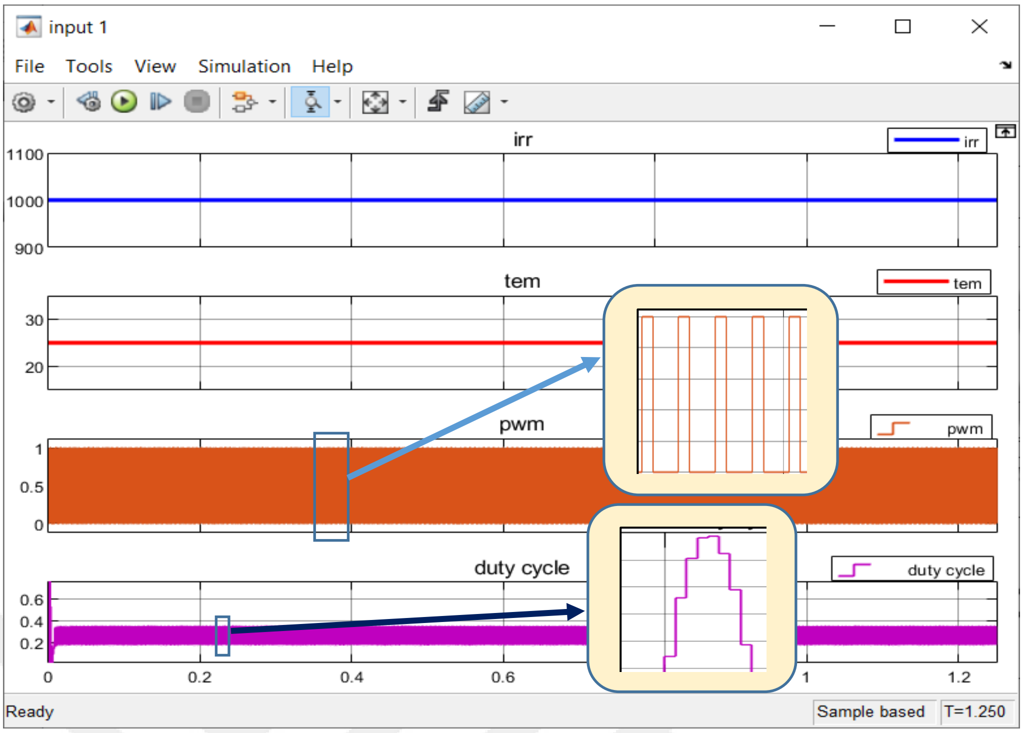

Figure 3.39 Shows the radiation intensity, the temperature applied to the photovoltaic cell, the control signal, and the duty cycle.

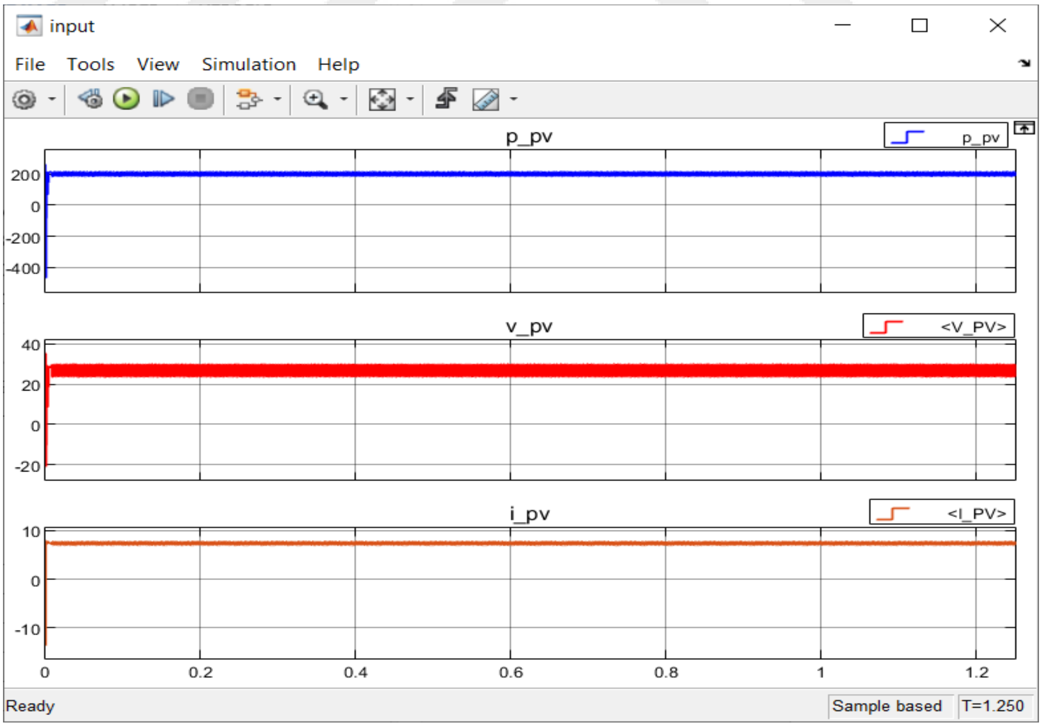

Figure 3.40 Shows the signal (power, voltage, current) generated in the photovoltaic cell.

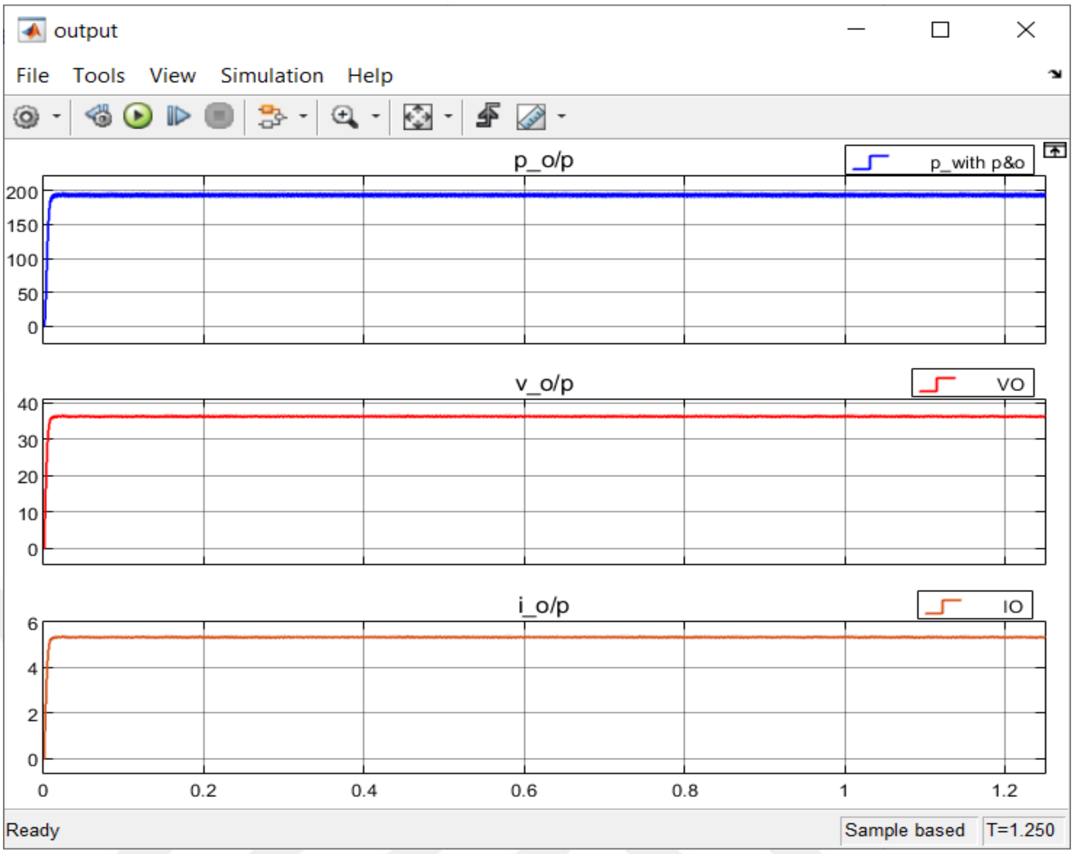

Figure 3.41 Shows the signal (power, voltage, current) of a DC-DC Boost Converter.

Table 3.6 represents the simulation results of a photovoltaic system using MPPT technology based on the P&O algorithm when tested under standard test conditions of radiation intensity (1000 W/m²) and temperature (25°C) and calculating the efficiency of the system.

Table 3.6 P&O algorithm simulation results under standard test conditions

Irradiation at 25^{O} C	$P_{I/P}$ (W)	$V_{I/P}$ (V)	$I_{I/P}$ (A)	Efficiency of extracting power %	$P_{O/P}$ (W)	$V_{O/P}$ (V)	$I_{O/P}$ (A)	MPPT Technology Efficiency %
1000 W/m^2	206	26.89	6.934	96.64	196	36.49	5.37	95.14

2. Testing the P&O algorithm under changing weather conditions:

Change in the intensity of the solar radiation [600 1000 800 650 980 700] W/m^2 and the temperature is constant(25°C) Figure 3.42, Figure 3.43 and Figure 3.44.

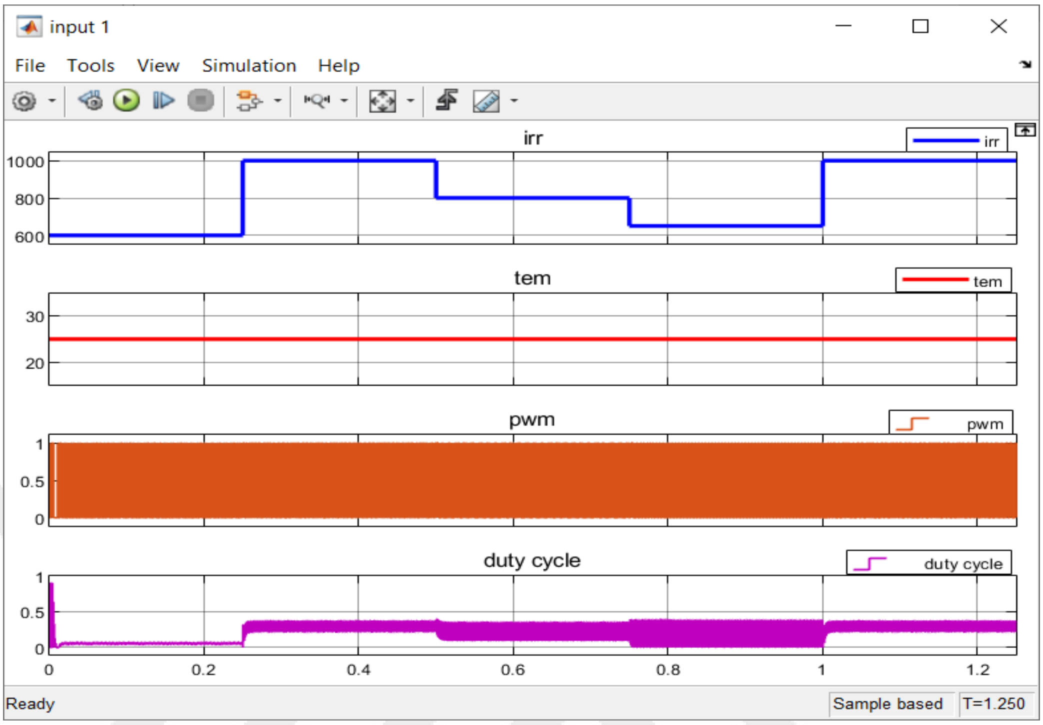

Figure 3.42 Shows the radiation intensity, the temperature applied to the photovoltaic cell, the control signal, and the duty cycle.

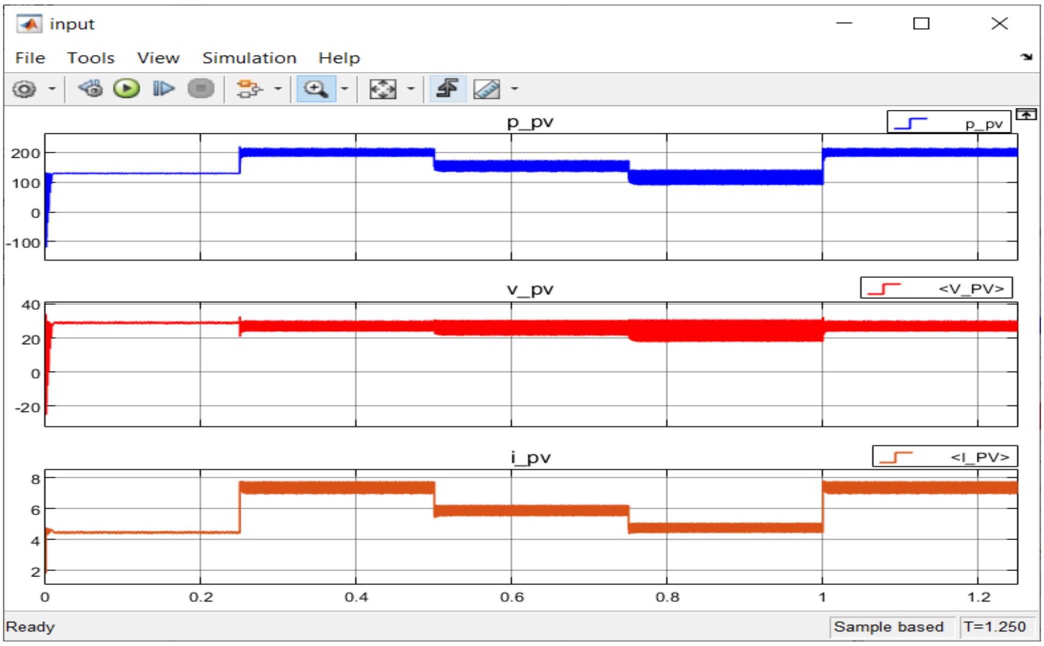

Figure 3.43 Shows the signal(power, voltage, current) generated in the photovoltaic cell when the radiation intensity is variable.

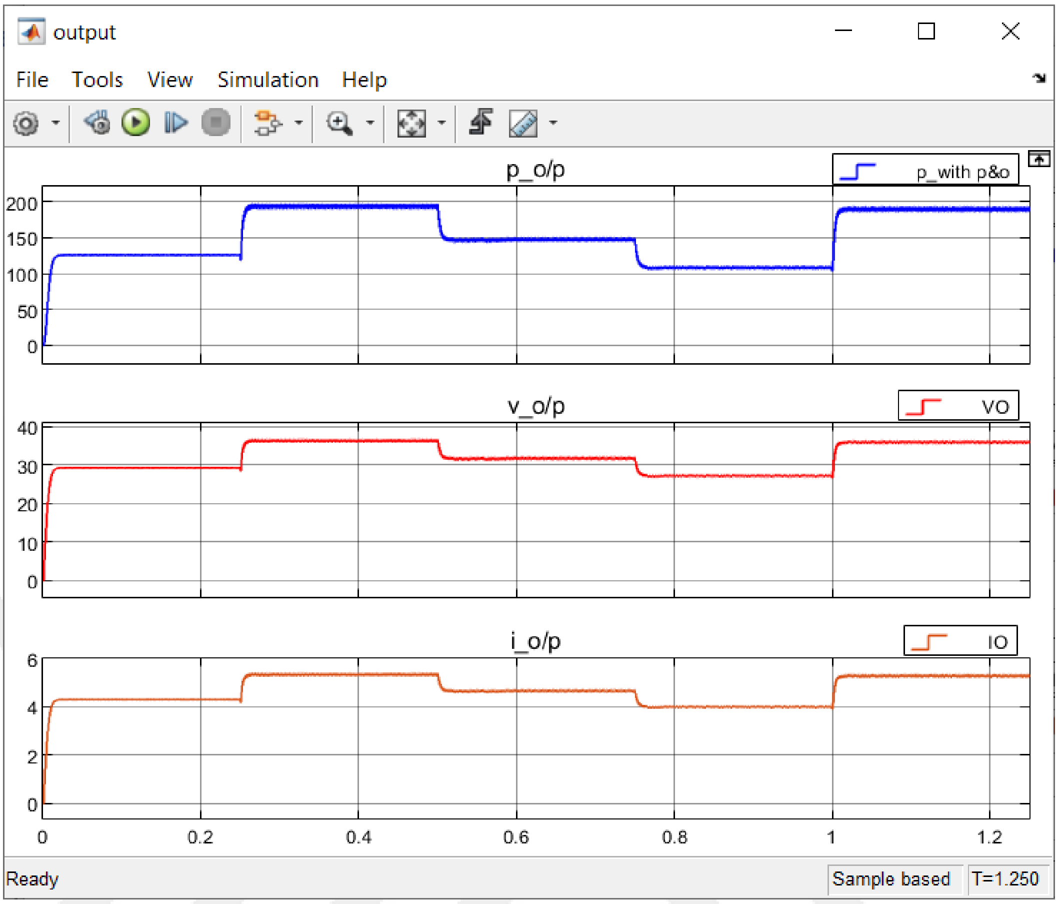

Figure 3.44 Shows the signal (power, voltage, current) of a DC-DC Boost Converter when the radiation intensity is variable.

Table 3.7 represents the simulation results of a photovoltaic system using MPPT control technology based on the P&O algorithm when tested under variable weather conditions when the solar radiation intensity is variable [600 1000 800 650 980 700] W/m^2 and the temperature is constant (25°C).

Table 3.7 P&O algorithm simulation results when the irradiation intensity is variable.

Irradiation at 25^O C	$P_{I/P}$ (W)	$V_{I/P}$ (V)	$I_{I/P}$ (A)	efficiency of extracting power %	$P_{O/P}$ (W)	$V_{O/P}$ (V)	$I_{O/P}$ (A)	MPPT Technology Efficiency %
variable	201.2	26.8	8.394	96.31	186.7	35.62	5.242	92.79

Change in the temperature [55°C, 45°C, 35°C, and 27°C] and the intensity of the solar radiation is constant (1000) W/m^2 Figure 3.45, Figure 3.46, and Figure 3.47.

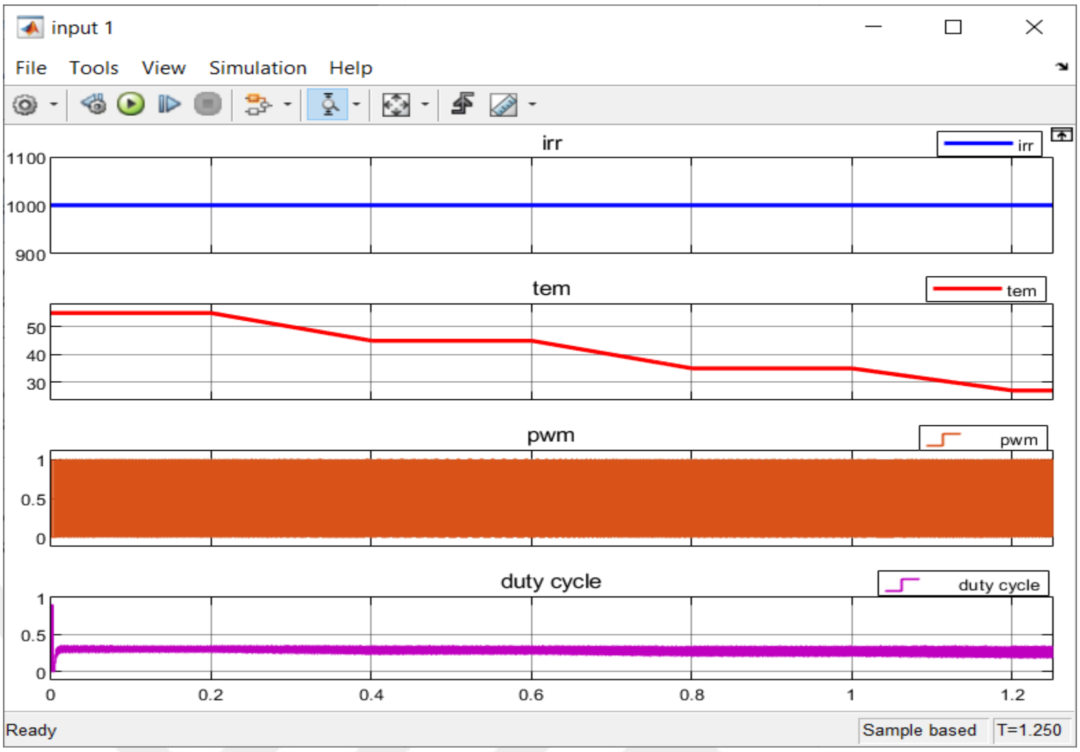

Figure 3.45 Shows the radiation intensity, the temperature applied to the photovoltaic cell, the control signal, and the duty cycle.

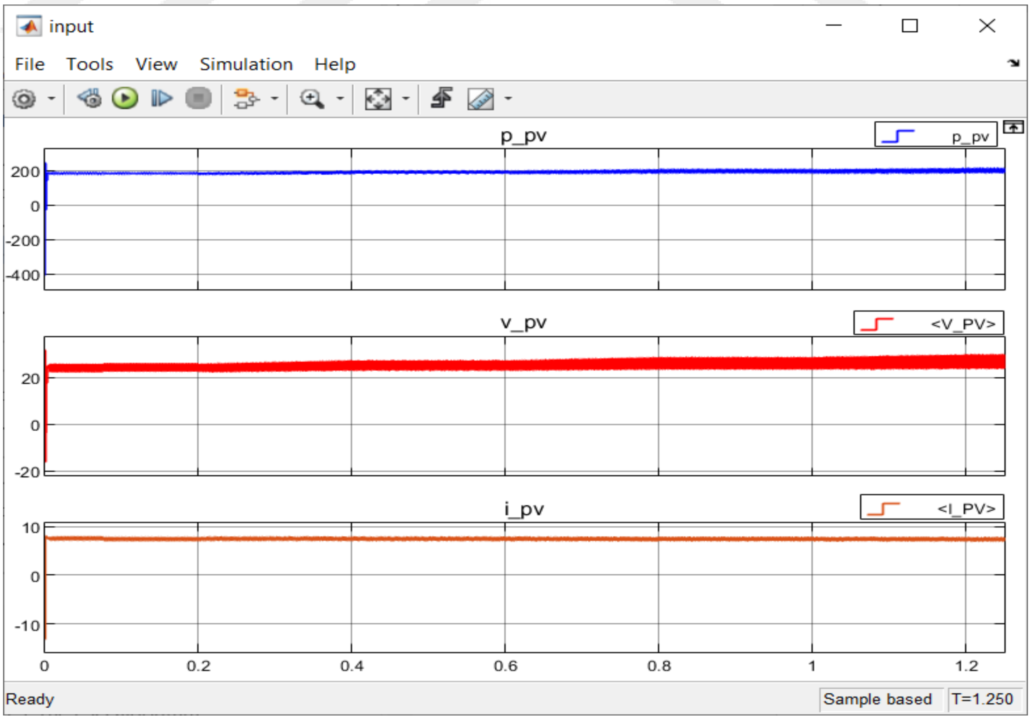

Figure 3.46 Shows the signal (power, voltage, current) generated in the photovoltaic cell when the temperature is variable.

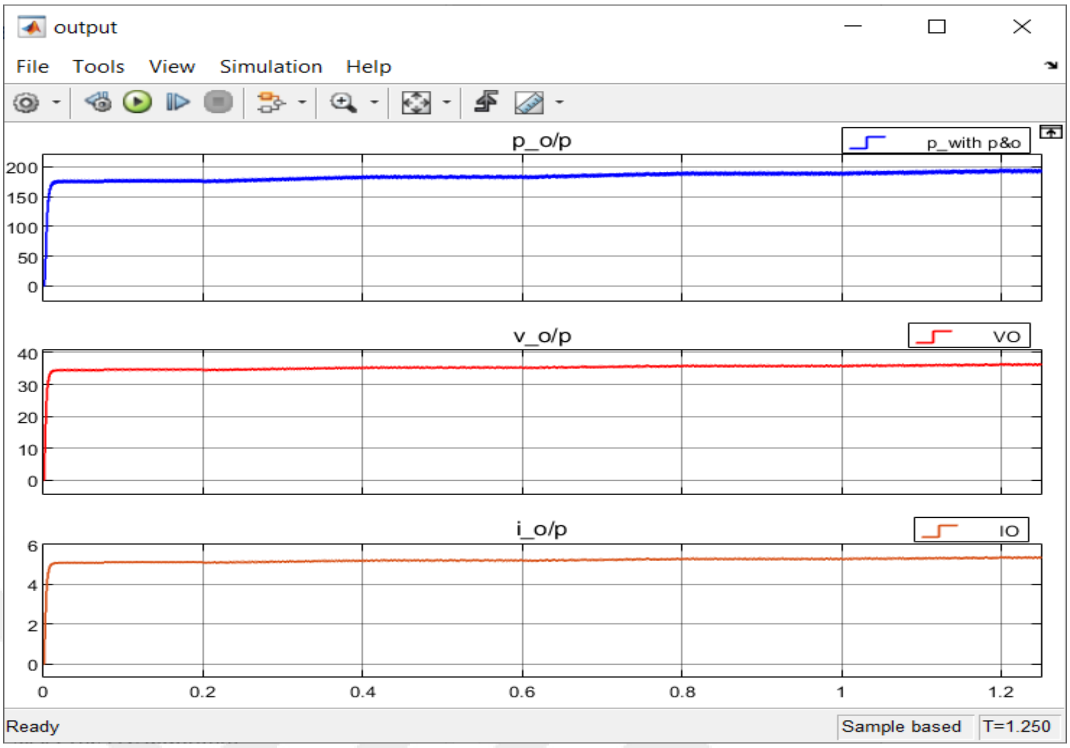

Figure 3.47 Shows the signal (power, voltage, current) of a DC-DC Boost Converter when the temperature is variable.

Table 3.8 represents the simulation results of a photovoltaic system using MPPT technology based on the P&O algorithm when tested under variable test conditions when the temperature is variable and the radiation intensity is constant (1000 W/m²).

Table 3.8 P&O algorithm simulation results when the temperature is different.

temperature at [1000] W/m^2	$P_{I/P}$ (W)	$V_{I/P}$ (V)	$I_{I/P}$ (A)	Efficiency of extracting power %	$P_{O/P}$ (W)	$V_{O/P}$ (V)	$I_{O/P}$ (A)	MPPT Technology Efficiency %
variable	199.2	25.82	8.423	94.31	190.6	35.99	5.296	95.68

Photovoltaic system simulation with MPPT technology based on Fuzzy Logic Controller (FLC) algorithm: Figure 3:48 shows a simulation of a photovoltaic system with MPPT technology based on the fuzzy logic controller (FLC) algorithm using MATLAB/Simulink. Where the FLC algorithm tracks the MPP that extracts the maximum power from the solar panels by controlling the duty cycle of the DC-DC boost converter connected to the solar panel, which contains two inputs, one for the intensity of solar radiation and the other for the temperature. A simulation of an MPPT controller circuit based on a fuzzy logic controller (FLC) is designed in MATLAB/Simulink Figure 3.48.

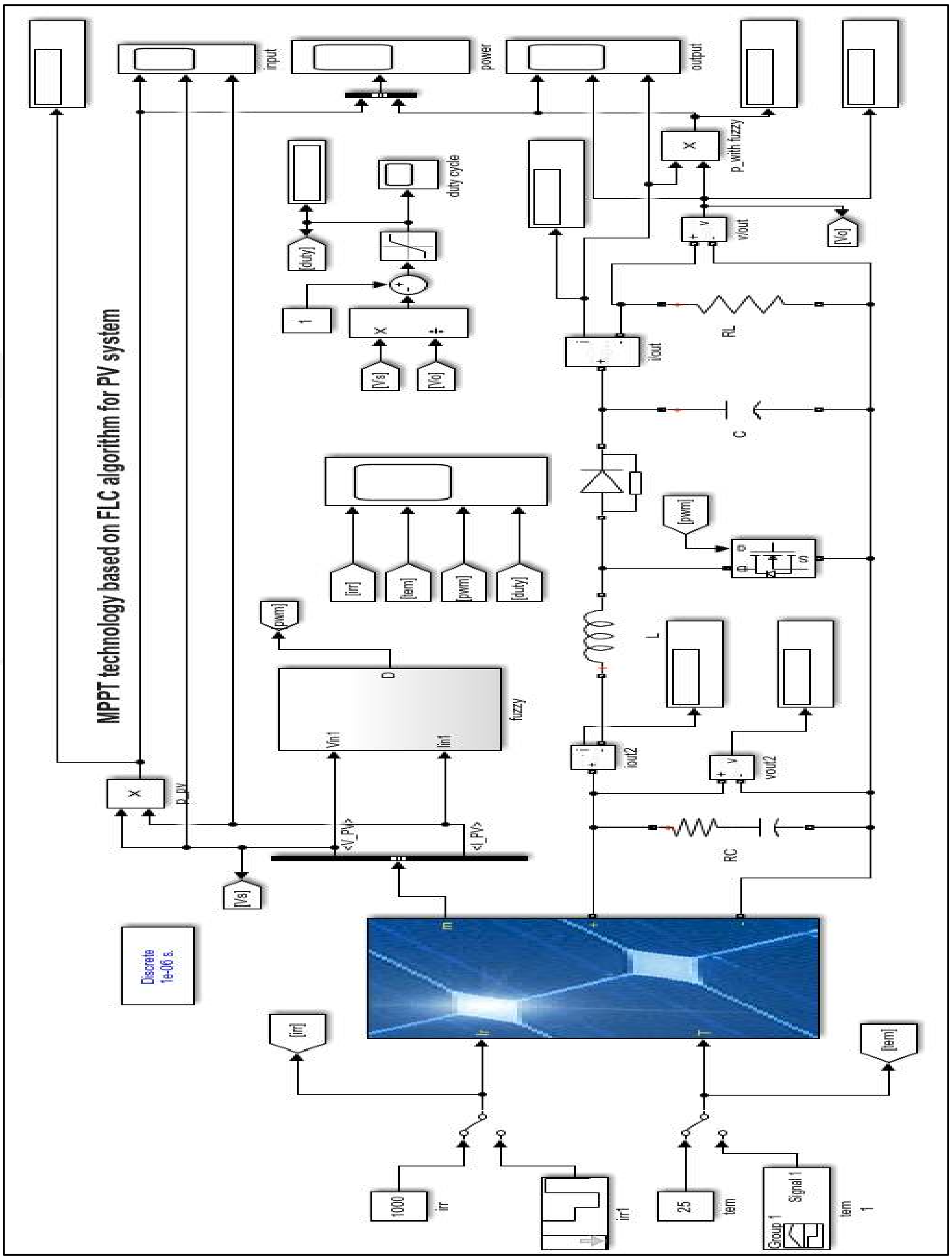

Figure 3.48 MPPT technology based on FLC algorithm with a DC-DC boost converter.

Design of fuzzification segment: Numerical inputs are converted to linguistic variables based on the membership function at this step. This controller has two inputs and one output in this research. The fuzzy inputs 'change in voltage' and 'change in current' include seven fuzzy variables. The number of membership functions determines these variables. These membership functions are called NB (Negative Big), NM (Negative Medium), NS (Negative Small), ZE (Zero), PS (Positive Small), PM (Positive Medium), and PB (Positive Big). The duty cycle changes are the output of the fuzzy logic system. Figure 3.49 and Figure 3.50 demonstrate the membership functions of change in voltage and current, respectively. Figure 3.51 depicts the final output, which is the duty cycle change.

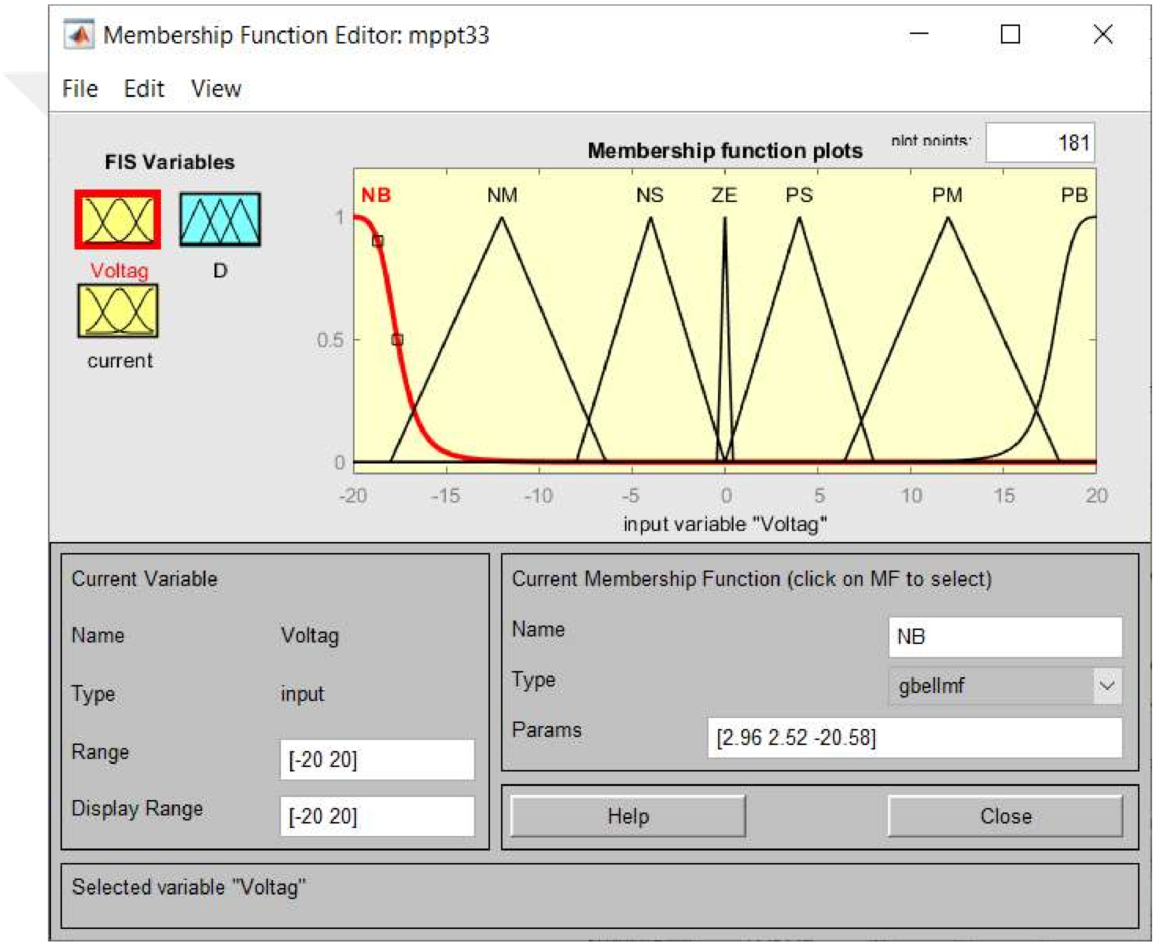

Figure 3.49 The input of FLC Voltage).

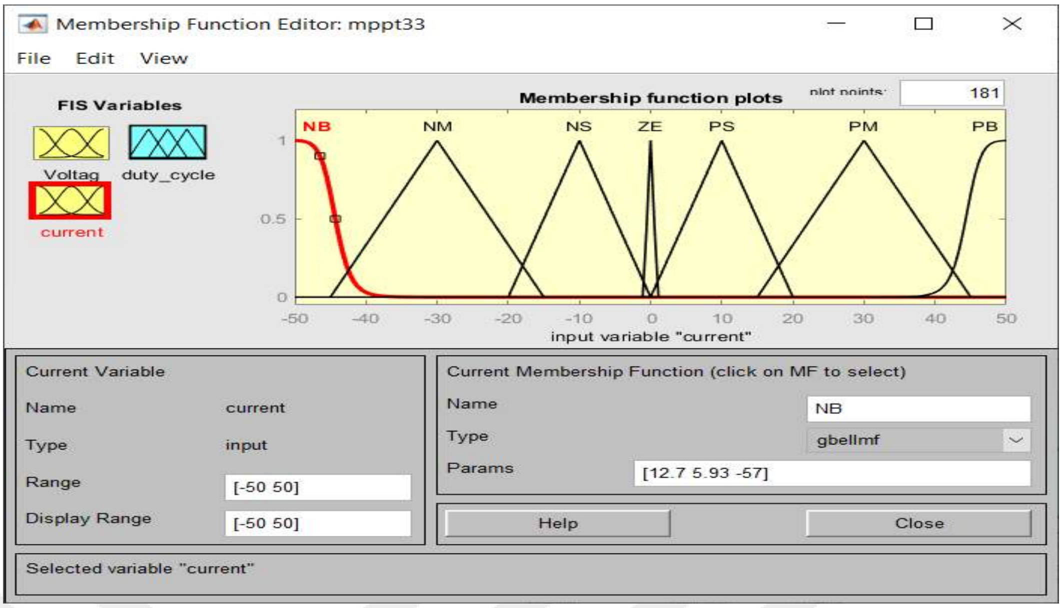

Figure 3.50 The input of FLC (current)

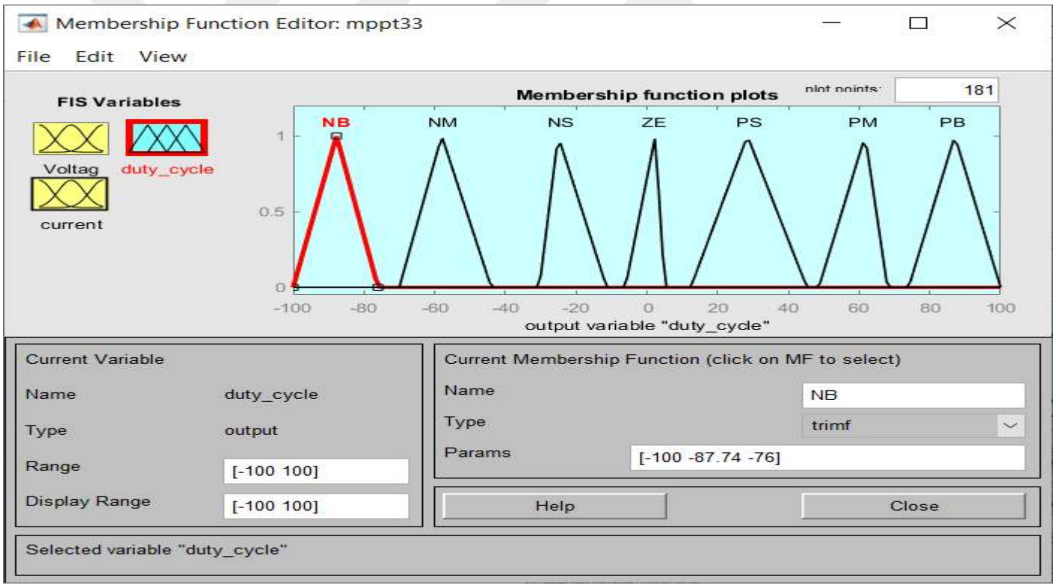

Figure 3.51 The output of FLC (duty cycle)

Design of inference system: One of the most crucial processes in the fuzzy logic controller is the inference step. This part is motivated by people's ability to infer and make decisions. Which rules are employed in the rule base and the inference process is done using the membership functions produced by fuzzification. In the extraction process, four different inference techniques are typically used. Inference techniques such as Max-Dot, Min-Max, Tsukamoto, and Takagi- Sugeno are used. The Mamdani approach, which is similar to the max-min methodology, is employed in this research Figure 3.52.

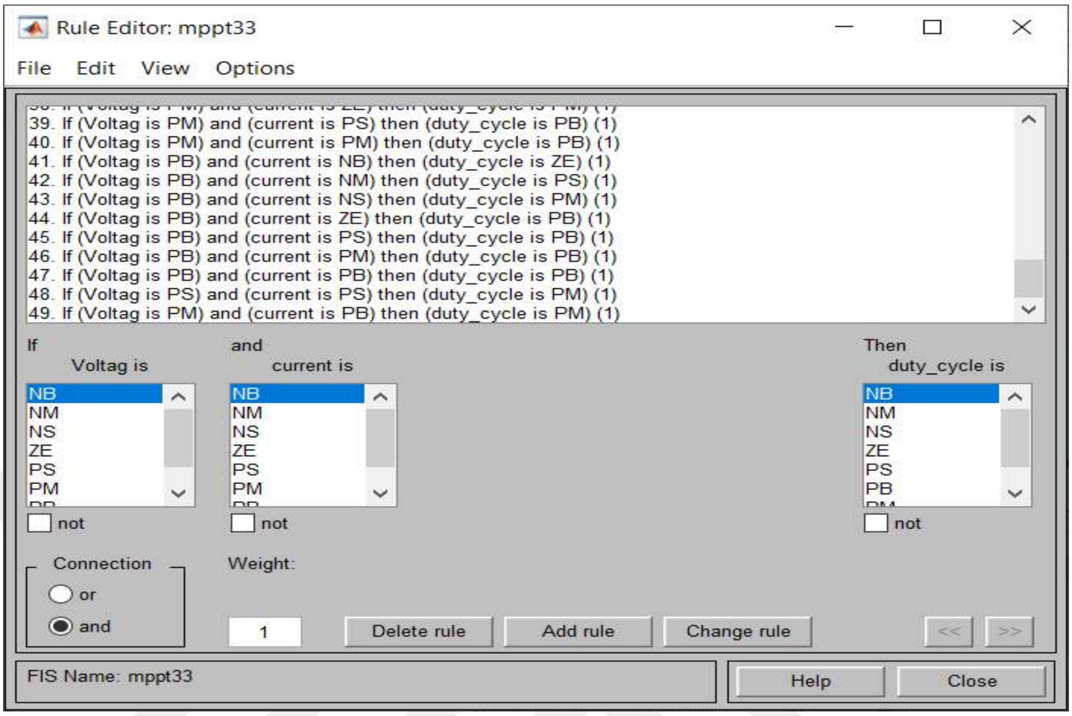

Figure 3.52 A screenshot of the FLC-based MPPT's designed rule editor.

Two inputs and one output system have been implemented in the fuzzification segment in this study, and membership functions are determined. Each input has seven various status possibilities, which are detailed in the fuzzification section. For the design of two-input and single-output systems, 49 distinct rules have been devised. Table 3.9 shows these rules.

Table 3.9 Rules implemented in Fuzzy logic inference system.

ΔI / Δv	NB	NM	NS	ZE	PS	PM	PB
NB	NB	NB	NB	NB	NM	NS	ZE
NM	NB	NB	NB	NM	NS	ZE	PS
NS	NB	NB	NM	NS	ZE	PS	PM
ZE	NB	NM	NS	ZE	PS	PM	PB
PS	NM	NS	ZE	PS	PM	PB	PB
PM	NS	ZE	PS	PB	PB	PB	PM
PB	ZE	PS	PM	PB	PB	PB	PB

Design of defuzzification segment: The inference methods, it was discovered, give a function for the resulting membership variable, and therefore behave as fuzzy information. Given that the DC-DC converter requires a precise control signal D at its entry, it is required to consider a transformation of this fuzzy data into deterministic data, which is referred to as defuzzification.

The output of fuzzy logic control, duty ratio, is used to control MOSFET switches in DC-DC converters using PWM, which generates a pulse. The fuzzy logic controller for MPPT algorithm configuration is shown in Figure 3.53 where the input is current and photovoltaic voltage, and the output is duty cycle to the DC-DC boost converter.

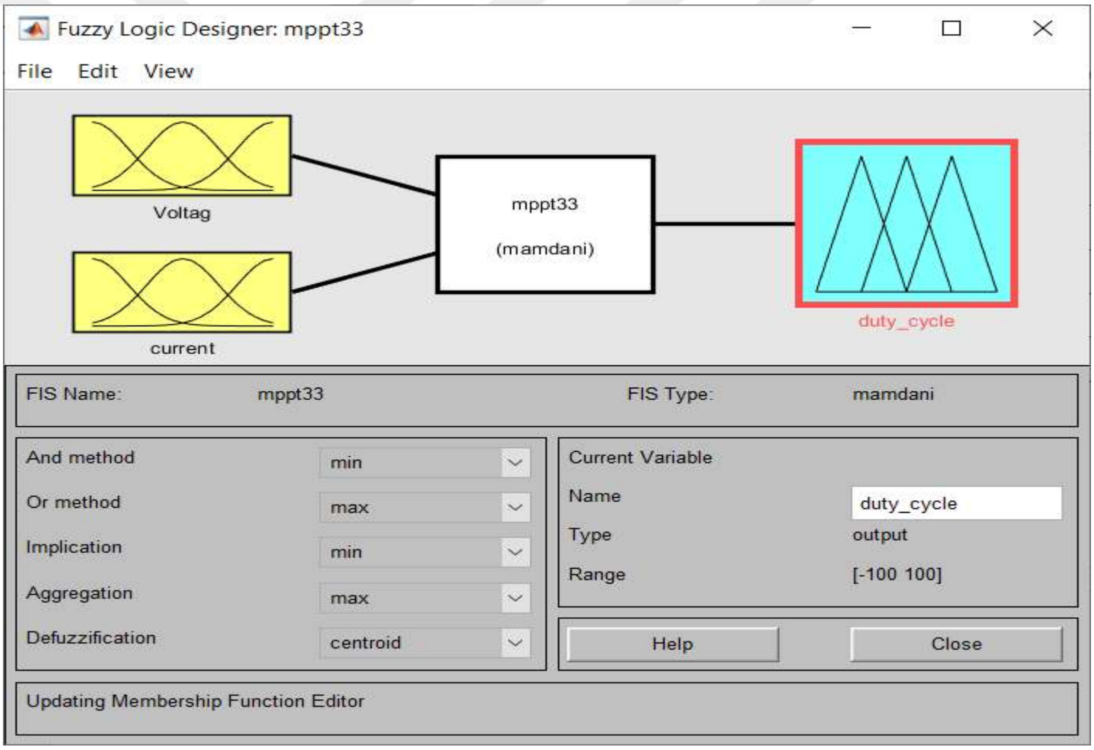

Figure 3.53 The interface of FLC with defuzzification.

Table 3.10 shows simulation results using the resulting MATLAB/Simulink values (current, voltage, and power) obtained from solar panels as well as DC-DC boost converter output after applying the fuzzy logic controller (FLC) algorithm when tested under volatile weather conditions (radiation different and constant temperature).

Table 3.10 FLC algorithm simulation results when the irradiation intensity is variable.

Irradiation at 25^{O} C	$P_{I/P}$ (W)	$V_{I/P}$ (V)	$I_{I/P}$ (A)	$P_{O/P}$ (W)	$V_{O/P}$ (V)	$I_{O/P}$ (A)	MPPT Technology Efficiency %
1000 W/m^2	210.1	30.05	6.914	204.6	33.26	6.152	97.38
800 W/m^2	163.4	26.54	6.087	158.6	29.28	5.416	97.06
600 W/m^2	94.99	20.32	.462	91.46	22.24	4.113	96.28
400 W/m^2	43.2	13.82	3.087	40.9	14.87	2.75	94.67
200 W/m^2	11.41	7.277	1.547	10.28	7.457	1.379	90.09

Table 3.11 shows simulation results using the resulting MATLAB/Simulink values (current, voltage, and power) obtained from solar panels as well as DC-DC boost converter output after applying the fuzzy logic controller (FLC) algorithm when tested under volatile weather conditions) The intensity of solar radiation is constant and the temperature is variable).

Table 3.11 FLC algorithm simulation results when the temperature is different.

Temperature at 1000 W/m^2	$P_{I/P}$ (W)	$V_{I/P}$ (V)	$I_{I/P}$ (A)	$P_{O/P}$ (W)	$V_{O/P}$ (V)	$I_{O/P}$ (A)	MPPT Technology Efficiency %
15^o C	221	30.8	7.092	215.3	34.12	6.31	97.42
25^o C	210.1	30.05	6.914	204.6	33.26	6.152	97.38
35^o C	198.1	29.19	6.711	192.8	32.28	5.971	97.32
45^o C	185.4	28.25	6.491	180.3	31.22	5.775	97.24
55^o C	172.5	27.27	6.259	167.7	30.11	5.569	97.21

Solar system test with MPPT based on FLC algorithm in two test cases:

1. Testing the FLC algorithm under standard test conditions (STC):

In this case, the photovoltaic system based on the (FLC) algorithm was tested under standard test conditions (irr = 1000W/m^2, tem = 25°C) and plotted the input and output signals (voltage, current, power) Using MATLAB / Simulink Figure 3.54, Figure 3.55 and Figure 3.56.

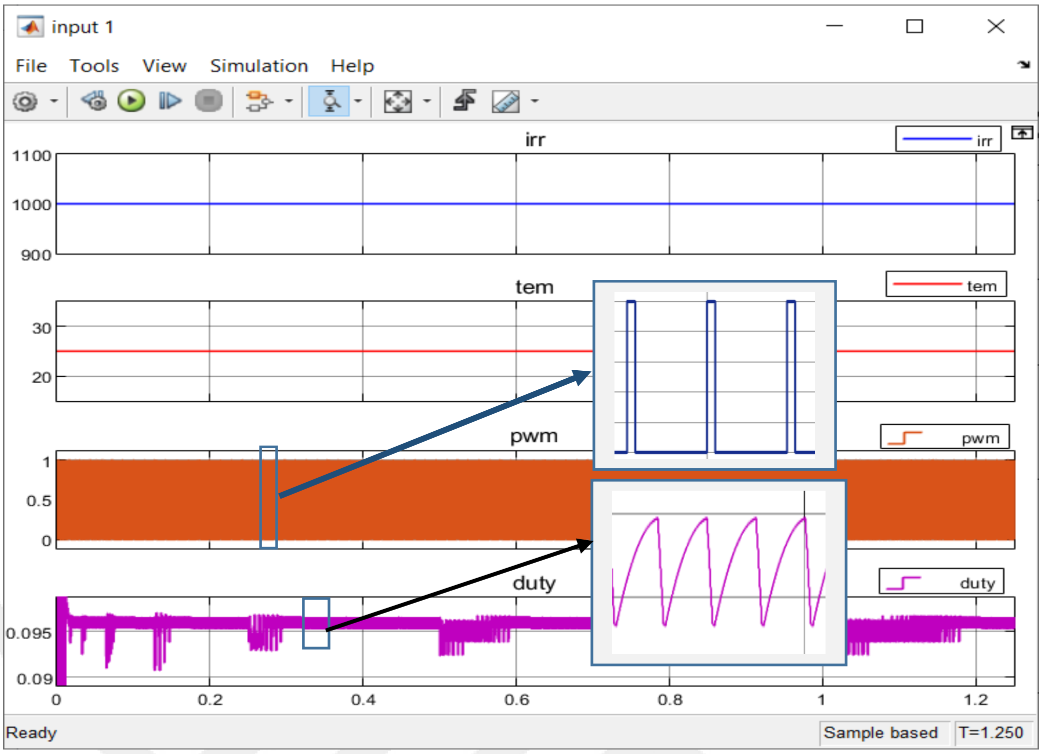

Figure 3.54 Shows the radiation intensity, the temperature applied to the photovoltaic cell, the control signal, and the duty cycle.

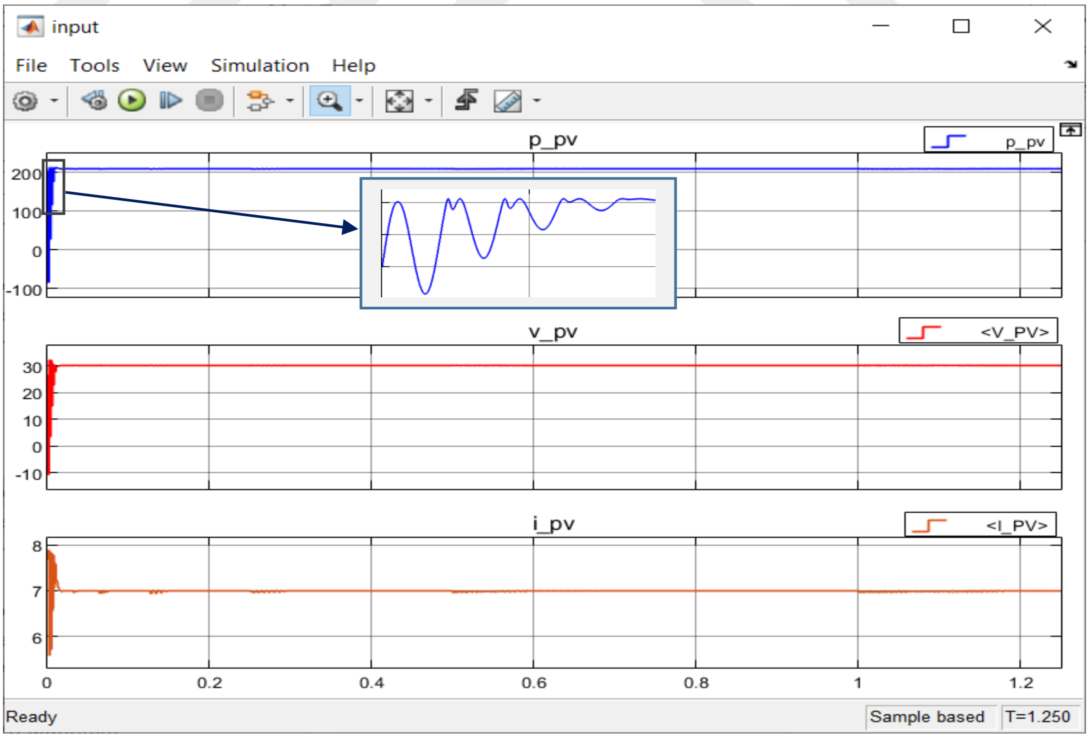

Figure 3.55 Shows the signal (power, voltage, current) generated in the photovoltaic cell.

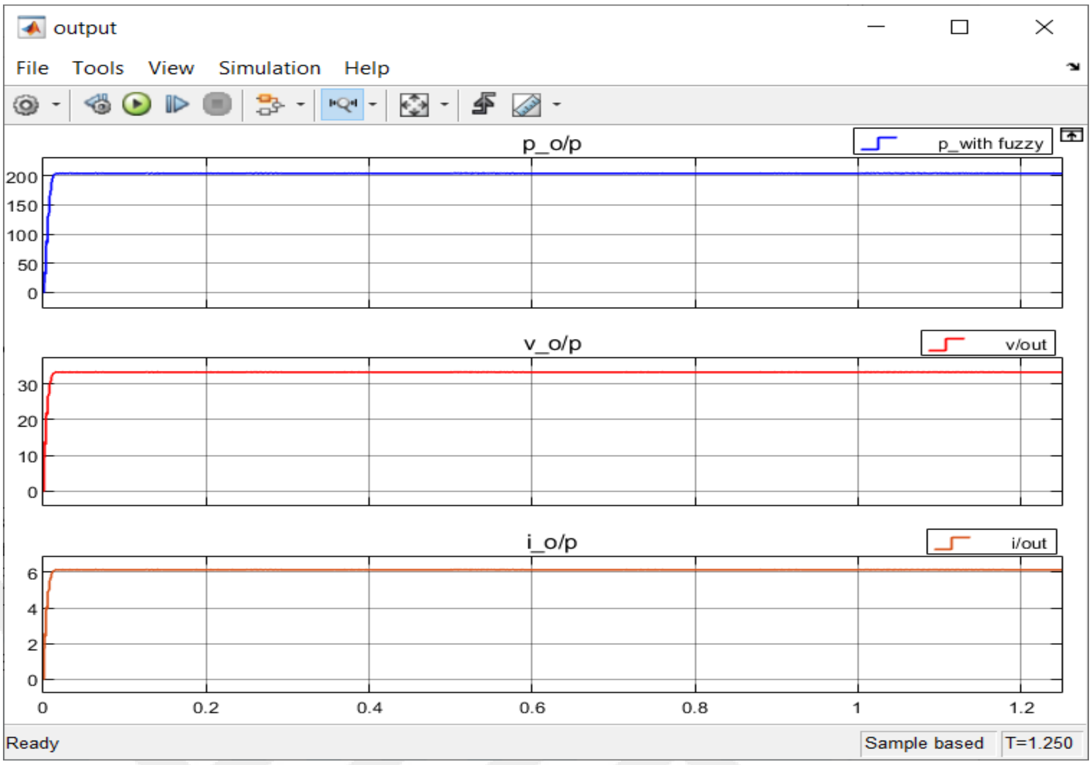

Figure 3.56 Shows the signal (power, voltage, current) of a DC-DC Boost Converter.

Table 3.12 represents the simulation results of a photovoltaic system using MPPT technology based on the FLC algorithm when tested under standard test conditions of radiation intensity (1000 W/m²) and temperature (25°C) and calculating the efficiency of the system.

Table 3.12 FLC algorithm simulation results under standard test conditions.

Irradiation at 25^{O}C	$P_{I/P}$ (W)	$V_{I/P}$ (V)	$I_{I/P}$ (A)	Efficiency of extracting power %	$P_{O/P}$ (W)	$V_{O/P}$ (V)	$I_{O/P}$ (A)	MPPT Technology Efficiency %
1000 W/m^2	210.1	30.05	6.914	98.56	204.6	33.26	6.152	97.38

2. Testing the FLC algorithm under changing weather conditions:

Change in the intensity of the solar radiation [600 1000 800 650 980 700] W/m^2 and the temperature is constant(25°C) Figure 3.57, Figure 3.58 and Figure 3.59.

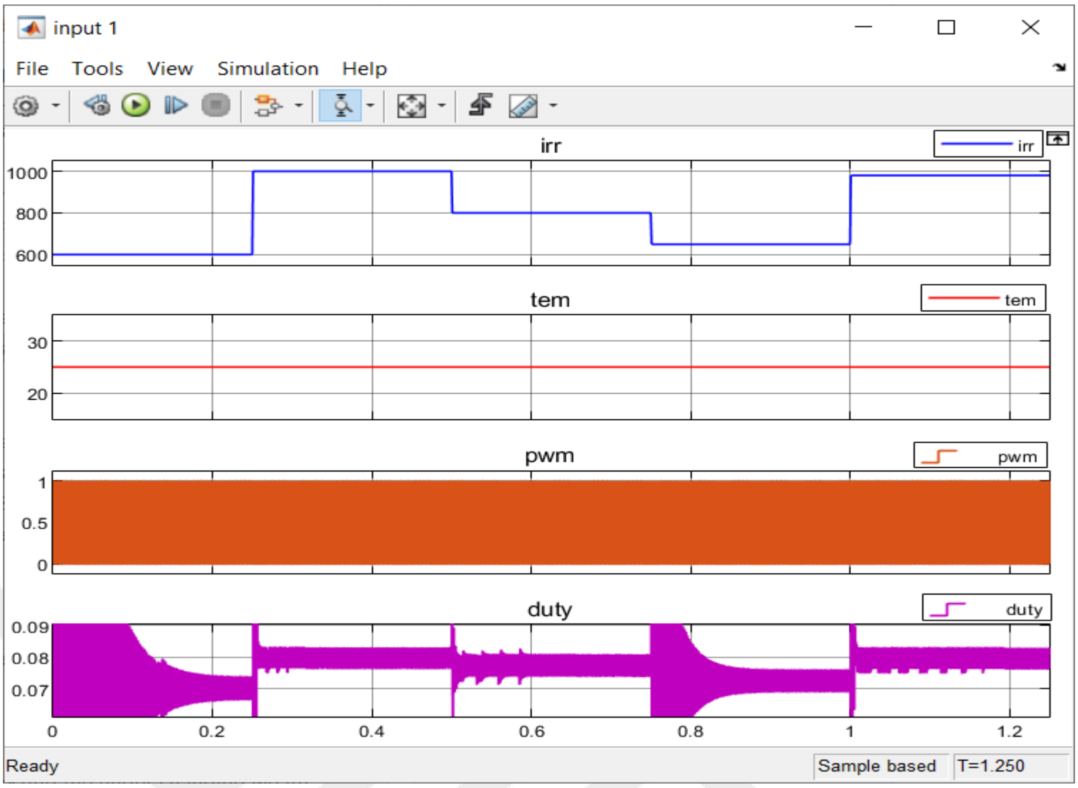

Figure 3.57 Shows the radiation intensity, the temperature applied to the photovoltaic cell, the control signal, and the duty cycle.

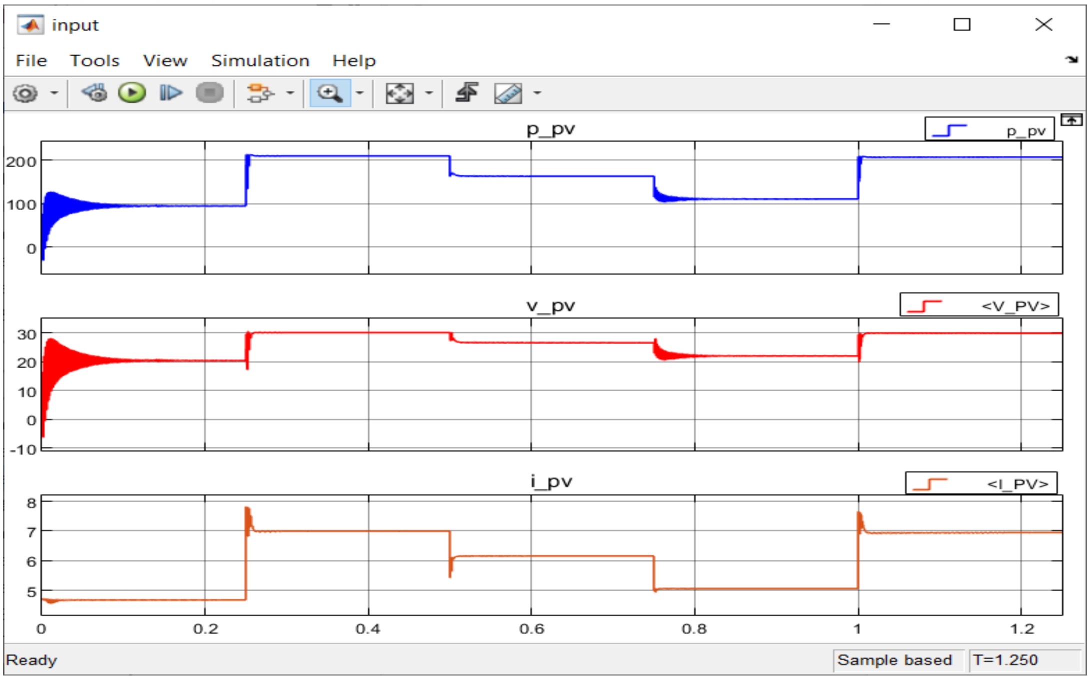

Figure 3.58 Shows the signal(power, voltage, current) generated in the photovoltaic cell When the irradiation intensity is variable.

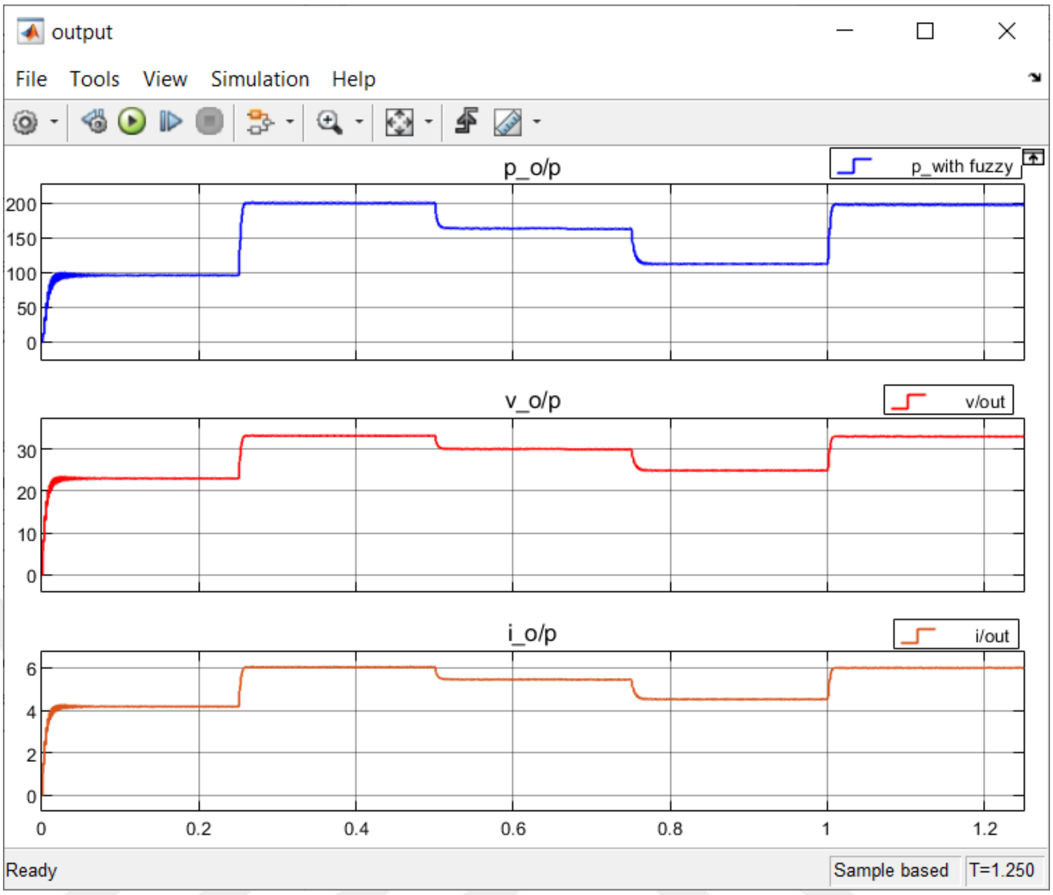

Figure 3.59 Shows the signal (power, voltage, current) of a DC-DC Boost Converter when the radiation intensity is variable.

Table 3.13 represents the simulation results of a photovoltaic system using MPPT technology based on the FLC algorithm when tested under variable test conditions when the temperature is variable and the radiation intensity is constant (1000 W/m²).

Table 3.13 FLC algorithm simulation results when the irradiation intensity is variable.

Irradiation at 25^{O} C	$P_{I/P}$ (W)	$V_{I/P}$ (V)	$I_{I/P}$ (A)	Efficiency of extracting power %	$P_{O/P}$ (W)	$V_{O/P}$ (V)	$I_{O/P}$ (A)	MPPT Technology Efficiency %
variable	205.7	29.95	6.869	98.46	200.3	33.01	6.067	97.37

Change in the temperature [55°C, 45°C, 35°C, and 27°C] and the intensity of the solar radiation is constant (1000) W/m^2 Figure 3.60, Figure 3.61 and Figure 3.62.

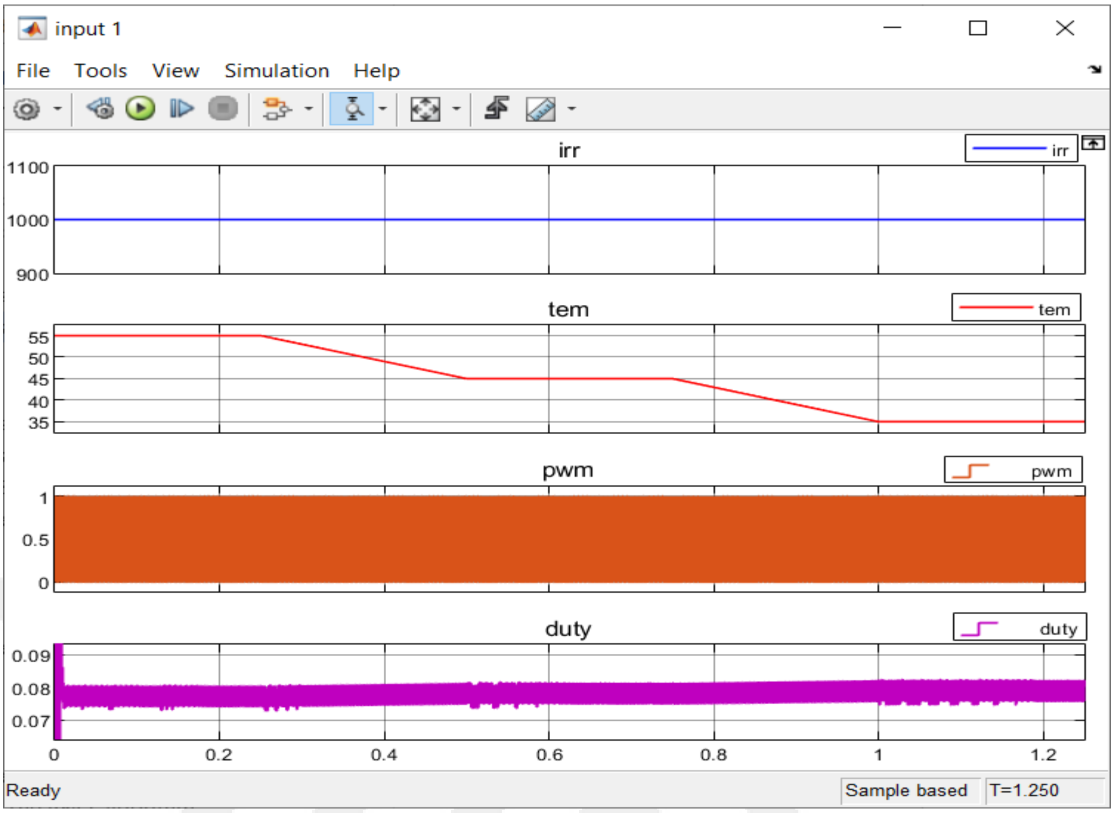

Figure 3.60 Shows the change in the temperature and constant radiation intensity.

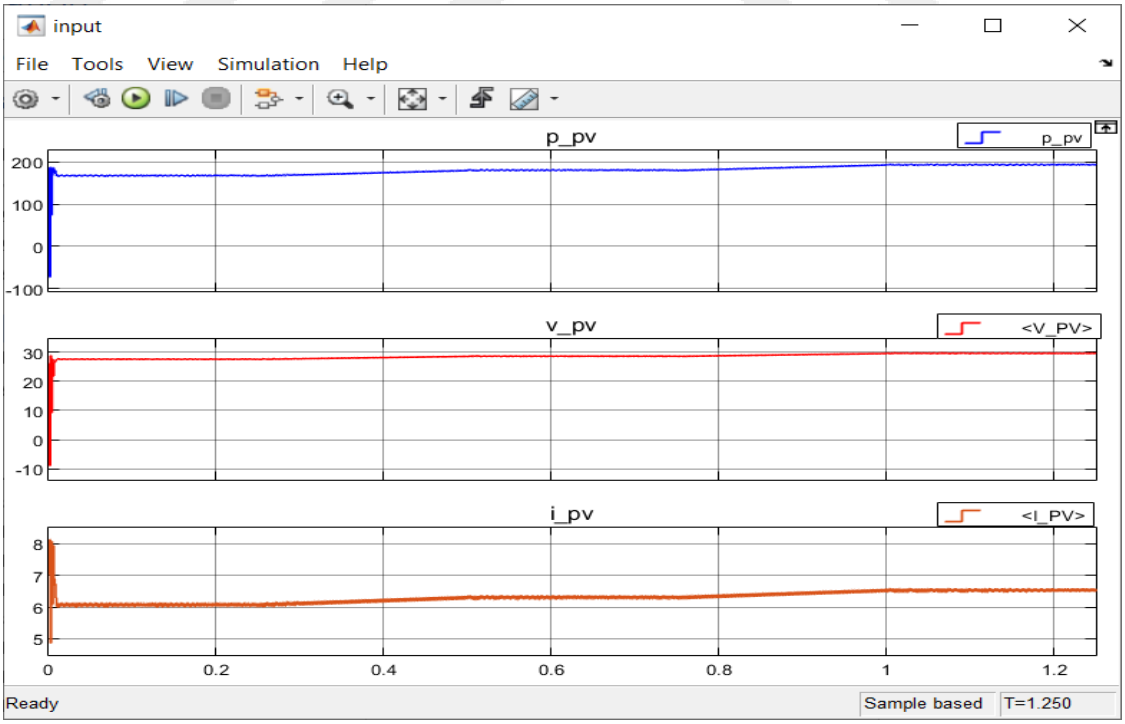

Figure 3.61 Shows the signal (power, voltage, current) generated in the photovoltaic cell when the temperature is variable.

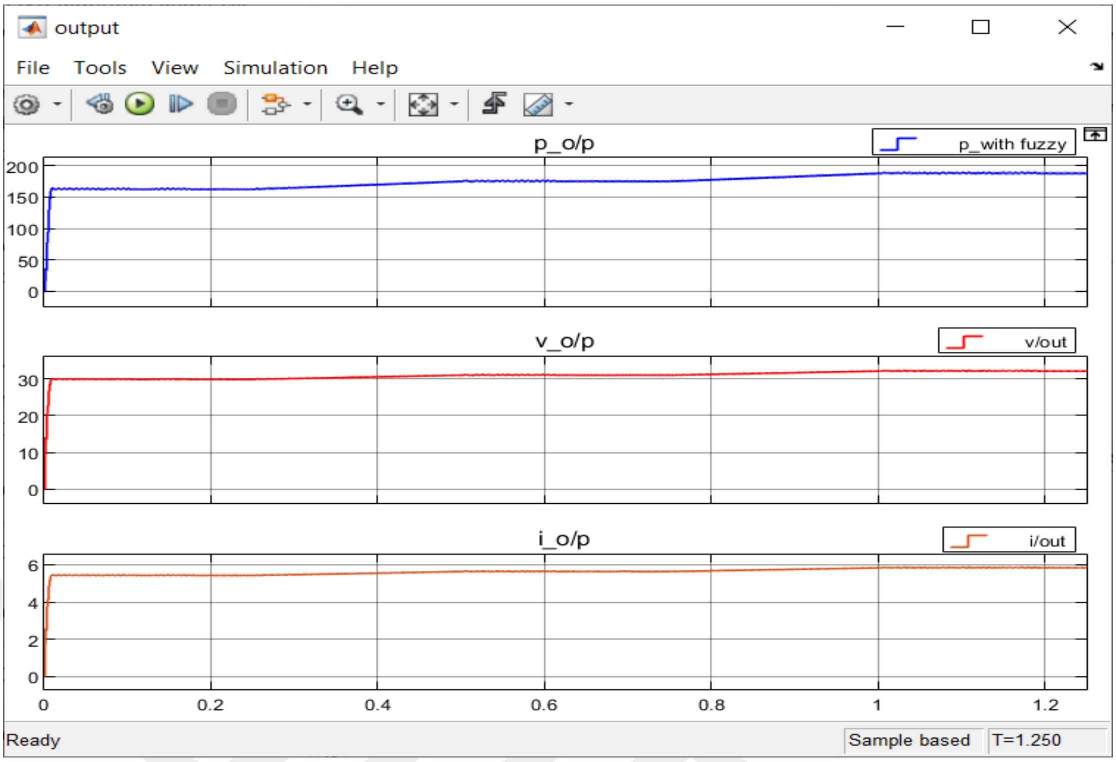

Figure 3.62 Shows the signal (power, voltage, current) of a DC-DC Boost Converter when the temperature is variable.

Table 3.14 represents the simulation results of a photovoltaic system using MPPT technology based on the FLC algorithm when tested under variable test conditions when the temperature is variable and the radiation intensity is constant (1000 W/m²).

Table 3.14 FLC algorithm simulation results when the temperature is different.

Temperature at [1000] W/m^2	$P_{I/P}$ (W)	$V_{I/P}$ (V)	$I_{I/P}$ (A)	Efficiency of extracting power %	$P_{O/P}$ (W)	$V_{O/P}$ (V)	$I_{O/P}$ (A)	MPPT Technology Efficiency %
variable	207.8	29.88	6.875	98.39	202.3	33.07	6.117	97.35

Photovoltaic system simulation with MPPT technology based on Particle Swarm Optimization (PSO) algorithm: Figure 3.63 shows a simulation of a photovoltaic system with MPPT technology based on the particle swarm optimization (PSO) algorithm using MATLAB/Simulink. Where the PSO algorithm tracks the MPP that extracts the maximum power from the solar panels by controlling the duty cycle of the DC-DC boost converter connected to the solar panel, which contains two inputs, one for the intensity of solar radiation and the other for the temperature. A simulation of an MPPT controller circuit based on particle swarm optimization (PSO) is designed in MATLAB/Simulink.

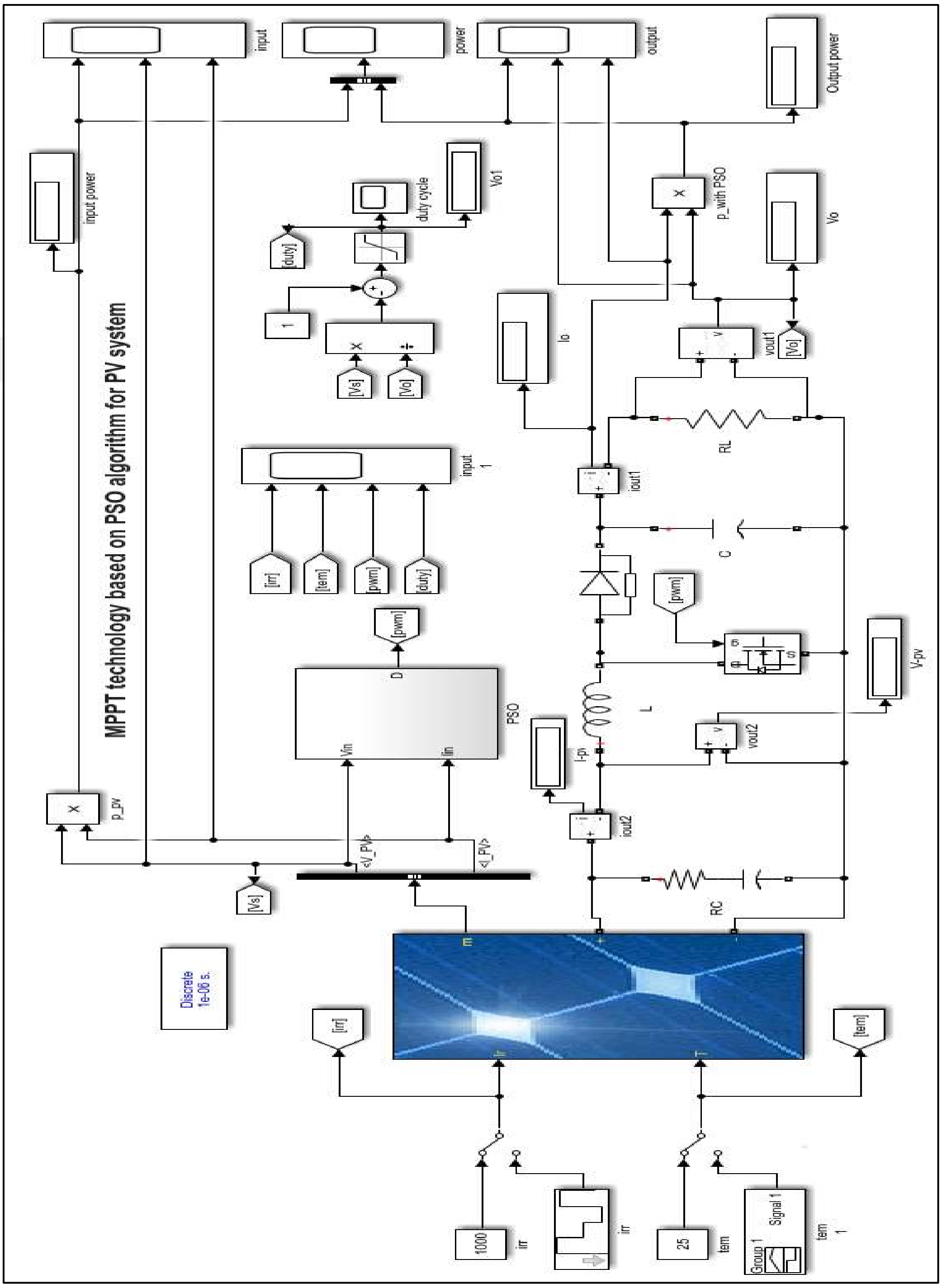

Figure 3.63 MPPT technology based on PSO algorithm with a DC-DC boost converter.

Table 3.15 shows simulation results using the resulting MATLAB/Simulink values (current, voltage, and power) obtained from solar panels as well as DC-DC boost converter output after applying the particle swarm optimization (PSO) algorithm when tested under volatile weather conditions (radiation different and constant temperature).

Table 3.15 PSO algorithm simulation results when the radiation intensity is variable.

Irradiation at 25^{O}C	$P_{I/P}$ (W)	$V_{I/P}$ (V)	$I_{I/P}$ (A)	$P_{O/P}$ (W)	$V_{O/P}$ (V)	$I_{O/P}$ (A)	MPPT Technology Efficiency %
1000 W/m^2	211.5	28.14	6.763	206.6	39.38	5.246	97.68
800 W/m^2	145	23.32	5.581	140.9	32.52	4.332	97.17
600 W/m^2	82.71	17.67	4.196	79.83	24.48	3.261	96.51
400 W/m^2	37.5	11.99	2.798	35.66	16.36	2.18	95.09
200 W/m^2	9.851	6.28	1.394	8.969	8.201	1.092	91.04

Table 3.16 shows simulation results using the resulting MATLAB/Simulink values (current, voltage, and power) obtained from solar panels as well as DC-DC boost converter output after applying the particle swarm optimization (PSO) algorithm when tested under volatile weather conditions (the intensity of solar radiation is constant and the temperature is variable).

Table 3.16 PSO algorithm simulation results when the temperature is different.

Temperature at 1000 W/m^2	$P_{I/P}$ (W)	$V_{I/P}$ (V)	$I_{I/P}$ (A)	$P_{O/P}$ (W)	$V_{O/P}$ (V)	$I_{O/P}$ (A)	MPPT Technology Efficiency %
15^{o} C	214.8	28.33	6.813	209.7	39.67	5.285	97.62
25^{o} C	211.5	28.14	6.763	206.6	39.38	5.246	97.68
35^{o} C	204.3	27.68	6.65	199.8	38.72	5.158	97.79
45^{o} C	194.3	27.03	6.488	190.2	37.79	5.033	97.88
55^{o} C	182.6	26.24	6.295	179	36.66	4.884	98.02

Solar system test with MPPT based on PSO algorithm in two test cases:

1. Testing the PSO algorithm under standard test conditions (STC):

In this case, the photovoltaic system based on the (PSO) algorithm was tested under standard test conditions (irr = 1000W/m^2, tem = 25°C) and plotted the input and output signals (voltage, current, power) Using MATLAB / Simulink Figure 3.64, Figure 3.65 and Figure 3.66.

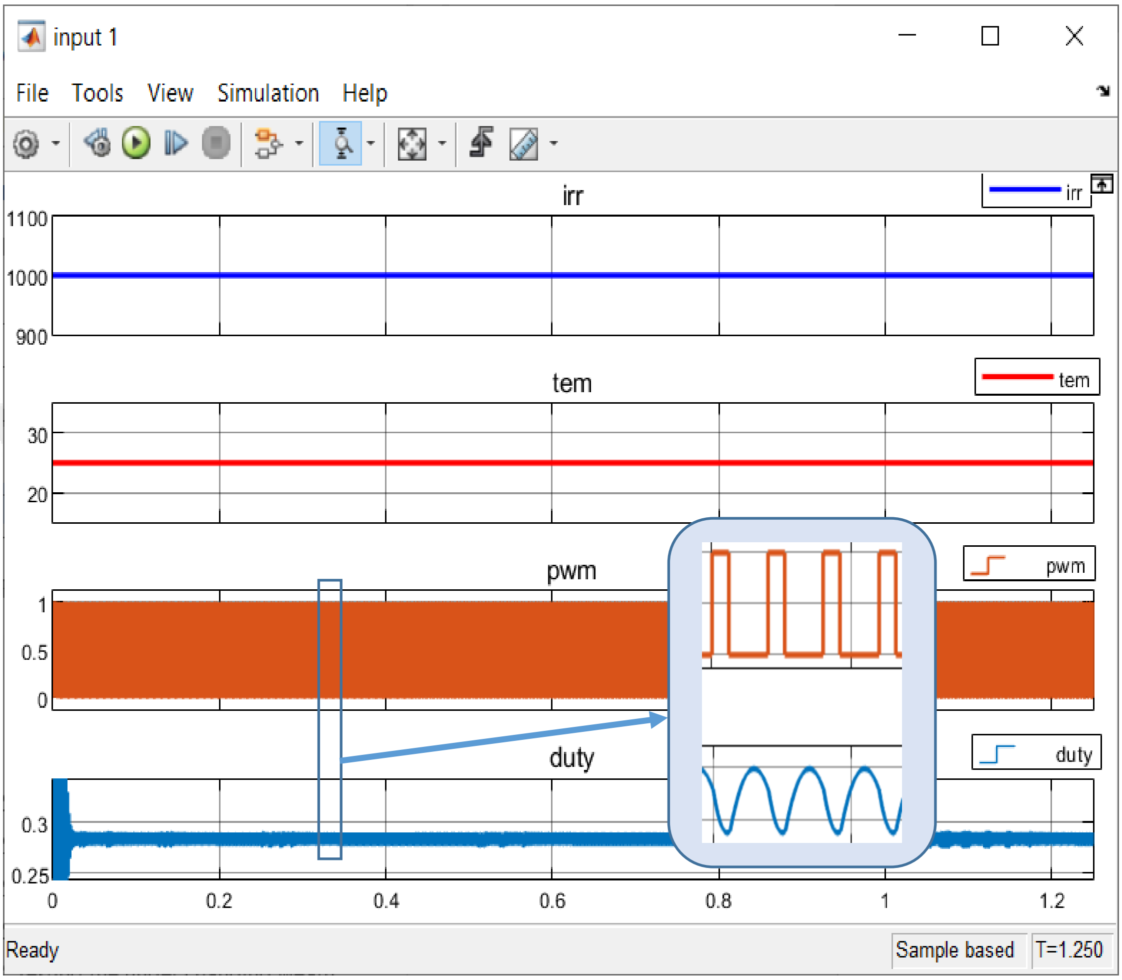

Figure 3.64 Shows the radiation intensity, the temperature applied to the photovoltaic cell, the control signal, and the duty cycle.

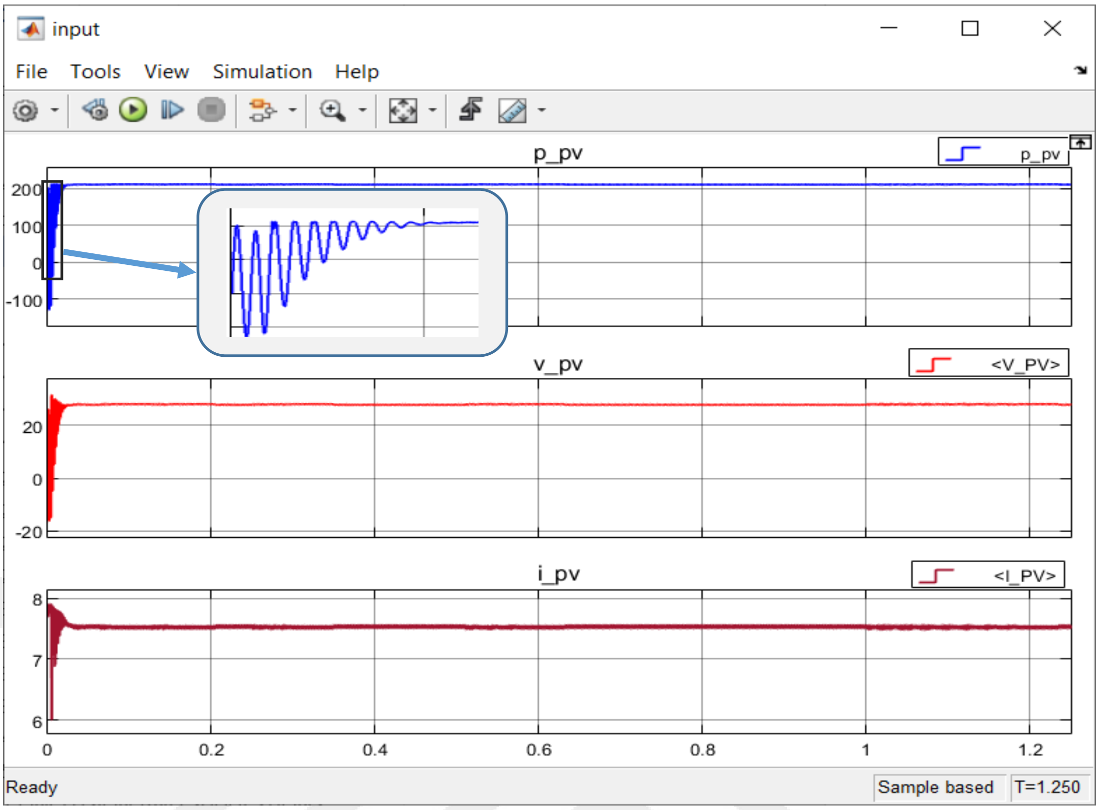

Figure 3.65 Shows the signal (power, voltage, current) generated in the photovoltaic cell.

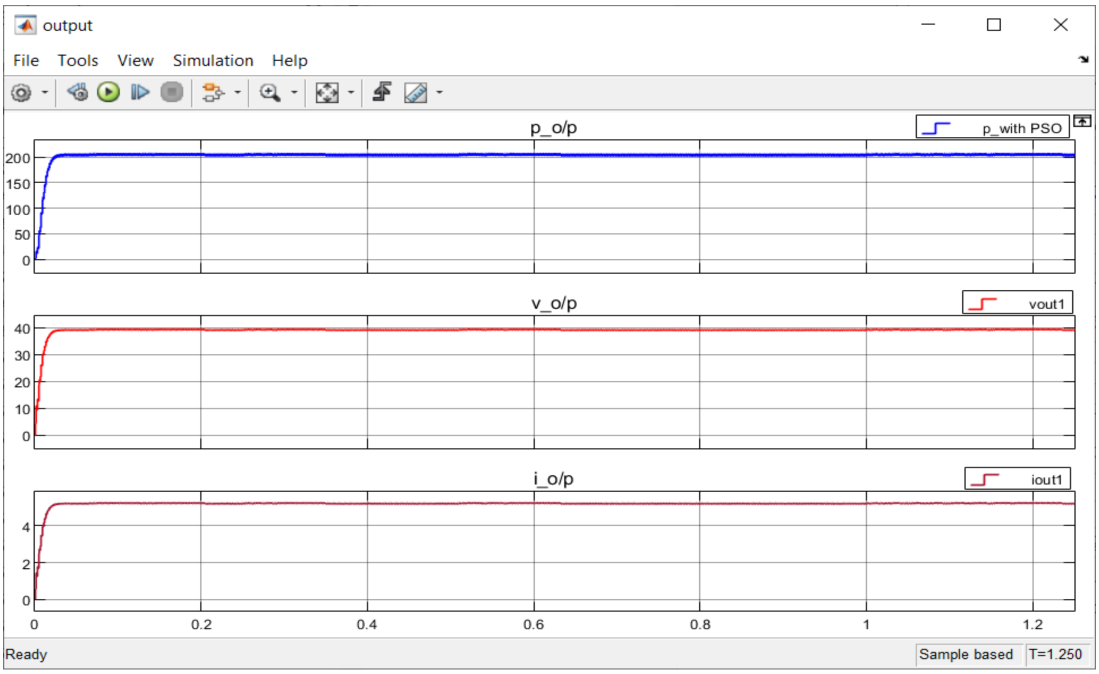

Figure 3.66 Shows the signal (power, voltage, current) of a DC-DC Boost Converter.

Table 3.17 represents the simulation results of a photovoltaic system using MPPT technology based on the PSO algorithm when tested under standard test conditions of radiation intensity (1000 W/m²) and temperature (25°C) and calculating the efficiency of the system.

Table 3.17 PSO algorithm simulation results under standard test conditions.

Irradiation at 25^{O} C	$P_{I/P}$ (W)	$V_{I/P}$ (V)	$I_{I/P}$ (A)	Efficiency of extracting power %	$P_{O/P}$ (W)	$V_{O/P}$ (V)	$I_{O/P}$ (A)	MPPT Technology Efficiency %
1000 W/m^2	211.5	28.14	6.763	99.22	206.6	39.38	5.246	97.68

2. Testing the PSO algorithm under changing weather conditions:

Change in the intensity of the solar radiation [600, 1000, 800, 650, 980, 700] W/m^2 and the temperature is constant(25°C) Figure 3.67, Figure 3.68 and Figure 3.69.

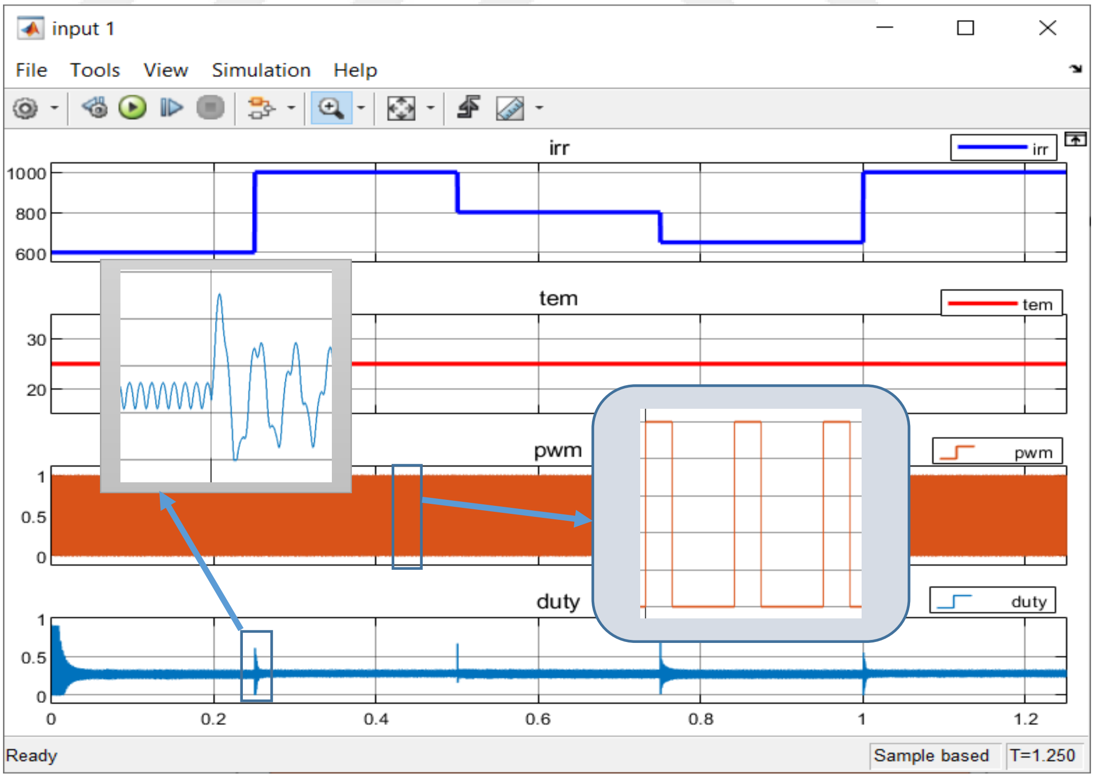

Figure 3.67 Shows the radiation intensity, the temperature applied to the photovoltaic cell, the control signal, and the duty cycle.

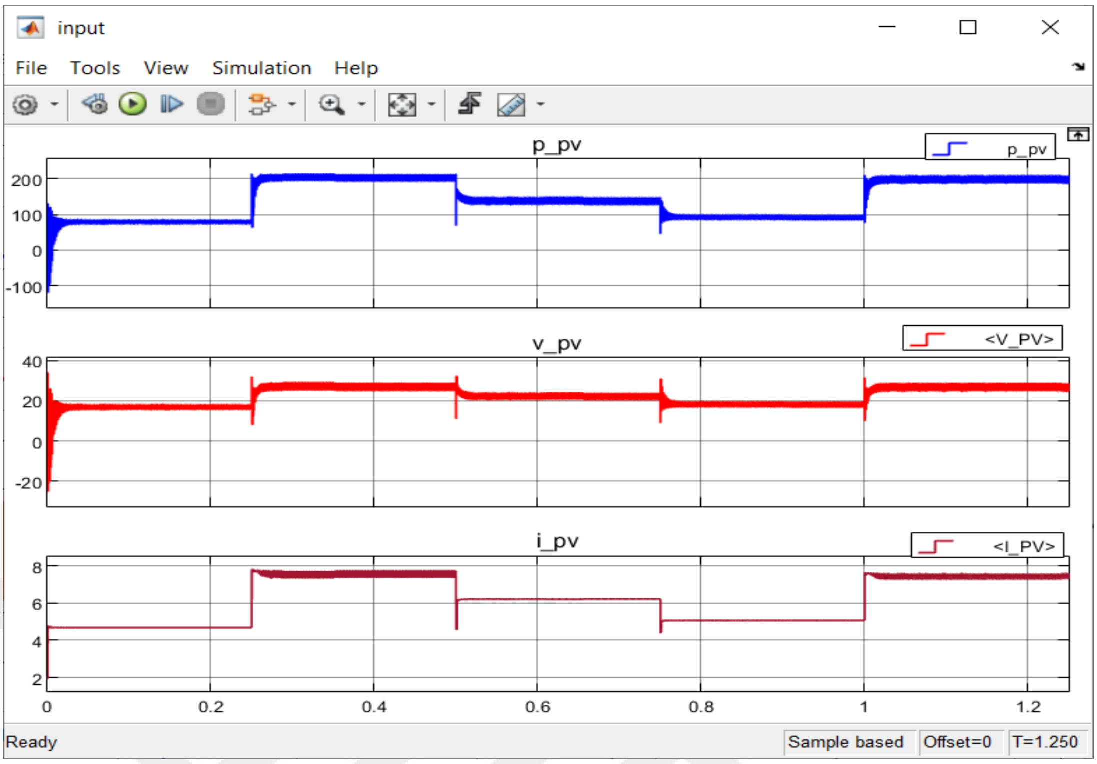

Figure 3.68 Shows the signal(power, voltage, current) generated in the photovoltaic cell When the irradiation intensity is variable.

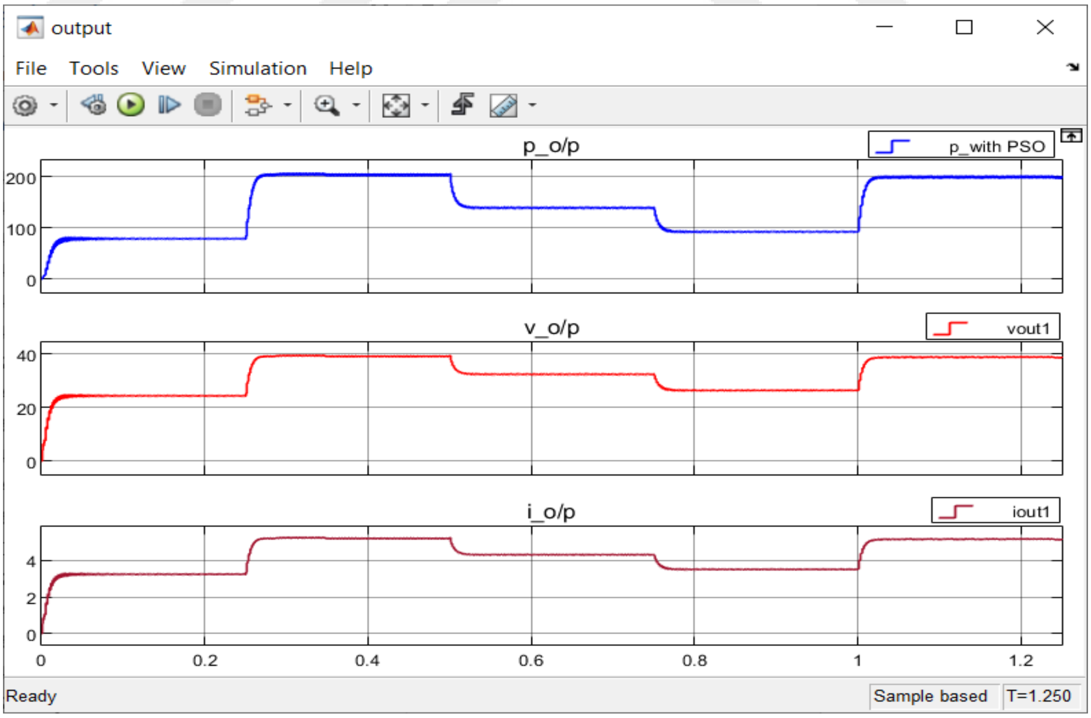

Figure 3.69 Shows the signal (power, voltage, current) of a DC-DC Boost Converter when the irradiation intensity is variable.

Table 3.18 represents the simulation results of a photovoltaic system using MPPT control technology based on the PSO algorithm when tested under variable weather conditions when the solar radiation intensity is variable [600 1000 800 650 980 700] W/m^2 and the temperature is constant (25°C).

Table 3.18 PSO algorithm simulation results when the irradiation intensity is variable.

Irradiation at 25^O C	$P_{I/P}$ (W)	$V_{I/P}$ (V)	$I_{I/P}$ (A)	Efficiency of extracting power %	$P_{O/P}$ (W)	$V_{O/P}$ (V)	$I_{O/P}$ (A)	MPPT Technology Efficiency %
variable	206.1	27.77	6.673	98.65	201.2	38.86	5.177	97.62

Change in the temperature [50°C, 45°C, 35°C, and 27°C] and the intensity of the solar radiation is constant (1000) W/m^2 Figure 3.70, Figure 3.71 and Figure 3.72.

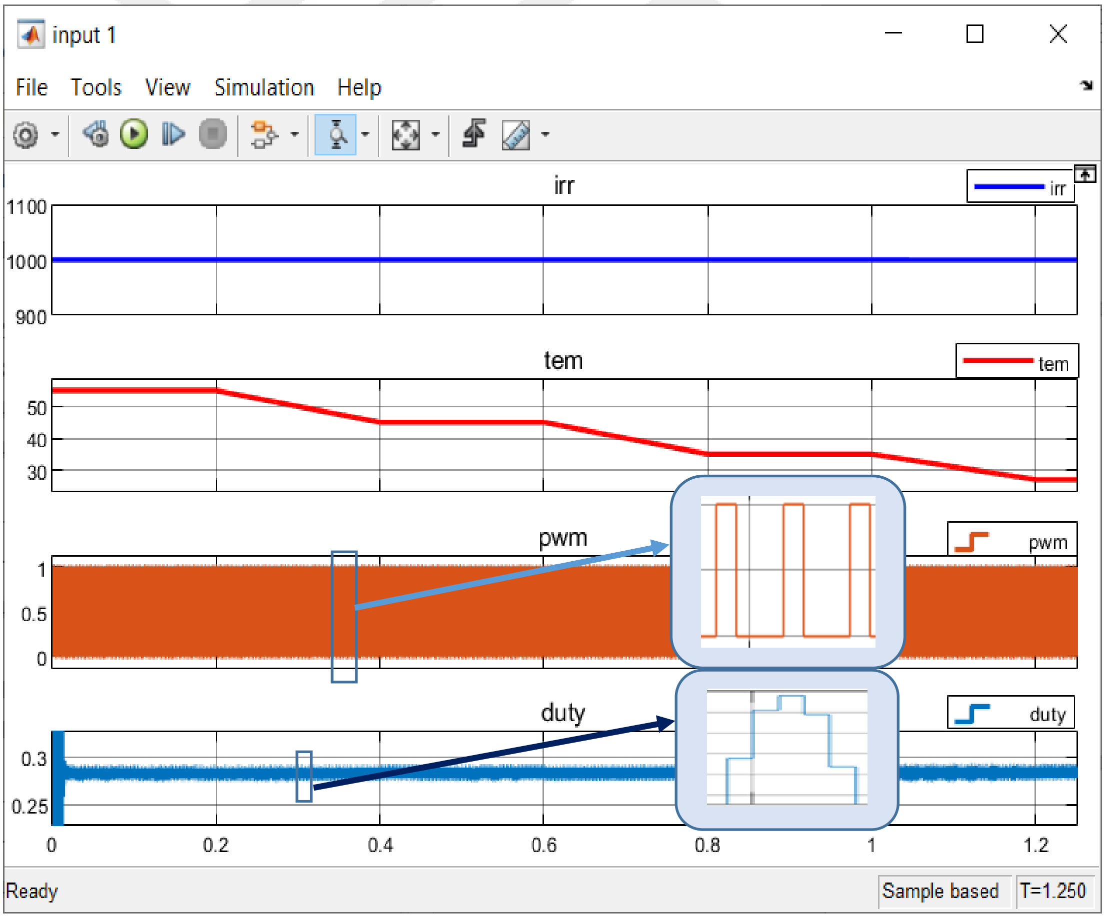

Figure 3.70 Shows the radiation intensity, the temperature applied to the photovoltaic cell, the control signal, and the duty cycle.

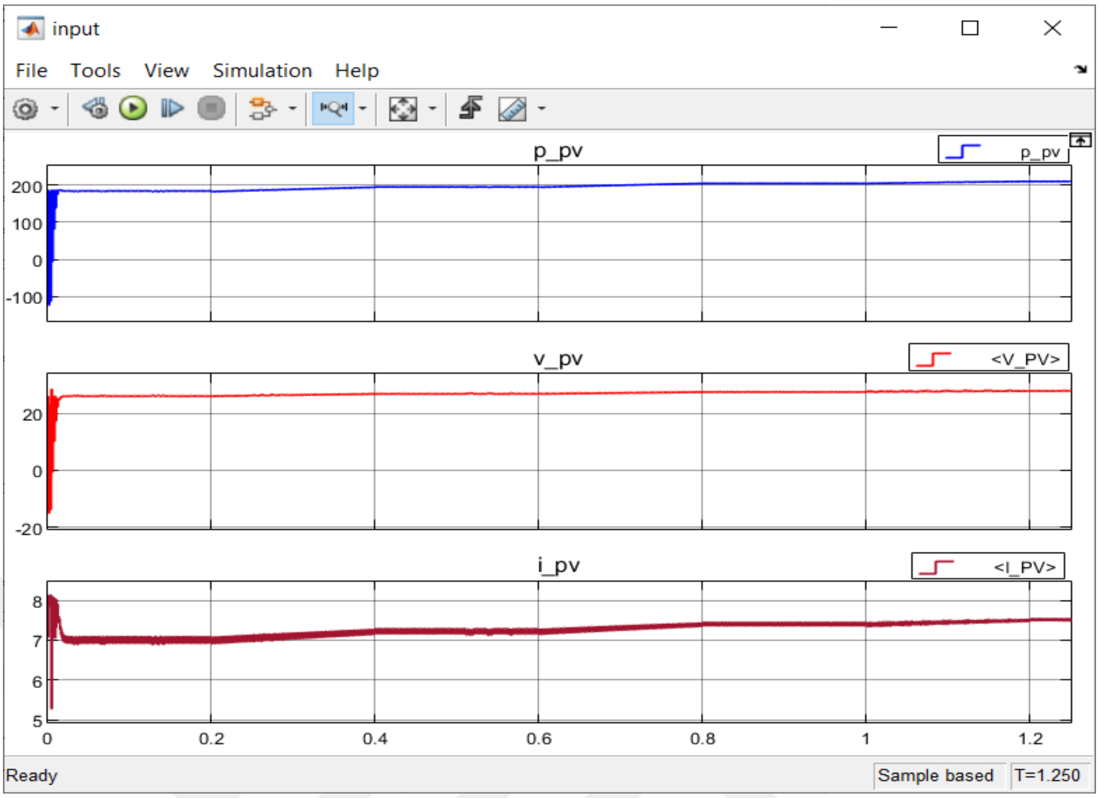

Figure 3.71 Shows the signal (power, voltage, current) generated in the photovoltaic cell when the temperature is variable.

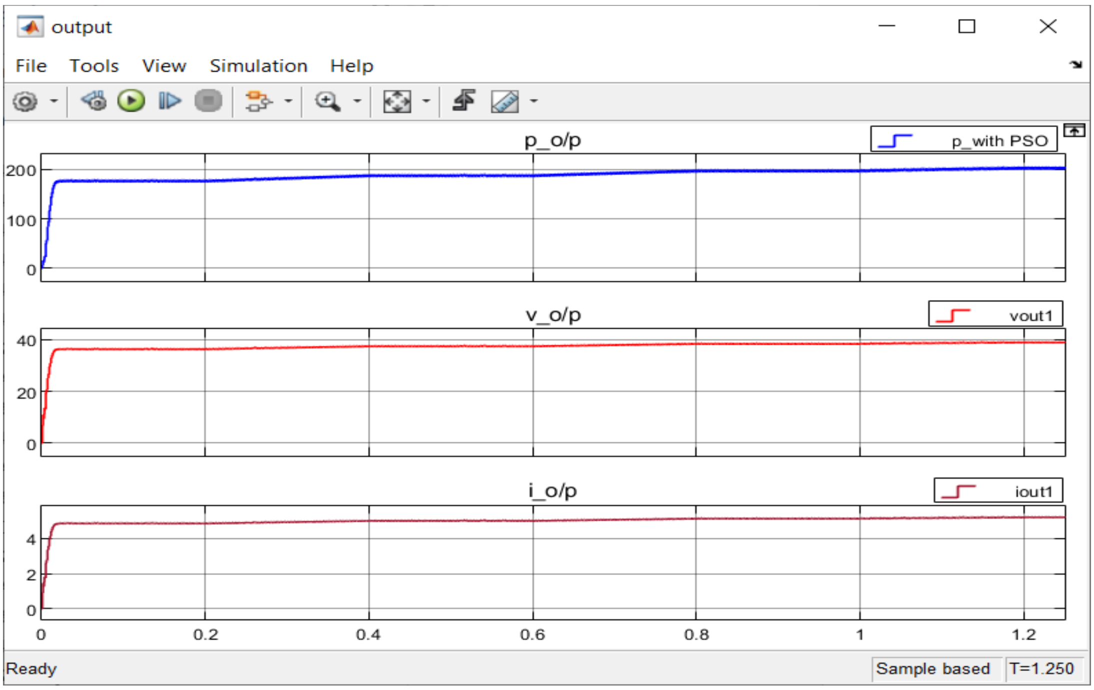

Figure 3.72 Shows the signal (power, voltage, current) of a DC-DC Boost Converter when the temperature is variable.

Table 3.19 represents the simulation results of a photovoltaic system using MPPT technology based on the PSO algorithm when tested under variable test conditions when the temperature is variable and the radiation intensity is constant (1000 W/m²).

Table 3.19 PSO algorithm simulation results when the temperature is different.

Temperature at [1000] W/m^2	$P_{I/P}$ (W)	$V_{I/P}$ (V)	$I_{I/P}$ (A)	efficiency of extracting power %	$P_{O/P}$ (W)	$V_{O/P}$ (V)	$I_{O/P}$ (A)	MPPT Technology Efficiency %
variable	210.4	28.06	6.745	99.62	205.5	39.28	5.232	97.67

4. RESULTS AND DISCUSSION

The results we obtained by simulating the photovoltaic system using MATLAB / Simulink, which contains an MPPT type charge controller based on three types of algorithms (P&O, FLC, PSO), where the system was operated under standard test conditions(irr=1000W/m2, tem=250C) and other variable weather conditions (Variation of solar irradiation intensity and temperature change) with each algorithm for MPP point tracking and extracting the maximum energy from solar panels and supplying constant power to batteries or loads.

In the following, I will present the results obtained for (current, voltage, power) by simulating a photovoltaic system with electrical characteristic curves obtained from solar panels (current, voltage, power) and output signals of a DC-DC boost converter that Its work cycle is controlled by MPPT technology based on the three algorithms (P&O, FLC, PSO) under standard and variable test conditions.

4.1 Testing Under Standard Test Conditions (STC)

4.1.1 The P&O algorithm

In Table 4.1 see P&O algorithm simulation results under standard test conditions and Figure 4.1 shows the signal of the input power and the output power when the P&O algorithm is applied

Table 4.1 P&O algorithm simulation results under standard test conditions.

Irradiation at 25^{O} C	$P_{I/P}$ (W)	$V_{I/P}$ (V)	$I_{I/P}$ (A)	Efficiency of extracting power %	$P_{O/P}$ (W)	$V_{O/P}$ (V)	$I_{O/P}$ (A)	MPPT Technology Efficiency %
1000 W/m^2	206	26.89	6.934	96.64	196	36.49	5.37	95.14

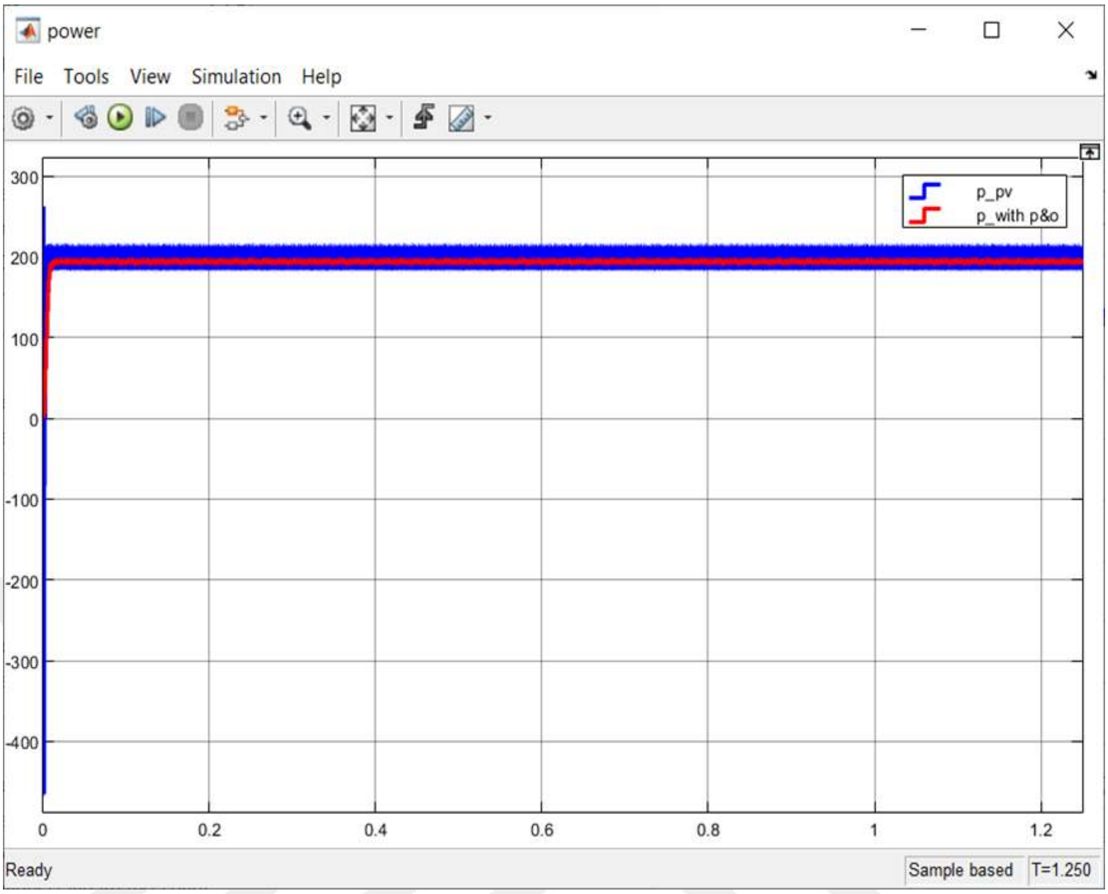

Figure 4.1 Shows the signal of the input power and the output power when the P&O algorithm is applied.

4.1.2 The FLC algorithm

In Table 4.2 we can see FLC algorithm simulation results under standard test conditions and Figure 4.2 shows the signal of the input power and the output power when the FLC algorithm is applied.

Table 4.2 FLC algorithm simulation results under standard test conditions.

Irradiation at 25^{O}C	$P_{I/P}$ (W)	$V_{I/P}$ (V)	$I_{I/P}$ (A)	Efficiency of extracting power %	$P_{O/P}$ (W)	$V_{O/P}$ (V)	$I_{O/P}$ (A)	MPPT Technology Efficiency %
1000 W/m^2	210.1	30.05	6.914	98.56	204.6	33.26	6.152	97.38

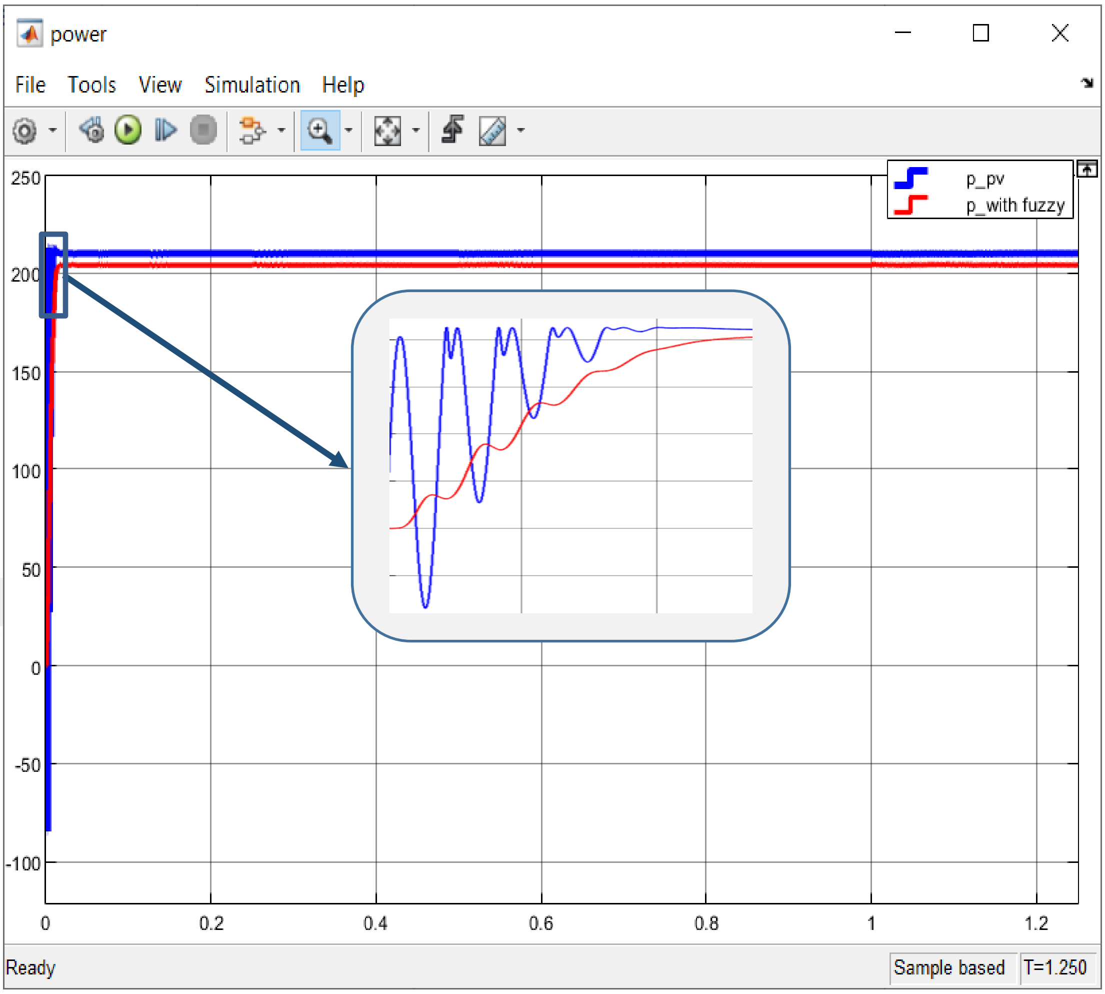

Figure 4.2 Shows the signal of the input power and the output power when the FLC algorithm is applied.

4.1.3 The PSO algorithm

In Table 4.3 we can see PSO algorithm simulation results under standard test conditions and Figure 4.3 shows the signal of the input power and the output power when the PSO algorithm is applied.

Table 4.3 PSO algorithm simulation results under standard test conditions.

Irradiation at 25^{O}C	$P_{I/P}$ (W)	$V_{I/P}$ (V)	$I_{I/P}$ (A)	Efficiency of extracting power %	$P_{O/P}$ (W)	$V_{O/P}$ (V)	$I_{O/P}$ (A)	MPPT Technology Efficiency %
1000 W/m^2	211.5	28.14	6.763	99.22	206.6	39.38	5.246	97.68

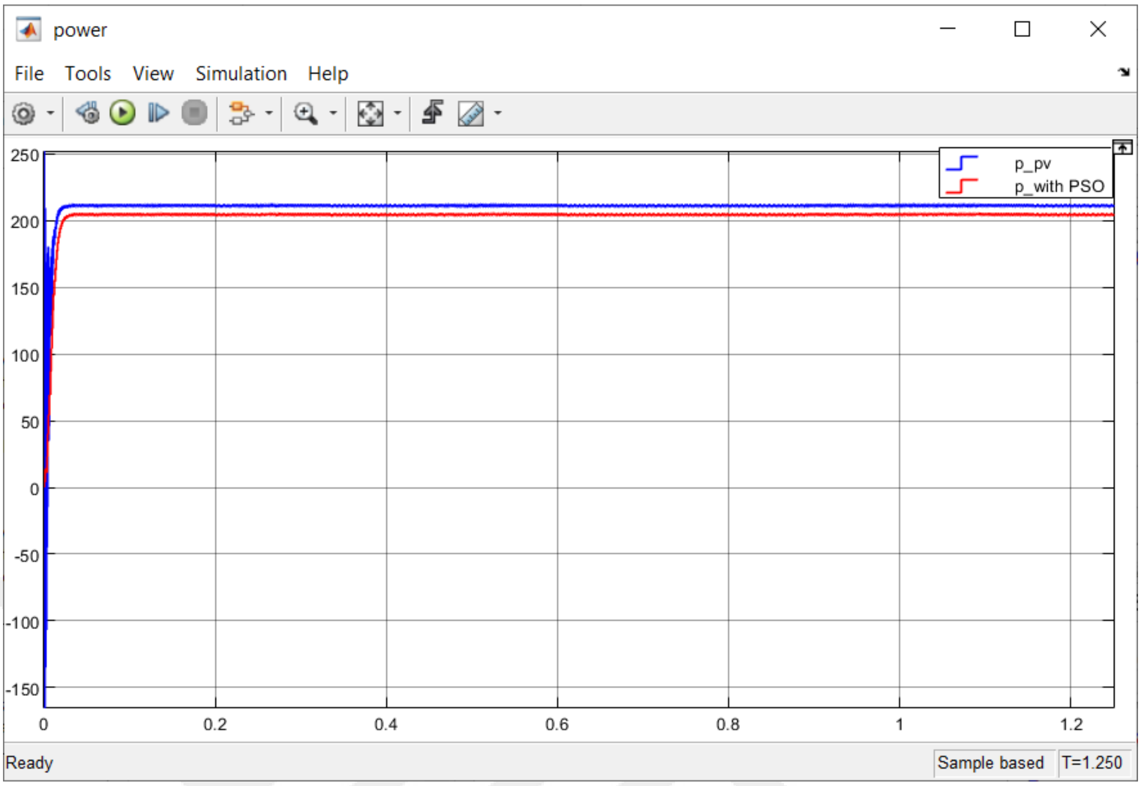

Figure 4.3 Shows the signal of the input power and the output power when the PSO algorithm is applied.

4.2 Testing the Under Changing Weather Conditions (Variable Irradiation Intensity)

4.2.1 The P&O algorithm

In Table 4.4 we can see P&O algorithm simulation results when the irradiation intensity is variable and Figure 4.4 shows the input and output power with the P&O algorithm when the irradiation intensity is variable.

Table 4.4 P&O algorithm simulation results when the irradiation intensity is variable.

Irradiation at 25^{O} C	$P_{I/P}$ (W)	$V_{I/P}$ (V)	$I_{I/P}$ (A)	efficiency of extracting power %	$P_{O/P}$ (W)	$V_{O/P}$ (V)	$I_{O/P}$ (A)	MPPT Technology Efficiency %
variable	201.2	26.8	8.394	96.31	186.7	35.62	5.242	92.79

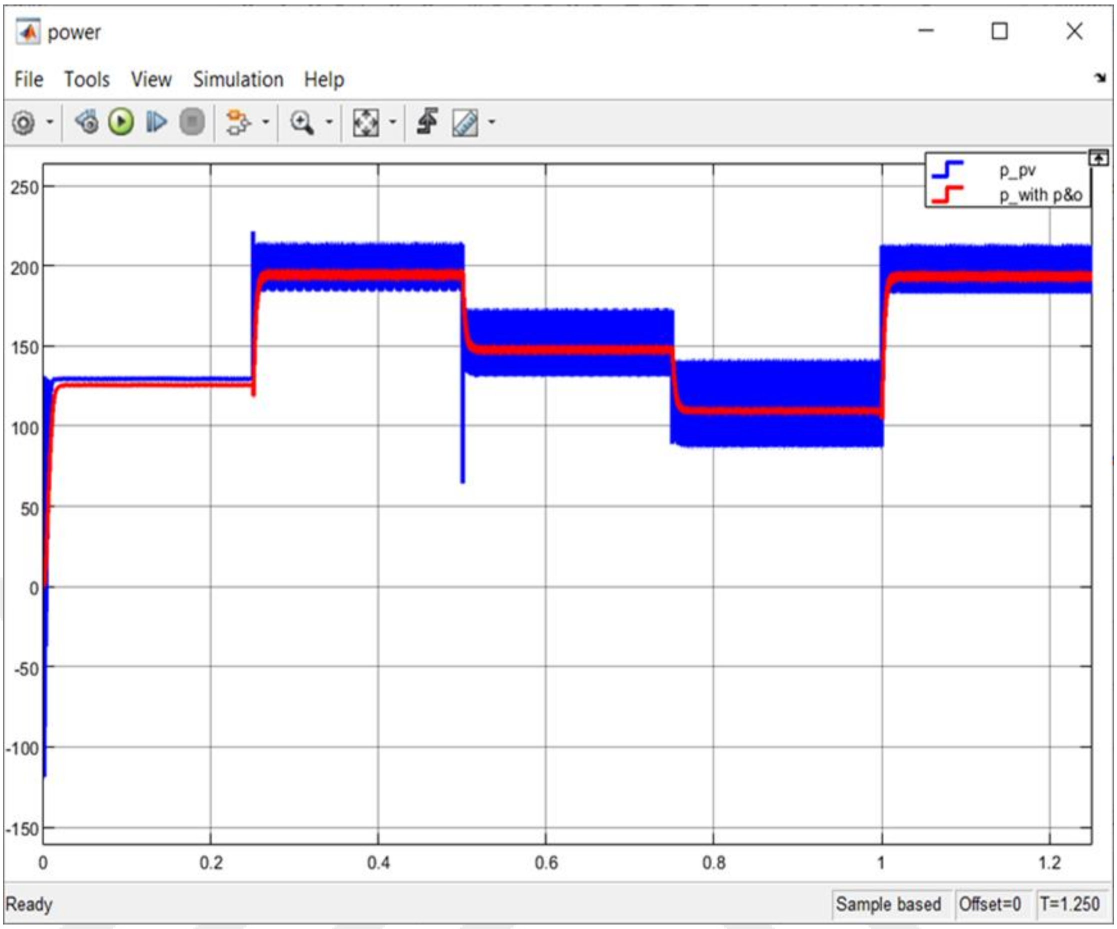

Figure 4.4 Shows the input and output power with the P&O algorithm when the irradiation intensity is variable.

4.2.2 The FLC algorithm

In Table 4.5 we can see FLC algorithm simulation results when the irradiation intensity is variable and Figure 4.5 shows the input power and the output power with the FLC algorithm when the radiation intensity is variable.

Table 4.5 FLC algorithm simulation results when the irradiation intensity is variable.

Irradiation at 25^{O} C	$P_{I/P}$ (W)	$V_{I/P}$ (V)	$I_{I/P}$ (A)	The efficiency of extracting power %	$P_{O/P}$ (W)	$V_{O/P}$ (V)	$I_{O/P}$ (A)	MPPT Technology Efficiency %
variable	205.7	29.95	6.869	98.46	200.3	33.01	6.067	97.37

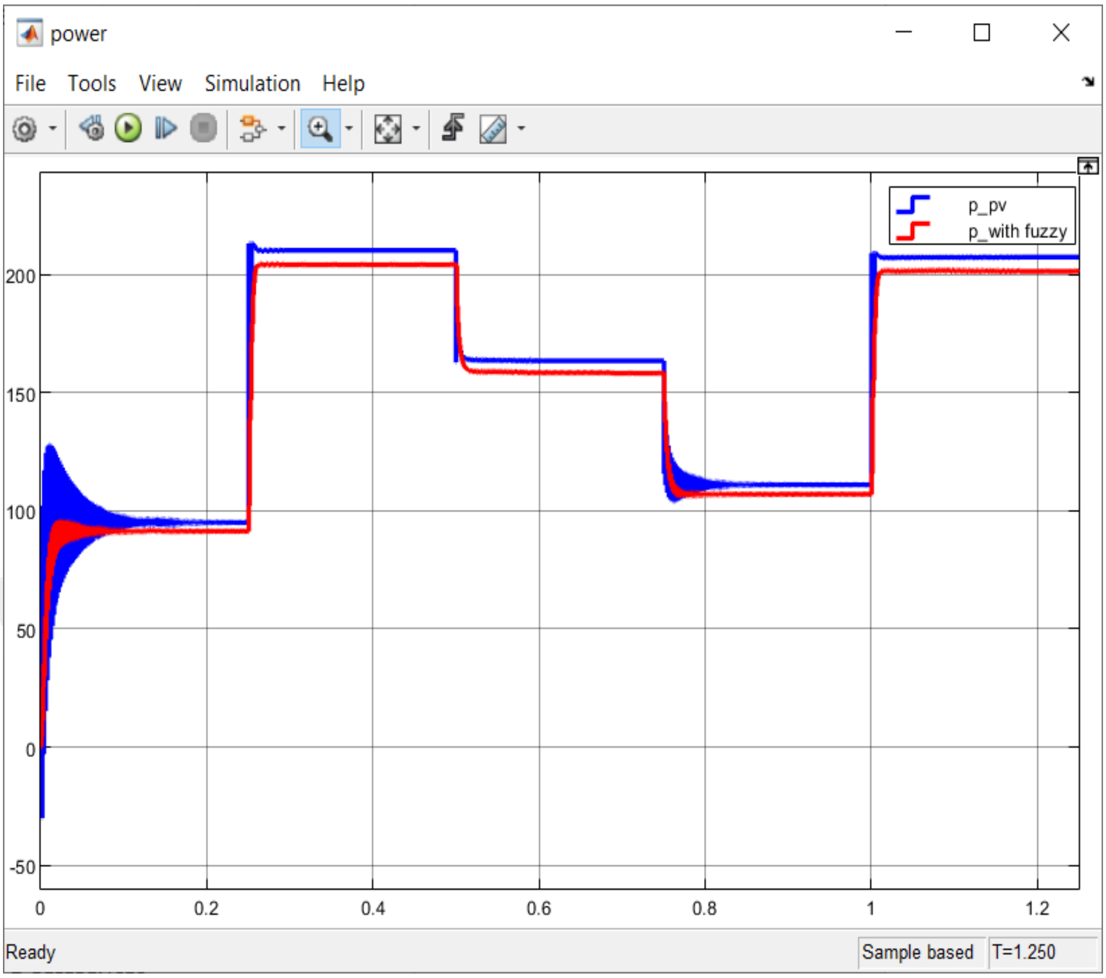

Figure 4.5 Shows the input power and the output power with the FLC algorithm when the radiation intensity is variable.

4.2.3 The PSO algorithm

In Table 4.6 we can see PSO algorithm simulation results when the irradiation intensity is variable and in Figure 4.6 shows the input power and the output power with the PSO algorithm when the radiation intensity is variable.

Table 4.6 PSO algorithm simulation results when the irradiation intensity is variable.

Irradiation at 25^{O} C	$P_{I/P}$ (W)	$V_{I/P}$ (V)	$I_{I/P}$ (A)	Efficiency of extracting power %	$P_{O/P}$ (W)	$V_{O/P}$ (V)	$I_{O/P}$ (A)	MPPT Technology Efficiency %
variable	206.1	27.77	6.673	98.65	201.2	38.86	5.177	97.62

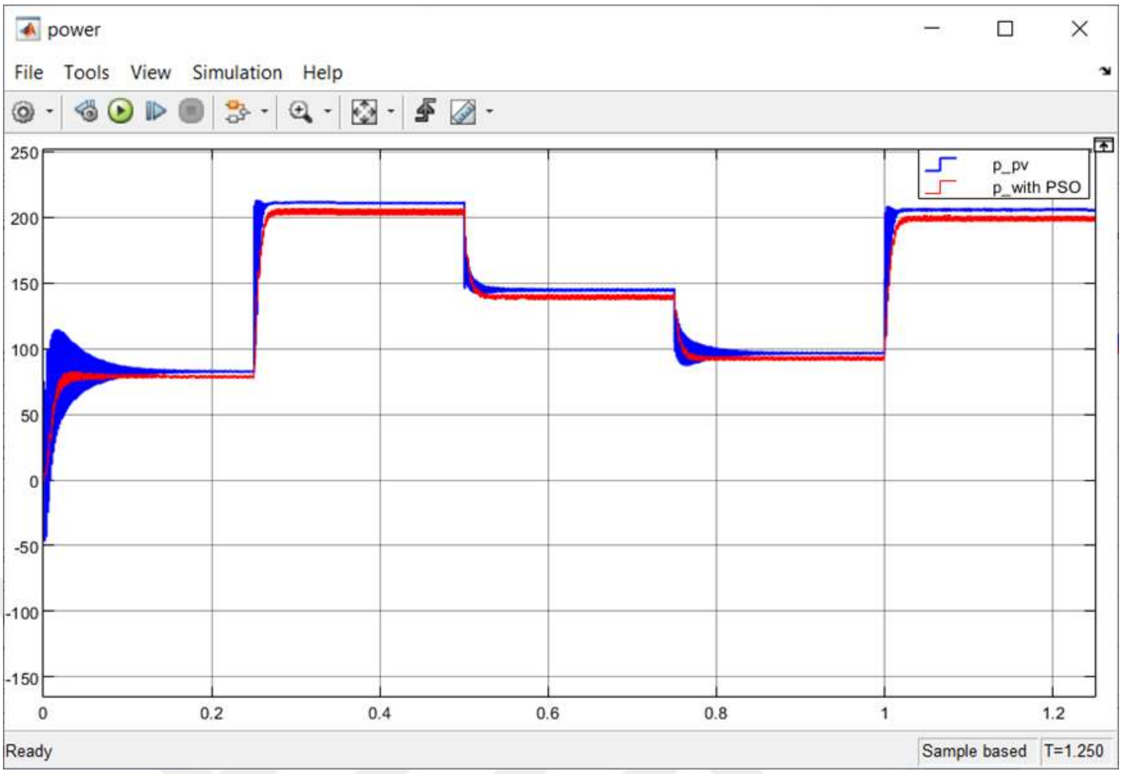

Figure 4.6 Shows the input power and the output power with the PSO algorithm when the radiation intensity is variable.

4.3 Testing the Under Changing Weather Conditions (Change in the Temperature)

4.3.1 The P&O algorithm

In Table 4.7 P&O algorithm simulation results when the temperature is different and in Figure 4.7 shows the input and output power with the P&O algorithm when the temperature is variable.

Table 4.7 P&O algorithm simulation results when the temperature is different.

temperature at [1000] W/m^2	$P_{I/P}$ (W)	$V_{I/P}$ (V)	$I_{I/P}$ (A)	Efficiency of extracting power %	$P_{O/P}$ (W)	$V_{O/P}$ (V)	$I_{O/P}$ (A)	MPPT Technology Efficiency %
variable	199.2	25.82	8.423	94.31	190.6	35.99	5.296	95.68

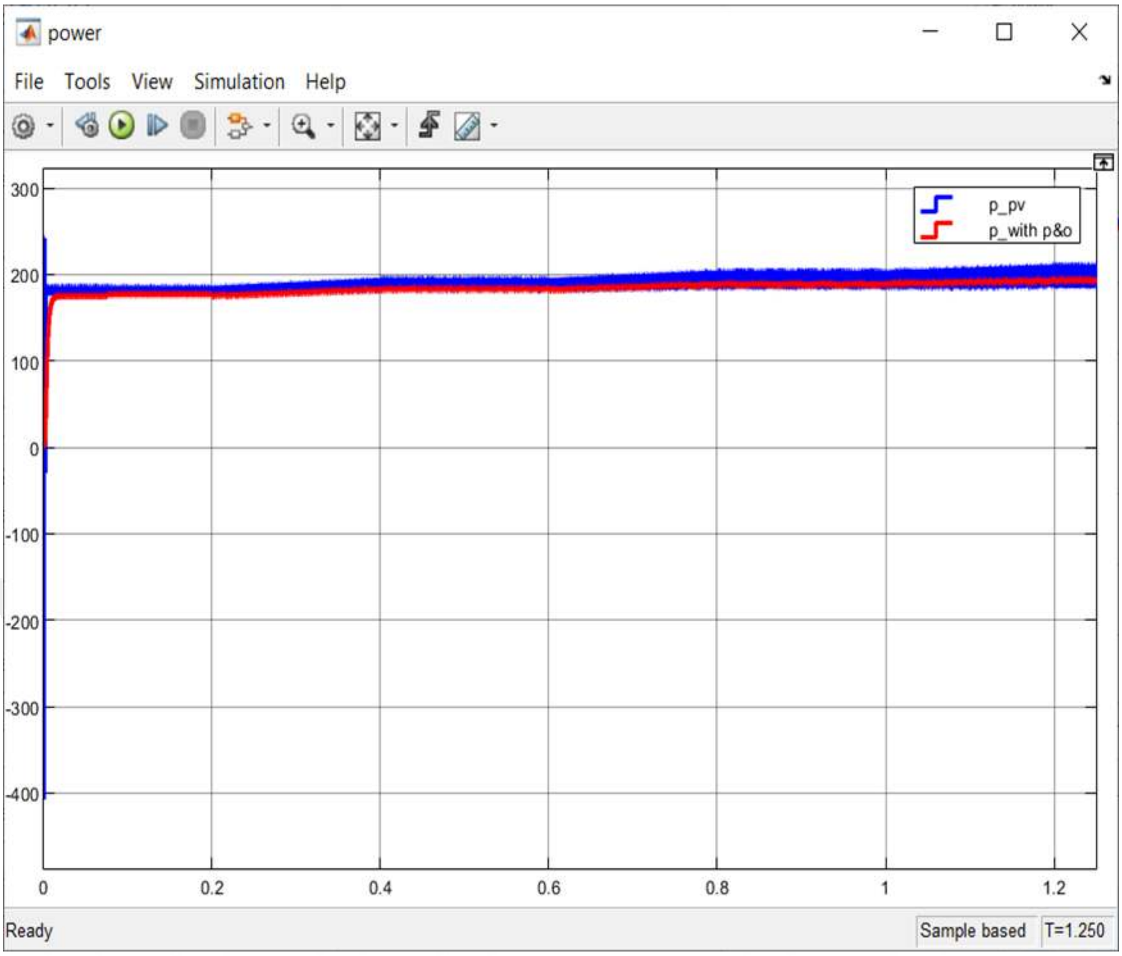

Figure 4.7 Shows the input and output power with the P&O algorithm when the temperature is variable

4.3.2 The FLC algorithm

In Table 4.8 we can see FLC algorithm simulation results when the temperature is different and in Figure 4.8 shows the input power and the output power with the FLC algorithm when the temperature is variable.

Table 4.8 FLC algorithm simulation results when the temperature is different.

Temperature at [1000] W/m^2	$P_{I/P}$ (W)	$V_{I/P}$ (V)	$I_{I/P}$ (A)	Efficiency of extracting power %	$P_{O/P}$ (W)	$V_{O/P}$ (V)	$I_{O/P}$ (A)	MPPT Technology Efficiency %
variable	207.8	29.88	6.875	98.39	202.3	33.07	6.117	97.35

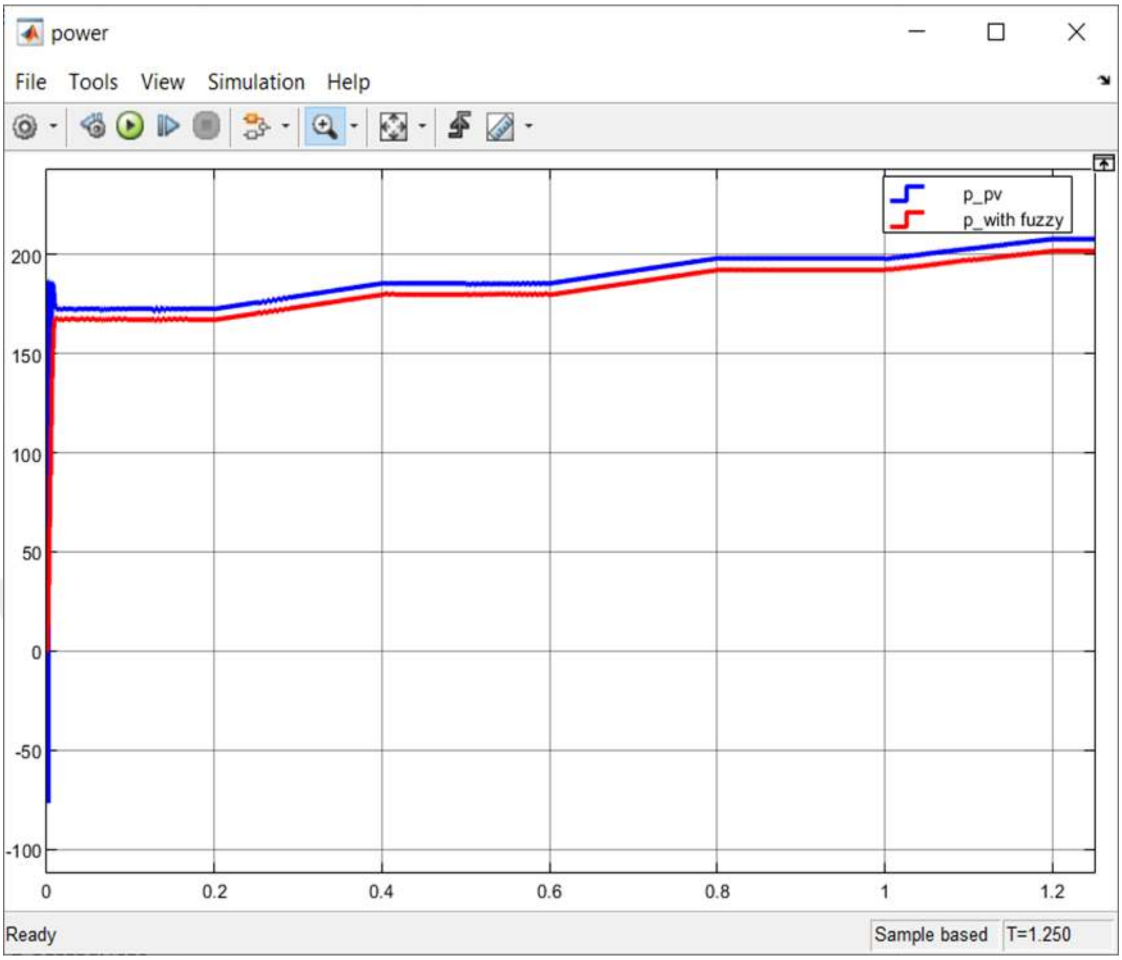

Figure 4.8 Shows the input power and the output power with the FLC algorithm when the temperature is variable.

4.3.3 The PSO algorithm

In Table 4.9 we can see PSO algorithm simulation results when the temperature is different and in Figure 4.9 shows the input power and the output power with the PSO algorithm when the temperature is variable.

Table 4.9 PSO algorithm simulation results when the temperature is different.

Temperature at [1000] W/m^2	$P_{I/P}$ (W)	$V_{I/P}$ (V)	$I_{I/P}$ (A)	efficiency of extracting power %	$P_{O/P}$ (W)	$V_{O/P}$ (V)	$I_{O/P}$ (A)	MPPT Technology Efficiency %
variable	210.4	28.06	6.745	99.62	205.5	39.28	5.232	97.67

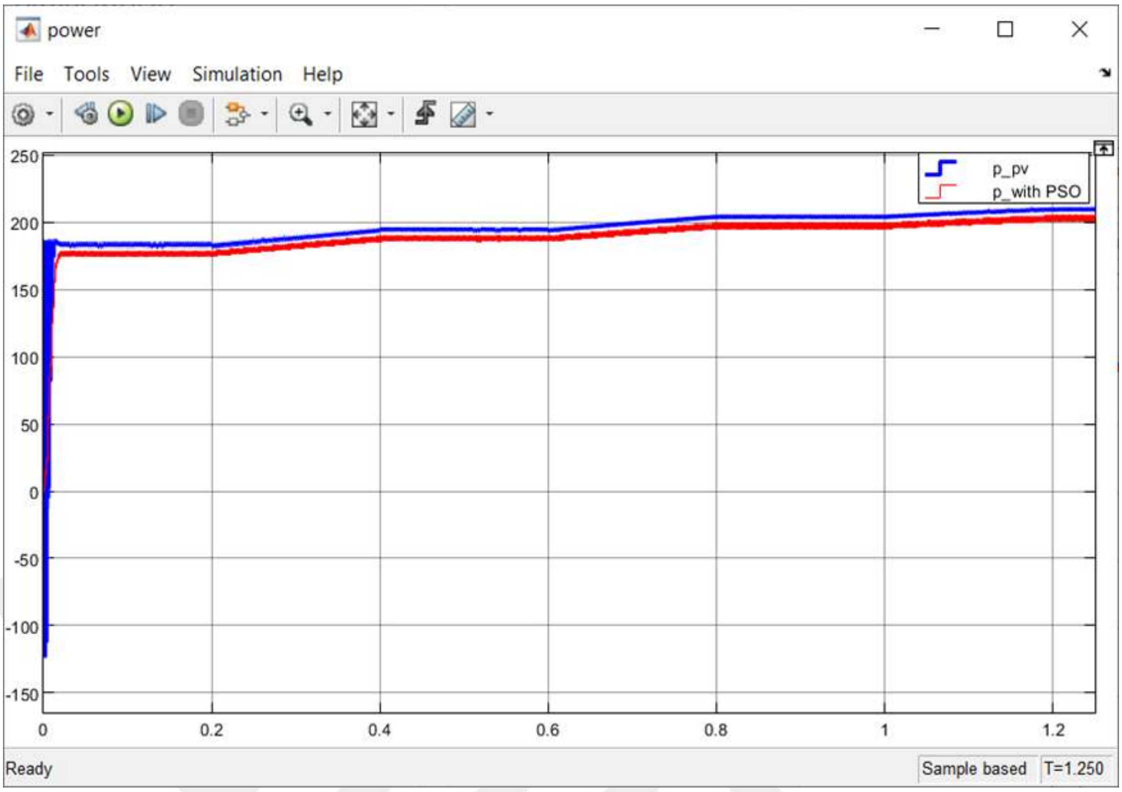

Figure 4.9 Shows the input power and the output power with the PSO algorithm when the temperature is variable.

4.4 Efficiency

In Table 4.10: Simulation results obtained for the energy extracted from the solar panel using MPPT technology and compared with the panel power mentioned in its datasheet (213.15 W) when operating under standard test conditions (irr=1000W/m2, tem=250C) and repeating the same process and calculations under variable test conditions (change of solar irradiation intensity(208.9W/m2), change in temperature (211.2W/m2), the efficiency of each algorithm (P&O, FLC, PSO) was calculated through the value of the power extracted from the solar panel and compared to the theoretical power value of the panel given in a datasheet.

Table 4.10 Calculation of the efficiency of the MPPT technique from the power.

	Efficiency Under standard test conditions (STC)			Efficiency Testing under changing weather conditions					
	irr=1000W/m^2, tem=25°C			Variable irradiation intensity.			variable temperature		
	P_{PV}	$P_{I/P}$	Efficiency (η)	P_{PV}	$P_{I/P}$	Efficiency (η)	P_{PV}	$P_{I/P}$	Efficiency (η)
P&O	213.15	206	96.64%	208.9	201.2	96.31%	211.2	199.2	94.31%
FLC	213.15	210.1	98.56%	208.9	205.7	98.46%	211.2	207.8	98.39%
PSO	213.15	211.5	99.22%	208.9	206.1	98.65%	211.2	210.4	99.62%

Figure 4.10 shows the efficiency chart obtained from Table 4.10 to compare the simulation results of the three algorithms

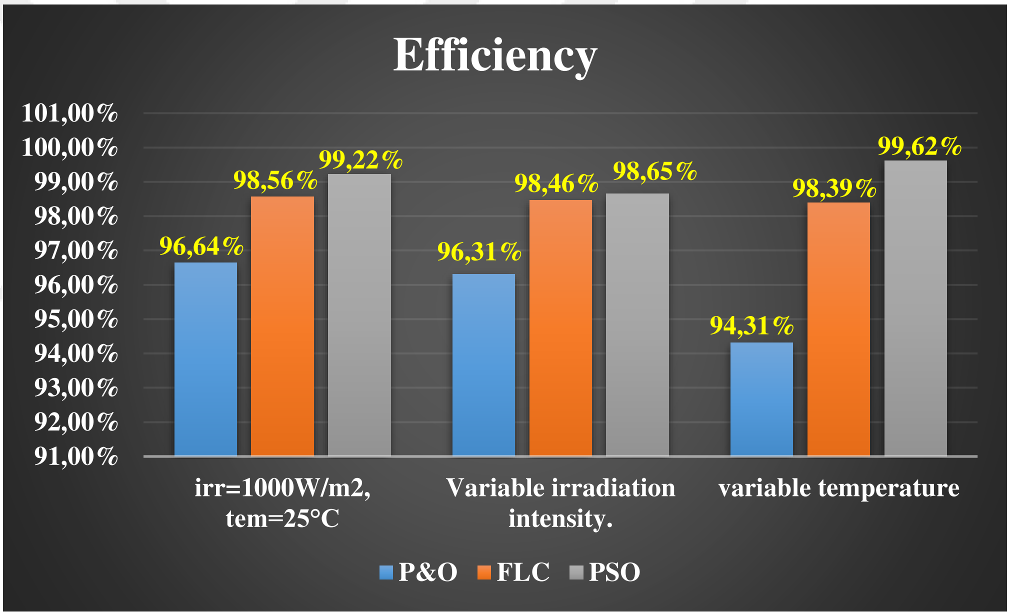

Figure 4.10 MPPT Technology Efficiency Chart.

We can also calculate the efficiency of a photovoltaic system using MPPT technology with a DC-DC boost converter by the output power of the converter and compare it with the input power extracted from solar panels under standard and variable test conditions (temperature change, solar irradiation intensity change), and for each of the three algorithms used in This thesis (P&O, FLC, PSO), through the efficiency results, we can determine which of the three algorithms is best for controlling the duty cycle of the converter for maximum power production in various weather conditions, and Table 4.11 shows the results of the efficiency calculation.

Table 4.11 Efficiency of MPPT technology with a DC-DC boost converter.

	Efficiency Under standard test conditions (STC)			Efficiency Testing under changing weather conditions					
	irr=1000W/m^2, tem=25°C			Variable irradiation intensity.			variable temperature		
	$P_{I/P}$	$P_{O/P}$	Efficiency (η)	$P_{I/P}$	$P_{O/P}$	Efficiency (η)	$P_{I/P}$	$P_{O/P}$	Efficiency (η)
P&O	206	196	95.14%	201.2	186.7	92.79%	199.2	190.6	95.68%
FLC	210.1	204.6	97.38%	205.7	200.3	97.37%	200.3	202.3	97.35%
PSO	211.5	206.6	97.68%	206.1	201.2	97.65%	210.4	205.5	97.67%

Figure 4.11 shows the efficiency Chart obtained from Table 4.11 by the results of the input power of MPPT and power output of DC-DC boost converter.

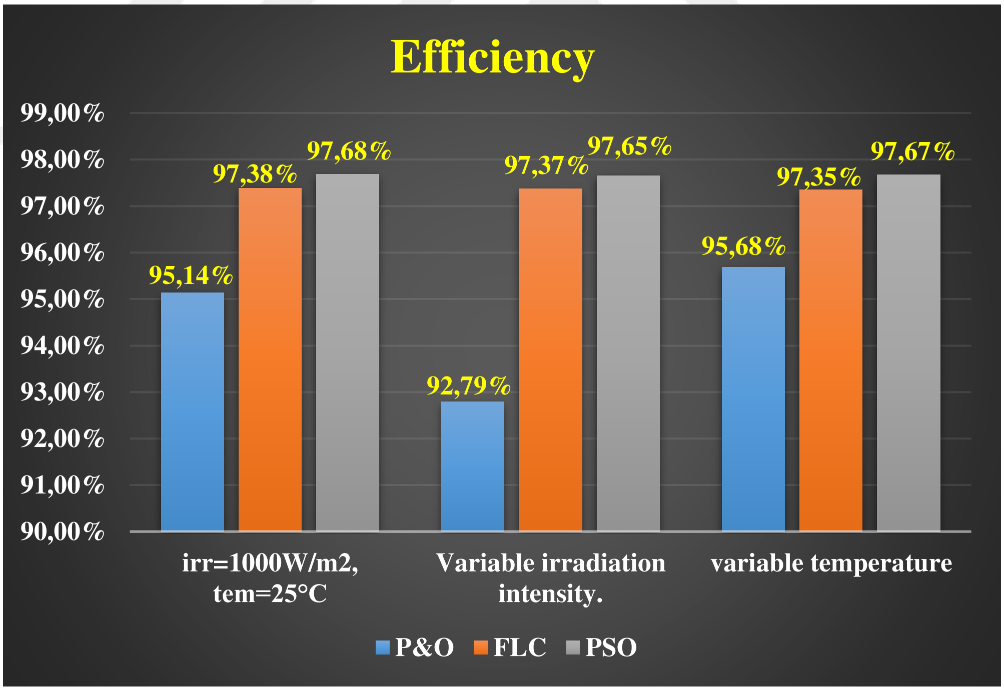

Figure 4.11 MPPT Efficiency Chart with DC-DC Boost Converter.

We can calculate the efficiency of a DC-DC boost converter by comparing the output voltage with the voltage designed to output it (40V) under standard and variable test conditions. By efficiency, we can determine which of the three algorithms is best in controlling the duty cycle of the converter, and Table 4.12 shows the voltage and efficiency results.

Table 4.12 Efficiency of the DC-DC boost converter.

	Efficiency Under standard test conditions (STC)		Efficiency Testing under changing weather conditions			
	irr=1000W/m^2, tem=25°C		Variable irradiation intensity.		variable temperature	
	$V_{O/P}$	Efficiency (η)	$V_{O/P}$	Efficiency (η)	$V_{O/P}$	Efficiency (η)
P&O	36.49	91.22%	35.62	89.05%	35.99	89.97%
FLC	33.26	83.15%	33.01	82.52%	33.07	82.67 %
PSO	39.38	98.45%	38.86	97.15%	39.28	98.20%

Figure 4.12 shows the efficiency diagram obtained from Table 5.11 for the results of the DC-DC boost converter.

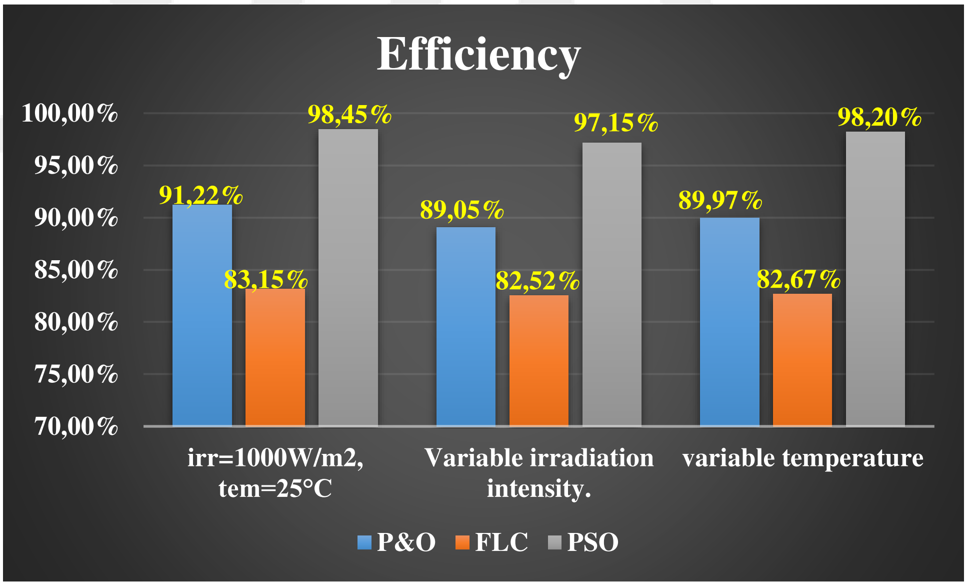

Figure 4.12 Efficiency Chart of a DC-DC boost converter.

4.5 Discussion

In this thesis, a photovoltaic system consisting of three main parts (solar panel, MPPT charge controller, and DC-DC boost converter) is simulated. The boost converter was designed using the equation mentioned in paragraph (3.4.1) and the constants generated by the cell from the values of voltage (29 V), current (7.35 A), and power (213.15 W) during standard test conditions (STC). The boost transformer is designed to supply a voltage (36 V-40 V) to the load in different weather conditions. MPPT technology based on three different algorithms (P&O, FLC, and PSO) generates pulses that control the duty cycle of the converter.

Through the obtained simulation results, it was found that the MPPT technique works very well in tracking the MPP point, extracting the maximum power from the solar panels in the various test conditions, and reducing the signal fluctuation to a minimum. It is also possible to compare the incoming electrical characteristic curves (current, voltage, and power) and the amount of oscillation in them with the curves of the outgoing signals and the amount of improvement and oscillation reduction around the MPP point. The efficiency was also calculated for each algorithm under standard and variable test conditions and DC-DC boost converter.

The efficiency was theoretically calculated for each algorithm under different measurement conditions by the output power divided by the input power multiplied by a percentage and as shown in Equation 4.1.

$$\eta = \frac{P_{I/P}}{P_{PV}} * 100\% \tag{4.1}$$

That the input power (P_PV) is the power generated by the solar cell and prepared in the cell datasheet here in the type used in this thesis Power value (213.15 W) under standard test conditions (irr = 1000 W/m², temperature = 25 °C) This value varies as the irradiation intensity and temperature change and is calculated at each step. As for the output power value (P_(I/P)), it represents the amount of power output from and extracted from the solar panels using MPPT technology, which is fed directly to a DC-DC boost converter.

The results of calculating the efficiency from the power shown in Table 4.10 showed that all the algorithms that were developed and worked on in this thesis to be applied in the MPPT technique have very good results and work well in extracting the maximum power from solar panels in various test conditions and addressing the fluctuations in the MPP point follow-up, the duty cycle of the DC-DC boost converter is well controlled. But we can see that there is a difference in the speed of performance and efficiency between the three algorithms (P&O, FLC, and PSO). Through the efficiency calculation results, we observe a difference in extracting maximum power from the solar panel, processing the oscillation around the MPP point in the electrical characteristic curves, and controlling the duty cycle of a DC-DC boost converter to produce a certain level of voltage under different test conditions.

The results of extracting maximum power from solar panels shown in Table 4.10 prove that MPPT technology based on particle swarm optimization (PSO) algorithm has great superiority and high performance in extracting maximum power from solar panels, tracking MPP points, and reducing signal fluctuation under standard and variable test conditions. Where the (PSO) algorithm achieved an efficiency of (99.22%) under the standard test conditions, while the fuzzy logic control (FLC) algorithm achieved (98.56%) efficiency, and the perturbation and observation (P&O) algorithm achieved Efficiency (96.64%).

While under variable test conditions (change of irradiation intensity and constant temperature) the PSO algorithm achieved an efficiency of (98.65%), the FLC algorithm achieved an efficiency of (98.46%) and the P&O algorithm achieved an efficiency of (96.31%) in the same conditions.

The (PSO) algorithm achieved an efficiency of (99.62%), while the (FLC) algorithm achieved an efficiency of (98.39%) and the (P&O) algorithm achieved an efficiency of (94.31%) all under variable test conditions (temperature change and irradiation intensity were constant).

Table 4.11 shows the efficiency results that were calculated by comparing the power output from the PV system with the power values extracted from the solar panels. The results also show the superiority of the (PSO) algorithm in the speed of performance in tracking the maximum power point, reducing oscillation, and producing maximum power despite the change in weather conditions. Where the (PSO) algorithm achieved an efficiency of (97.68%) in the standard test conditions, while the (FLC) algorithm was the closest in performance and efficiency, which achieved an efficiency of (97.38%) and the (P&O) algorithm achieved an efficiency of (95.14%) under the same test conditions (STC).

Through the efficiency results given in Table 4.10 and Table 4.11 and efficiency plots, the superiority of the (PSO) algorithm can be distinguished in all standard and variable test conditions. And The (FLC) algorithm came in second place, while the (P&O) algorithm came in third place in tracking the maximum power point, processing the oscillation around the MPP point, and controlling the duty cycle of the DC-DC converter.

We can measure the efficiency of the DC-DC boost converter by comparing the output voltage results of the converter shown in Table 4.12 with the voltage value for which the converter is designed (40V) under standard and variable test conditions.

The DC-DC boost converter provides a voltage (39.38V) when using MPPT technology based on the PSO algorithm to control the duty cycle of the converter under standard test conditions, while the converter outputs a voltage of)36.49V) with the P&O algorithm, and the use of the FLC algorithm achieves a voltage of (33.26V). Where the efficiency of the converter with the PSO algorithm reached (98.45%), which is the highest compared to the other two algorithms (P&O, FLC), where the (FLC) algorithm achieved an efficiency of (83.15%) and the (P&O) algorithm achieved an efficiency of (91.22%) under the same standard test conditions.

The DC-DC boost converter provided the highest voltage values under changing test conditions (change of solar irradiation intensity and temperature change) as shown in Table 4.12.

Through the results of the voltage provided by the DC-DC boost converter, we note that the application of MPPT technology based on the (PSO) algorithm to control its work cycle achieved the best performance and the closest electrical voltage (39.38 volts) compared to the voltage that the transformer was designed based on providing (40 volts) under standard test conditions and also the best effort under variable test conditions compared to the other two algorithms (P&O, FLC).

5 CONCLUSIONS AND RECOMMENDATION

The main objective of this thesis is to improve the performance of the MPPT charge controller to increase the efficiency of the photovoltaic system, by tracking the MPP point, reducing oscillation around it, extracting maximum power from the solar panels, and controlling the duty cycle of the DC-DC boost converter to provide a constant voltage on the Despite the changing weather conditions. As solar energy is today one of the most important sources of renewable energy, and we hope that it will be the most important source of electrical energy in the coming years, it has become the focus of researchers' attention to conduct their research. To develop its performance, increase its efficiency, and reduce its initial costs.

To increase the efficiency of the photovoltaic system, three algorithms have been developed to be applied in MPPT technology. These algorithms are the Perturbation and Observation (P&O) Algorithm, the Fuzzy Logic Controller (FLC) Algorithm, and the Particle Swarm Optimization (PSO) Algorithm. To extract the maximum amount of electrical power from solar panels under standard and variable test conditions, maximum power point (MPP) tracking, duty cycle control of the boost converter.

After simulating the photovoltaic system (solar panels, MPPT technology, DC-DC boost converter) using MATLAB / Simulink, we obtained three sets of results (the first group relates to MPPT technology in extracting the maximum power generated from the solar panel, and the second group relates to the results of electrical power which we obtained at the output of the photovoltaic system, the last group relates to the level of voltage supplied by the DC-DC boost converter to supply it to the load), As shown sequentially in Tables (4.10, 4.11, and 4.12), all the results showed that the three developed algorithms applied in MPPT technology gave very well results.

In the first set, the three algorithms (P&O, FLC, PSO) developed in MPPT technology are applied to extract maximum power from solar panels under standard and variable test conditions. Where the application of the (PSO) algorithm achieved the best performance and the highest efficiency, as it achieved an efficiency of (99.22%) in the standard test conditions and an efficiency of (98.65%) under changing weather conditions (changing the intensity of solar irradiation) while achieving an efficiency of (99.62%) at (temperature change), which is the highest efficiency compared to the two algorithms (P&O, FLC).

The results in the second group, Table (4.11), proved that the developed algorithms work very well, but there are slight differences in performance and efficiency, as the PSO algorithm achieved the best performance and the highest efficiency (97.68%) in tracking the maximum power point. The FLC algorithm came in second place with an efficiency of (97.38%), while the P&O algorithm achieved an efficiency of (95.14%) under the standard test conditions (STC). The (PSO) algorithm also demonstrated high efficiency and better performance when tested under changing weather conditions, as it achieved an efficiency of (97.65%) at (change of solar irradiation intensity), and efficiency of (97.67%) at (change of temperature) compared to the two algorithms (P&O). , FLC).

The last group is the voltage results shown in Table 4.12 from which the efficiency of the DC-DC boost converter was calculated by comparing the voltage coming out of the photovoltaic system with the voltage on which the converter was designed (40 volts). We got very well results by applying MPPT technology based on three developed algorithms (PSO, P&O, and FLC) to control the duty cycle of the transformer. The best value for voltage was obtained under standard test conditions (39.38V) when using the PSO algorithm. The PSO algorithm also achieved the highest values of electrical voltage in the variable test conditions, as it achieved a voltage value of (38.86V) when changing the intensity of solar irradiation, and we obtained a voltage of (39.28V) when applying the PSO algorithm at a variable temperature, And it is the closest electrical voltage values to the value required to prepare it for the load (40 volts).

So the (PSO) algorithm is considered the best performance and efficiency compared to the two algorithms (P&O, FLC). Through the results we obtained in this thesis, the developed PSO algorithm achieved the best results and increased the efficiency of the system compared to the two algorithms (P&O, FLC) as it achieved the highest efficiency under standard and variable test conditions and also achieved the best results when controlling the duty cycle of the boost converter to produce the highest value an effort.

As future work, he suggested applying new algorithms such as Artificial Neural Network (ANN) algorithm and Ant colony optimization algorithm (ACO) algorithm and using a traditional algorithm such as the traditional Incremental conductance (IC) algorithm and comparing their results to increase system efficiency and extract the greatest amount of electrical power. Application of the three algorithms (P&O, FLC, PSO) to operate the DC motor used in water pumps in remote villages for agriculture as well as in water pumps from wells. It can also be used to operate street surveillance cameras in desert and mountainous areas, where the national electric grid is not available, and its applications in the manufacture of smart cars that run on renewable energy.

REFERENCES

Abdellatif, W. S. E., Mohamed, M. S., Barakat, S. and Brisha, A. 2021. A fuzzy logic controller based mppt technique for photovoltaic generation system. International Journal on Electrical Engineering and Informatics., 13(2): 394–417.

Abo-Sennah, M. A., El-Dabah, M. A. and Mansour, A. E. B. 2021. Maximum power point tracking techniques for photovoltaic systems: A comparative study. International Journal of Electrical and Computer Engineering., 11(1): 57–73.

Acharya, P. S. and Aithal, P. S. 2020. A Comparative Study of MPPT and PWM Solar Charge Controllers and their Integrated System. Journal of Physics: Conference Series., 17(1): 12.

Ahmed, J. and Salam, Z. 2017. An Accurate Method for MPPT to Detect the Partial Shading Occurrence in a PV System. IEEE Transactions on Industrial Informatics., 13(5): 2151–2161.

Akiza, B., Akoro, E. and Douti, D.-B. L. 2021. Design and Simulation of an MPPT Charge Controller for a PV Application. TH Wildau Engineering and Natural Sciences Proceedings., 1: 257–261.

Al-Ghezi, M. K., Ahmed, R. T. and Chaichan, M. T. 2022. The Influence of Temperature and Irradiance on Performance of the photovoltaic panel in the Middle of Iraq. International Journal of Renewable Energy Development., 11(2): 501–553.

Ali, A., Almutairi, K., Padmanaban, S., Tirth, V., Algarni, S., Irshad, K., Islam, S., Zahir, M. H., Shafiullah, M. and Malik, M. Z. 2020. Investigation of MPPT Techniques under Uniform and Non-Uniform Solar Irradiation Condition-A Retrospection. IEEE Access., 8: 127368–127392.

Ali, M. N., Mahmoud, K., Lehtonen, M. and Darwish, M. M. F. 2021. Promising mppt methods combining metaheuristic, fuzzy-logic and ann techniques for grid-connected photovoltaic. Sensors (Switzerland)., 21(4): 1–18.

Al-Majidi, S. D., Abbod, M. F. and Al-Raweshidy, H. S. 2018. A novel maximum power point tracking technique based on fuzzy logic for photovoltaic systems. International Journal of Hydrogen Energy., 43(31): 14158–14171.

Alshareef, M. 2021. An Improved MPPT Method Based on Fuzzy Logic Controller for a PV System. Studies in Informatics and Control., 30(1): 89–98.

Alsumiri, M. 2019. Residual Incremental Conductance Based Nonparametric MPPT Control for Solar Photovoltaic Energy Conversion System. IEEE Access., 7: 87901–87906.

Aly, M. and Rezk, H. 120211. An improved fuzzy logic control-based MPPT method to enhance the performance of PEM fuel cell system. Neural Computing and Applications., 34(6): 4555-4566.

Anowar, M. H. and Roy, P. 2019. A modified incremental conductance based photovoltaic MPPT charge controller. In 2019 International Conference on Electrical, Computer and Communication Engineering (ECCE)., 1: 5.

Arunkumari, T. and Indragandhi, V. 2017. An overview of high voltage conversion ratio DC-DC converter configurations used in DC micro-grid architectures. Renewable and Sustainable Energy Reviews., 77: 670–687.

Asif, R. M., Ur Rehman, A., Ur Rehman, S., Arshad, J., Hamid, J., Tariq Sadiq, M. and Tahir, S. 2020. Design and analysis of robust fuzzy logic maximum power point tracking based isolated photovoltaic energy system. Engineering Reports., 2(9): 1–16.

Ayop, R. and Tan, C. W. 2018. Design of boost converter based on maximum power point resistance for photovoltaic applications. Solar Energy., 160: 322–335.

Azad, M. L., Sadhu, P. K. and Das, S. (2020). Comparative Study between PO and Incremental Conduction MPPT Techniques- A Review. Proceedings of International Conference on Intelligent Engineering and Management., 2(20): 217–222.

Ba, A., Ehssein, C. O., Mahmoud, M. E. M. O. M., Hamdoun, O. and Elhassen, A. 2018. Comparative Study of Different DC/DC Power Converter for Optimal PV System Using MPPT (PandO) Method. Applied Solar Energy (English Translation of Geliotekhnika)., 54(4): 235–245.

Baramadeh, M. Y., Abouelela, M. A. A. and Alghuwainem, S. M. 2021. Maximum Power Point Tracker Controller Using Fuzzy Logic Control with Battery Load for Photovoltaics Systems. Smart Grid and Renewable Energy., 12(10): 163–181.

Bollipo, R. B., Mikkili, S. and Bonthagorla, P. K. 2020. Critical Review on PV MPPT Techniques: Classical, Intelligent and Optimisation. IET Renewable Power Generation., 14(9): 1433–1452.

Bollipo, R. B., Mikkili, S. and Bonthagorla, P. K. 2021. Hybrid, optimal, intelligent and classical PV MPPT techniques: A review. CSEE Journal of Power and Energy Systems., 7(1): 9–33.

Boutabba, T., Drid, S., Chrifi-Alaoui, L. and Benbouzid, M. E. 2018. A new implementation of maximum power point tracking based on fuzzy logic algorithm for solar photovoltaic system. International Journal of Engineering, Transactions B: Applications., 31(4): 580–587.

Chaibi, Y., Allouhi, A., Malvoni, M., Salhi, M. and Saadani, R. 2019. Solar irradiance and temperature influence on the photovoltaic cell equivalent-circuit models. Solar Energy., 188: 1102–1110.

Chao, K. H. and Rizal, M. N. 2021. A hybrid mppt controller based on the genetic algorithm and ant colony optimization for photovoltaic systems under partially shaded conditions. Energies., 14(10): 20-29.

Converter, B. (2017). Perturb and Observation MPPT algorithm for Solar Photovoltaic System., 12: 17-20.

Dhaouadi, G., Djamel, O., Youcef, S. and Salah, C. 2019. Implementation of Incremental Conductance Based MPPT Algorithm for Photovoltaic System. Proceedings - 2019 4th International Conference on Power Electronics and Their Applications., 8(9): 105-111.

Elbarbary, Z. M. S. and Alranini, M. A. 2021. Review of maximum power point tracking algorithms of PV system. Frontiers in Engineering and Built Environment., 1(1): 68–80.

Eltamaly, A. M. and Abdelaziz, A. Y. (2020). Modern Maximum Power Point Tracking Techniques for Photovoltaic Energy Systems., 1: 10-20.

Farooqui, S. A., Khan, R. A., Islam, N. and Ahmed, N. 2022. Cuckoo Search Algorithm and Artificial Neural Network-based MPPT: A Comparative Analysis., 10: 1–5.

Guran, I. C. and Perișoară, L. 2020. MPPT solar charge controller for automotive industry., 2: 118.

Hashim, N., Salam, Z., Johari, D. and Nik Ismail, N. F. 2018. DC-DC Boost Converter Design for Fast and Accurate MPPT Algorithms in Stand-Alone Photovoltaic System. International Journal of Power Electronics and Drive Systems (IJPEDS)., 9(3): 1038.

Hu, K., Cao, S., Li, W. and Zhu, F. 2019. An Improved Particle Swarm Optimization Algorithm Suitable for Photovoltaic Power Tracking under Partial Shading Conditions. IEEE Access., 7: 143217–143232.

Irwanto, M., Leow, W. Z., Ismail, B., Baharudin, N. H., Juliangga, R., Alam, H. and Masri, M. 2020. Photovoltaic powered DC-DC boost converter based on PID controller for battery charging system. Journal of Physics: Conference Series., 1432(1): 012055.

Jeannot, B. G., Jacques, M. J. and Jeannot, M. M. 2020. Reliability of the MPPT Control on the Energy Parameters of a Photovoltaic Generator. World Journal of Engineering and Technology., 08(03): 537–550.

Junichi, O., Yuren, T., Naoko, S., Yoshinori, F. and Tanji, H. 2003. Covariance structure analysis of health-related indicators in the elderly at home with a focus on subjective health (Special feature: People's health) (How to support). Comprehensive Urban Studies., 8(1): 19-30.

Jyothy, L. P. N. and Sindhu, M. R. 2018. An Artificial Neural Network based MPPT Algorithm for Solar PV System. Proceedings of the 4th International Conference on Electrical Energy Systems ICEES., 21(8): 375–380.

Kabalci, E. and Boyar, A. 2020. Design and Comparison of MPPT Controllers with Fuzzy Logic and Particle Swarm Optimization for PV Power Conversion. Proceedings - 2020 2nd International Conference on Control Systems, Mathematical Modeling, Automation and Energy Efficiency, SUMMA., 22: 993–998.

Kamran, M., Mudassar, M., Fazal, M. R., Asghar, M. U., Bilal, M. and Asghar, R. 2020. Implementation of improved Perturb and Observe MPPT technique with confined search space for standalone photovoltaic system. Journal of King Saud University - Engineering Sciences., 32(7): 432–441.

Khodair, D., Salem, M. S., Shaker, A., El Munim, H. E. A. and Abouelatta, M. 2020. Application of Modified MPPT Algorithms: A Comparative Study between Different Types of Solar Cells. Applied Solar Energy (English Translation of Geliotekhnika)., 56(5): 309–323.

Kota, V. R. and Bhukya, M. N. 2019. A novel global MPP tracking scheme based on shading pattern identification using artificial neural networks for photovoltaic power generation during partial shaded condition. IET Renewable Power Generation., 13(10): 1647–1659.

Kumar, R., Choudhary, A., Koundal, G., Singh, A. and Yadav, A. 2017. Modelling/Simulation of MPPT Techniques for Photovoltaic Systems Using Matlab. International Journal of Advanced Research in Computer Science and Software Engineering., 7(4): 178–187.

Majaw, T., Deka, R., Roy, S. and Goswami, B. 2018. Solar Charge Controllers using MPPT and PWM: A Review. ADBU Journal of Electrical and Electronics Engineering., 2(1): 1–4.

Mala, I., Zia, S. S., Naseem, M., Mobeen, T. and Mughal, T. J. A. 2019. Fuzzy Logic Based Obstacle Avoidance Autonomous Robots. Sindh University Research Journal -Science Series., 51(01): 119–128.

Mao, M., Cui, L., Zhang, Q., Guo, K., Zhou, L. and Huang, H. 2020. Classification and summarization of solar photovoltaic MPPT techniques: A review based on traditional and intelligent control strategies. Energy Reports., 6(174): 1312–1327.

Mars, N., Grouz, F., Essounbouli, N. and Sbita, L. 2017. Synergetic MPPT Controller for Photovoltaic System. Journal of Electrical and Electronic Systems., 06(02): 2332-0796.

Mnati, M. J., Gino, V., Araujo, M., Abed, J. and Bossche, A. Van Den. 2019. Review Different Types of MPPT Techniques for Photovoltaic Systems Review Different Types of MPPT Techniques for Photovoltaic Systems. Ieee., 2: 0–7.

Mohamed Abdelwahab, S. A., Hamada, A. M. and Abdellatif, W. S. E. 2020. Comparative analysis of the modified perturb and observe with different MPPT techniques for PV grid connected systems. International Journal of Renewable Energy Research., 10(1): 155–164.

Mohamed, S. A. and Abd El Sattar, M. 2019. A comparative study of PandO and INC maximum power point tracking techniques for grid-connected PV systems. SN Applied Sciences., 1: 2.

Naderpour, A., Sardroud, J. M. and Mofid, M. 2017. Presenting a Model Based on Fuzzy Application to Optimize the Time of IBS Projects in Gas Refineries. MATEC Web of Conferences., 95: 4–7.

Nadkarni, S. S., Angadi, S. and Raju, A. B. 2018. Simulation and Analysis of MPPT Algorithms for Solar PV based Charging Station. Proceedings of the International Conference on Computational Techniques, Electronics and Mechanical Systems., 21(8): 45–50.

Nasser, K. W., Yaqoob, S. J. and Hassoun, Z. A. 2020. Improved dynamic performance of photovoltaic panel using fuzzy logic-MPPT algorithm. Indonesian Journal of Electrical Engineering and Computer Science., 21(2): 617–624.

Necaibia, S., Kelaiaia, M. S., Labar, H. and Necaibia, A. 2017. Implementation of an Improved Incremental Conductance MPPT Control Based Boost Converter in Photovoltaic Applications. International Journal of Emerging Electric Power Systems., 18(4): 1–19.

Nkambule, M. S., Hasan, A. N. and Ali, A. 2019. MPPT under partial shading conditions based on Perturb and Observe and Incremental Conductance. ELECO 2019 - 11th International Conference on Electrical and Electronics Engineering., 9: 85–90.

Nour Ali, M. 2019. Improved Design of Artificial Neural Network for MPPT of Grid-Connected PV Systems. 2018 20th International Middle East Power Systems Conference., 11: 97–102.

Owusu-Nyarko, I., Elgenedy, M. A., Abdelsalam, I. and Ahmed, K. H. 2021. Modified variable step-size incremental conductance mppt technique for photovoltaic systems. Electronics (Switzerland)., 10(19): 10-19.

Palanisamy, R., Vijayakumar, K., Venkatachalam, V., Narayanan, R. M., Saravanakumar, D. and Saravanan, K. 2019. Simulation of various DC-DC converters for photovoltaic system. International Journal of Electrical and Computer Engineering (IJECE)., 9(2): 917.

Panchal, S., Navalkar, O., Jadhav, P. and Malekar, P. N. 2019. Automated Solar Tracking System for Efficient Energy Utilization., 1(2): 1–5.

Pathare, M., Shetty, V., Datta, D., Valunjkar, R., Sawant, A. and Pai, S. 2017. Designing and implementation of maximum power point tracking(MPPT) solar charge controller. 2017 International Conference on Nascent Technologies in Engineering., 1: 5.

Pathy, S., Subramani, C., Sridhar, R., Thamizh Thentral, T. M. and Padmanaban, S. 2019. Nature-inspired MPPT algorithms for partially shaded PV systems: A comparative study. Energies., 12(8): 1–21.

Pilakkat, D., Kanthalakshmi, S. and Navaneethan, S. 2020. A Comprehensive Review of Swarm Optimization Algorithms for MPPT Control of PV Systems under Partially Shaded Conditions. Electronics., 24(1): 3–14.

Prabhu, H. U. and Babu, M. R. 2021. Performance study of mppt algorithms of dc-dc boost converters for pv cell applications. Proceedings of the 7th International Conference on Electrical Energy Systems, ICEES., 9: 201–205.

Putri, R. I., Wiyanto, S., Syamsiana, I. N., Junus, M., Rifa'I, M. and Putra, E. S. 2019. Maximum power point tracking based on particle swarm optimization for photovoltaic system on greenhouse application. Journal of Physics: Conference Series., 1402(3): 2–9.

R.Kareem, P. 2019. Simulation of the Incremental Conductance Algorithm for Maximum Power Point Tracking of Photovoltaic System Based On Matlab. Djes., 12(1): 34–43.

RAOF, A. A. 2020. a Comparative Study of Mppt Methods for Pv Array Under Partial Shading Condition in Matlab/Simulink., 8: 9.

Remoaldo, D. and Jesus, I. S. 2021. Analysis of a traditional and a fuzzy logic enhanced perturb and observe algorithm for the mppt of a photovoltaic system. Algorithms., 1: 41.

Ritu, K. R., Mishra, B. and Wadhwani, A. K. 2020. Simulation And Analysis Of Particle Swarm Optimization Algorithm Based MPPT For PV System Operating Under Partial Shading Condition., 9(09): 356–363.

Ronilaya, F., Setiawan, B., Kusuma, A. A., Mahfudi, I. and Yuliawan, D. M. 2018. Design Maximum Power Point Tracking of Wind Energy Conversion Systems Using PandO and IC Methods. IOP Conference Series: Materials Science and Engineering., 4:71.

ROUGAB, I., CHEKNANE, A. and ABOUCHABANA, N. 2021. Study and simulation of MPPT techniques to control a stand-alone photovoltaic system under varying irradiance. Revista Română de Informatică Și Automatică., 31(4): 109–122.

Salleh, Z., Sulaiman, M., Patakor, F. A. and Omar, R. 2017. Rules reduction and optimization of fuzzy logic membership functions for induction motor speed controller. Journal of Theoretical and Applied Information Technology., 95(19): 4922–4934.

Salman, S., Ai, X. and Wu, Z. 2018. Design of a P-and-O algorithm based MPPT charge controller for a stand-alone 200W PV system. Protection and Control of Modern Power Systems., 3(1): 8-18.

Sampaio, P. G. V. and González, M. O. A. 2017. Photovoltaic solar energy: Conceptual framework. Renewable and Sustainable Energy Reviews., 74: 590–601.

Sarvi, M. and Azadian, A. 2021. A comprehensive review and classified comparison of mppt algorithms in pv systems. Energy Systems., 21: 1-40.

Sasi, M. A. 2017. Fuzzy Logic Control of MPPT Controller for PV Systems., 1: 17.

Senthilkumar, S., Mohan, V., Mangaiyarkarasi, S. P. and Karthikeyan, M. 2022. Analysis of Single-Diode PV Model and Optimized MPPT Model for Different Environmental Conditions. International Transactions on Electrical Energy Systems., 2(2): 1–17.

Sepulveda Mora, S. B., Luna Paipa, E. A., Laguado Serrano, M. A. and Bustos Márquez, L. F. 2019. Performance comparison between PWM and MPPT charge controllers. Scientia et Technica., 24(1): 6.

Shadlu, M. S. 2018. Comparison of Maximum Power Point Tracking (MPPT) Algorithms to Control DC-DC Converters in Photovoltaic Systems. Recent Advances in Electrical and Electronic Engineering (Formerly Recent Patents on Electrical and Electronic Engineering)., 12(4): 355–367.

Siddique, M. A. B., Khan, M. A., Asad, A., Rehman, A. U., Asif, R. M. and Rehman, S. U. 2020. Maximum power point tracking with modified incremental conductance technique in grid-connected PV array. CITISIA 2020 - IEEE Conference on Innovative Technologies in Intelligent Systems and Industrial Applications, Proceedings., 3: 16-20.

Soriano, L. A., Ponce, P. and Molina, A. 2017. Analysis of DC-DC converters for photovoltaic applications based on conventional MPPT algorithms. 2017 14th International Conference on Electrical Engineering, Computing Science and Automatic Control., 2: 7.

Sutikno, T., Subrata, A. C. and Elkhateb, A. (2021). Evaluation of Fuzzy Membership Function Effects for Maximum Power Point Tracking Technique of Photovoltaic System. IEEE Access., 9: 109157–109165.

Syafaruddin, Abubakar, M. I., Soma, H. G., Said, S. M. and Latief, S. 2018. Determination of sensorless input parameters of solar panel with adaptive neuro-fuzzy inference system (ANFIS) method. International Journal of Innovative Computing, Information and Control., 14(6): 2259–2271.

Szczepaniak, M., Otręba, P., Otręba, P. and Sikora, T. 2022. Use of the maximum power point tracking method in a portable lithium-ion solar battery charger. Energies., 15: 1.

Talbi, M., Mensia, N. and Ezzaouia, H. 2021. Modeling of a pv panel and application of maximum power point tracking command based on ann. International Arab Journal of Information Technology., 18(4): 568–577.

The MathWorks Inc. 2019. Build Fuzzy Systems Using Fuzzy Logic Designer - MATLAB and Simulink. MathWorks., 3: 1–18.

Victor, A., Mahato, D. K., Pundir, A. and Saxena, G. J. 2019. Design, Simulation and Comparative Analysis of Different Types of Solar Charge Controllers for Optimized Efficiency. Proceedings - 2019 Women Institute of Technology Conference on Electrical and Computer Engineering., 7: 17–21.

Villegas-Mier, C. G., Rodriguez-Resendiz, J., Álvarez-Alvarado, J. M., Rodriguez-Resendiz, H., Herrera-Navarro, A. M. and Rodríguez-Abreo, O. 2021. Artificial neural networks in mppt algorithms for optimization of photovoltaic power systems: A review. Micromachines., 12(10): 1–19.

Website. 2009. New Text Document (2). In Phil. Mag., 27: 77.

Yilmaz, A., Demirci, A. and Tercan, S. M. 2022. Technical Comparison of PWM and MPPT Charge Regulators., 5: 78–83.

Zafar, M. H., Al-Shahrani, T., Khan, N. M., Mirza, A. F., Mansoor, M., Qadir, M. U., Khan, M. I. and Naqvi, R. A. 2020. Group teaching optimization algorithm based mppt control of pv systems under partial shading and complex partial shading. Electronics (Switzerland)., 9(11): 1–24.

Zhang, F., Ye, W., Lei, G., Liu, Y., Wang, X. and He, C. 2021. Simulation and analysis of power-point tracking via photovoltaic sensors. Sensors and Materials., 33(11): 3991–4001.